PONTIFICAL CATHOLIC UNIVERSITY OF PARANÁ

SCHOOL OF MEDICINE AND LIFE SCIENCES

GRADUATE PROGRAM IN HEALTH SCIENCES

SALIVARY FRACTION FROM THE TICK *Amblyomma sculptum* INDUCES

INTRINSIC APOPTOSIS IN NEUROBLASTOMA CELLS

PhD Candidate: Sheron Campos Cogo

Advisors: Dr. Selene Elifio Esposito

Co-advisor: Dr. Olivier Micheau

Curitiba, April, 2022

PONTIFICAL CATHOLIC UNIVERSITY OF PARANÁ

SCHOOL OF MEDICINE AND LIFE SCIENCES

GRADUATE PROGRAM IN HEALTH SCIENCES

SALIVARY FRACTION FROM THE TICK *Amblyomma sculptum* INDUCES INTRINSIC APOPTOSIS IN NEUROBLASTOMA CELLS.

Thesis presented to the Graduate Program in Health Sciences, Escola de Medicina of Pontifícia Universidade Católica do Paraná, as a requirement for obtaining the title of Doctor in Health Sciences.

Advisors: Dr. Selene Elifio Esposito
Co-advisor: Dr. Olivier Micheau

Curitiba, April, 2022

PONTIFÍCIA UNIVERSIDADE CATÓLICA DO PARANÁ

ESCOLA DE MEDICINA E CIÊNCIAS DA VIDA

PROGRAMA DE PÓS-GRADUAÇÃO EM CIÊNCIAS DA SAÚDE

PUCPR

GRUPO MARISTA

FRAÇÃO SALIVAR DO CARRAPATO *Amblyomma sculptum* INDUZ APOPTOSE INTRÍNSECA EM CÉLULAS DO NEUROBLASTOMA.

Tese apresentada ao Programa de Pós-Graduação em Ciências da Saúde da Escola de Medicina da Pontifícia Universidade Católica do Paraná, como requisito para obtenção do título de Doutor em Ciências da Saúde.

Orientadores: Dra. Selene Elifio Esposito

Co-orientador: Dr. Olivier Micheau

Curitiba, Abril, 2022

Pontifícia Universidade Católica do Paraná
Escola de Medicina e Ciências da Vida
Programa de Pós-Graduação em Ciências da Saúde

ATA DA SESSÃO PUBLICA DE EXAME DE TESE DO PROGRAMA DE PÓS-GRADUAÇÃO EM CIÊNCIAS DA SAÚDE EM NÍVEL DE DOUTORADO DA PONTIFICIA UNIVERSIDADE CATÓLICA DO PARANÁ.

Aos **08** dias do mês de abril de 2022 às 10:00, realizou-se a sessão aberta de Defesa de Tese "FRAÇÃO SALIVAR DO CARRAPATO Amblyomma sculptum INDUZ APOPTOSE INTRÍNSECA EM CÉLULAS DO NEUROBLASTOMA" apresentado por **Sheron Campos Cogo** para obtenção do título de Doutor; Área de concentração: Medicina e áreas afins.

A banca examinadora foi composta pelos seguintes membros:

MEMBROS DA BANCA	ASSINATURA
Profa. Dra. Selene Eliflo Esposito - Presidente	*assinatura*
Prof. Dr. Roberto Hirochi Herai (PUCPR)	*assinatura*
Prof. Dr. Anderson de Sá Nunes (USP)	*assinatura*
Profa. Dra. Priscila Hess Lopes (Prevor S.P.R.L.)	*assinatura*
Profa. Dra. Joanna B Kitlinska (Georgetown University)	*assinatura*

De acordo com as normas regimentais a Banca Examinadora deliberou sobre os conceitos a serem distribuídos e que foram os seguintes:

Profa. Dra. Selene Eliflo Esposito   Conceito: Aprovada
Prof. Dr. Roberto Hirochi Herai   Conceito: Aprovada
Prof. Dr. Anderson de Sá Nunes   Conceito: Aprovada
Profa. Dra. Priscila Hess Lopes   Conceito: Aprovada
Profa. Dra. Joanna B Kitlinska   Conceito: Aprovada

Parecer Final: Aprovada

Observações da Banca Examinadora:

_____
Profa. Dra. Selene Eliflo Esposito
Presidente da Banca Examinadora

_____
Profa. Dra. Cristina Pellegrino Baena
Coordenadora do PPGCS-PUCPR

ACKNOWLEDGMENT

I would like to thank the following people for helping me finalize the project.

Professor Dr. Selene Elifio Esposito for her scientific knowledge, support and dedication to our work. Always kindly and regardfully teaching me, assisting me in the preparation of the present work and other professional projects. For her friendship, support and encouragement, representing my greatest model of scientist and mentor.

Dr. Olivier Micheau for welcoming me into his laboratory, guiding and providing assistance for the accomplishment of experiments and studies. For his great knowledge and disposition on supporting our project and the elaboration of the present thesis. Also, for the opportunity to participate in other scientific projects coordinated by him.

Dr. Simone Michaela Simons for the support and collaboration, for the collection and suppling of the tick saliva. As well as for the data collection related to the biochemical characterization of the saliva, carried out by her and her collaborators at the Butantan Institute, Brazil.

Professor Guilherme Sassaki from the Biochemistry Department at the Federal University of Paraná, in Brazil, for all his promptitude on assisting us on biochemical analysis of the tick saliva composition.

THESIS COMMITTEE

Selene Elifio Esposito – Graduate Program in Health Sciences, School of Medicine and Life Sciences, Pontifícia Universidade Católica do Paraná – Brazil

Olivier Micheau – Graduate Program in Health Sciences - UFR Science de Santé, INSERM U1231, University of Burgundy – France

Ricardo Aurino de Pinho – Graduate Program in Health Sciences, School of Medicine and Life Sciences, Pontifícia Universidade Católica do Paraná – Brazil

Anderson de Sá Nunes – Laboratory of Experimental Immunology, University of São Paulo – Brazil

Priscila Hess Lopes – Laboratory of Immunochemistry, Prevor – Belgium

Joanna Kitlinska – Department of Biochemistry and Molecular & Cellular Biology, Georgetown University – United States of America.

INFORMATIVE SECTION

The present study was developed as an interuniversity exchange doctorate coordinated by professor Dr. Selene Elifio Esposito, Pontifical Catholic University of Paraná (PUCPR), in collaboration with Professor Dr. Olivier Micheau from the University of Burgundy (UB) – France, and with Dr. Simone Simons from the Butantan Institute – SP, Brazil.

Tick *Amblyomma sculptum* and its crude saliva collection was coordinated by Dr. Simone Simons and her team at the Laboratory of Parasitology of the Butantan Institute. Experimental *in-vitro* studies were held at the Experimental Multiuser Laboratory – Toxins and Cancer Laboratory – of PUCPR, coordinated by professor Selene Esposito and at the Laboratory of Lipides, Nutrition and Cancer of UB coordinated by Professor Olivier Micheau, during a intership doctorate of one year (15th April 2019 – 15th of March 2020). The development of the present study also included with the collaboration of professor Dr. Guilherme Sassaki, from the Department of Biochemistry of Federal University of Paraná (UFPR), for analysis of the chemical composition of fractions extracted from the crude saliva of *A. sculptum.*

SUMMARY

LIST OF FIGURES

LIST OF ABREVIATIONS

7-AAD: 7-Aminoactinomycin D

ACE: angiotensin-converting enzyme

AMPK: 5' adenosine monophosphate-activated protein kinase

Apaf-1: Apoptotic protease activating factor-1

ASC: Associated speak-like protein containing caspase recruitment domain

ATCC: American type culture collection

ATG: autophagy related protein

AZA: 5-Aza-2-deoxycytidine

Bad: Bcl-2 antagonist of cell death

Bak: Bcl-2 antagonist killer 1

Bax: Bcl-2 associated x protein

Bcl-2: B-cell lymphoma 2

Bcl-W: Bcl-2 like 2

Bcl-xL: Bcl-2-related gene X, long isoform

BclXL/Mcl-1-OE: Overexpression of Bcl-XL and Mcl-1

Bid: BH3 interacting domain death agonist

Bik: Bcl -2 interacting killer

Bim: Bcl-2 interacting mediator of cell death

Bmf: Bcl-2-modifying factor

Bok: Bcl-2 related ovarian killer

BSA: Bovine Serum Albumin

CMPT: Camptothecin

CARD: Caspase recruitment domain

cIAP: Cellular Inhibitor of apoptosis

CRISPR: Clustered Regularly Interspaced Short Palindromic Repeats

CS: Crude saliva (*Amblyomma sculptum*)

CTX: Chlorotoxin

DAMPs: Damage-associated molecular patterns

DD: Death domain

DED: Death effector domain

DIABLO: Direct IAP binding protein with low pI

DISC: Death-inducing signaling complex

DKO: TRAIL-receptor-deficient

DR4: Death Receptor 4

DR5: Death Receptor 5

ER: Endoplasmic reticulum

FADD: Fas-Associated death domain

FAS: Death receptor CD95

FasL/CD95L: Fas ligand/CD95 ligand

FDA: Food and Drug Administration Agency (USA)

GC-MS: Gas chromatography – mass spectrometry

GSDM: Gasdermin

H^+-NMR: Proton nuclear magnetic resonance

HpaI: restriction enzyme that recognizes GTT^AAC sites

HRP: Horseradish Peroxidase

IAP: Inhibitor of apoptosis

IP3: inositol 1,4,5-trisphosphate receptor

IC: Ion exchange chromatography

JC-1: 5,5′,6,6′-tetrachloro-1,1′,3,3′-tetraethylbenzimidazolylcarbocyanine iodide

JNK: c-Jun NH2 terminal kinase

LC-3: Microtubule-associated protein 1A/1B-light chain 3

LPS: Lipopolysaccharide

MAP: Mitogen-activated protein

MAPK: Mitogen-activated protein Kinase

Mcl-1: Myeloid cell leukemia cell differentiation protein

MLKL: Mixed lineage kinase domain-like protein

MOCK: Cells transfected with plasmids without the gene of intrest – "empty plasmids"

MOMP: Mitochondria outer membrane permeabilization

MMP: Metalloproteinase

mPTP = mitochondrial permeability transition pores

mRNA: Messenger ribonucleic acid

mTORC: Mammalian target of rapamycin complex

NB: Neuroblastoma

Nec: Necrostatin-1 - RIPK1 inhibitor

NLR: NOD-like receptors

NF-kB: Nuclear factor kappa B

NOXA: Bcl-2-modifying factor

PAMPs: Pathogen Associated Molecular Patterns

PBS: Phosphate Buffer Saline

PCD: Programmed Cell Death

PEI: Polyethyleneimine

PI3K PhosphatidylInositol-3-Kinase

pVSV-G: Vesicular stomatitis virus expressing G glycoprotein

PUMA: Bcl-2-modifying factor

QVD: Q-V-D-Oph pan-caspase inhibitor

RIP: Receptor-interacting serine/threonine-protein

RIPK1: Receptor-interacting serine/threonine-protein kinase 1

ProtK: Proteinase K

PRR: Pathogen recognition receptors

rBCL-XL: Recombinant BCL-XL

rMcl-1: Recombinant Mcl-1

SHED: Stem cells from human exfoliated deciduous teeth

SL10: 10% of *Amblyomma sculptum*'s crude saliva

SMAC: Second mitochondrial activator of caspase

svMP: Snake Venom Metalloproteinase

svLAAO: Snake Venom L-amino acid oxidase

SVV: Survivin

tBid: Truncated Bid

TLR: Toll-like receptor

TNF: Tumor necrosis factor

TRADD: TNF-associated death domain protein

TRAIL-R1/DR4: TRAIL receptor 1/Death Receptor 4

TRAIL-R2/DR5: TRAIL receptor 2/Death Receptor 5

TRAIL: TNF-related apoptosis-inducing ligand

ULK: unc-51 like autophagy activating kinase

VEGF: Vascular endothelial growth factor

XIAP: X-linked inhibitor of apoptosis protein

<3 kDa: 10% of *A. sculptum*'s saliva fraction with molecules smaller than 3 kDa

<10 kDa: 10% of *A. sculptum*'s saliva fraction with molecules smaller than 10 kDa

ABSTRACT

Animal secretions are promising sources of bioactive molecules. Previous works have demonstrated that the crude saliva of *Amblyomma sculptum (Fabricius, 1787)* show cytotoxic effects on different tumor cell lines, with no cytotoxicity in non-tumoral cells; however, little is known about the mechanisms involved. Here, we investigate the CS effect on the activation of programmed cell death pathways in tumoral cell lines. CS was collected using microcapillary tubes after dopamine stimulation in the tick salivary gland. Neuroblastoma (SH-SY5Y, SK-N-SH, CHLA-20, and Be(2)M17) lineages were treated *in vitro* with 10% of the crude saliva (SL10) or its derived fractions for 72 hours. Protein content profiles by western blot showed that neuroblastoma lineages have low levels of initiating caspases and death receptors. Caspase-8 level was recovered with 5-Aza-2-deoxycytidine demethylating agent, but it did not affect SL10 induced cell death. The RIPK1 inhibitor Necrostatin-1 did not affect the SL10 induced cell death either, while the pan-caspase-inhibitor Q-VD-Oph significantly reduced cell death. Cells overexpressing Bcl-XL and Mcl-1 were generated to evaluate the role of anti-apoptotic proteins and the mitochondrial outer membrane potential status. Apoptosis was prevented in the generated cell lines, as demonstrated by the absence in caspase-3, caspase-9, and lamin A/C cleavage, as well as the mitochondrial potential loss. Different fractionation protocols were performed by ion-exchange chromatography and molar mass fractionation. It demonstrated that the active anti apoptotic potential of the saliva from *A. sculptum* is within molecules smaller than 3 kDa. Finally, we showed by Gas Chromatography–Mass Spectrometry (GC-MS) and Nuclear Magnetic Resonance Spectroscopy (NMR) the presence of amino-acids, sugars and fatty acid methyl ester, along with side chains compatible with Ala, Leu, Val, Glutamate, Glutamine, Phenylalanine and Tyrosine, in addition to aliphatics and aromatic peptides in the low

molecular weight fraction. These represent the possible antitumor compounds present in the saliva of *A. sculptum*, responsible for the activation of intrinsic pathways of apoptosis in neuroblastoma cells.

KEY-WORDS: Tick saliva, apoptosis, neuroblastoma, bioactive molecules, antitumoral compounds.

ABSTRACT (IN PORTUGUESE)

Secreções animais são fontes promissoras de moléculas bioativas. Estudos anteriores mostraram que a saliva do carrapato Amblyomma sculptum (Fabricius, 1787) é citotóxica para diferentes linhagens tumorais, sem efeito significativo em células não tumorais. No entanto, pouco se sabe sobre os mecanismos envolvidos nessa atividade. No presente trabalho, nós investigamos o efeito da saliva na ativação das vias de morte celular programada em diferentes linhagens tumorais. A saliva bruta foi coletada em tubos microcapilares após estimulação das glândulas salivares do carrapato com dopamina. Linhagens tumorais de tumor de mama (MDA-MB-231), adenocarcinoma colorretal (HCT-116) e linhagens de neuroblastoma (SH-SY5Y, SK-N-SH e Be(2)-M17) foram tratadas com 10% da saliva bruta (SL10) e frações derivadas dela por 72 horas. Células de neuroblastoma demonstraram a maior susceptibilidade aos efeitos citotóxicos da saliva e o perfil proteico analisado por western-blotting mostrou que estas células têm baixos níveis de caspases iniciadoras e receptores de morte. A recuperação dos níveis de caspase-8 induzida pelo agente desmetilante 5-Aza-2-desoxicitidina (AZA), no entanto, não afetou a morte celular induzida por SL10. O inibidor de RIPK1 Necrostatina-1 também não afetou a morte celular induzida por SL10, enquanto o inibidor de pan-caspase Q-VD-Oph foi capaz de proteger totalmente as células de neuroblastoma contra a morte celular induzida pela saliva. Células de neuroblastoma superexpressando Bcl-XL e Mcl-1 foram geradas e tal superexpressão inibiu a apoptose e perda de potencial mitocondrial induzida pela saliva. Além disso, a clivagem de caspase-3, lamina A/C e caspase-9 foram detectadas apenas nas linhagens sem superexpressão de Mcl-1 e Bcl-XL. A saliva bruta foi fracionada por cromatografia de troca iônica e por filtração. Estas permitiram demonstrar que a atividade pró-apoptótica da saliva de A. sculptum está em moléculas menores que 3 kDa. Por fim, nós evidenciamos por

Cromatografia Gasosa–Espectrometria de Massa (CG-MS) e Espectroscopia de Ressonância Magnética Nuclear (RMN) a presença de cadeias laterais compatíveis com Ala, Leu, Val, Glutamato, Glutamina, Fenilalanina e Tirosina, além de peptídeos alifáticos e aromáticos na fração <3 kDa. Estes representam os possíveis compostos antitumorais presentes na saliva de *A. sculptum*, responsáveis pela ativação de vias intrínsecas de apoptose em células de neuroblastoma.

PALAVRAS-CHAVE: Saliva-de-carrapato, apoptose, neuroblastoma, moléculas bioativas, compostos antitumorais.

FACT SHEET

Animal secretions are promising sources of molecules with therapeutic potential. The crude saliva (CS) from the tick *Amblyomma sculptum*, popularly known as Star Tick, has demonstrated anti-tumoral effects on different cancer cell types without affecting non-tumoral healthy cells. However, little is known about the cellular mechanisms involved in such activity. Here, we investigate how such salivary secretion selectively induces tumor cells to death, in a "controlled" manner. CS was collected by collaborators from the Butantan Institute and the cancer cells were then treated *in vitro* with 10% of the CS, or its fractions, for up to 72 hours. After that, different approaches were used to evaluate different cellular death mechanisms in those cells. Our results showed that molecules found within the SL induced mitochondria-dependent cell death in tumor cells. What was controlled by the activation of enzymes called "caspases", known for controlling cell death mechanisms. Those anti-tumoral molecules are very small and highly stable, desirable characteristics for the development of new therapeutic drugs. Hereafter, new analyses are in progress to characterize such molecules and extend our findings to additional conventional chemotherapeutic drug development.

FACT SHEET (IN PORTUGUESE)

Secreções animais são fontes promissoras de moléculas com potencial terapêutico. A saliva bruta (CS) do carrapato *Amblyomma sculptum*, popularmente conhecido como Carrapato Estrela, demonstrou efeitos antitumorais em diferentes tipos de células cancerígenas, sem afetar as células saudáveis. No entanto, pouco se sabe sobre os mecanismos celulares envolvidos nessa atividade. Investigamos pela primeira vez como essa secreção salivar induz seletivamente as células tumorais à morte, de forma "controlada". A CS foi coletada por colaboradores do Instituto Butantan e as células tumorais foram então tratadas *in vitro* com 10% da CS, ou suas frações, por até 72 horas. Depois disso, diferentes abordagens foram utilizadas para avaliar os diferentes mecanismos de morte celular nessas células. Nossos resultados mostraram que moléculas encontradas na SL induzem morte mitocôndria-dependente em células tumorais. Tal atividade é controlada pela ativação de enzimas chamadas "caspases", conhecidas por controlar os mecanismos de morte celular programada. Essas moléculas antitumorais da saliva são muito pequenas e altamente estáveis, características desejáveis para o desenvolvimento de novos fármacos com ação terapêutica. Futuramente, novas análises serão realizadas para caracterizar tais moléculas e estender nossas descobertas ao desenvolvimento de novas drogas quimioterápicas.

1. INTRODUCTION

Neuroblastoma (NB) is an extracranial tumor associated with the development of the sympathetic nervous system and the adrenal medulla [1]. It is the most frequent solid tumor in children and comprehends 8 to 10% of all pediatric cancers [2]. According to the American Cancer Society, NB prognostic factors range from clinical factors such as tumor stage and the patient's age at diagnosis to biological features such as histology and cytogenetic factors. Based on accurate diagnosis and prognosis, treatment may include observation, chemotherapy, surgical resection, myeloablative chemotherapy with autologous stem cell transplantation, radiation therapy, differentiating treatment with 13-cis-retinoic acid, and immunotherapy. Most of those basically aim at inducing programmed cell death (PCD) in cancer cells [3].

PCD has been long described as one of the main strategies to improve clinical cancer treatment. It is a fundamental process that maintains tissue homeostasis, removes damaged cells and ensures the recycling of cellular constituents [4]. However, the development of cell death resistance by certain types of tumors opens the need for new molecules capable of bypassing the resistance developed by cancer cells. Some promising sources of biologically active molecules capable of inducing the activation of different cell death pathways include animal secretions. It was estimated that about 40% of all available anticancer drugs were developed from natural sources, such as plants, microorganisms, and animals [5]. Among arthropods, ticks are just starting to be investigated regarding bioactive components within their salivary secretion with antitumoral activities [6].

The tick *Amblyomma sculptum*, previously named *A. cajennense* (Fabricius, 1787), is one of the most widespread species in South America [8]. Although the composition of the

A. sculptum's saliva has been partially described by neutron activation analysis (NAA) [9] and Tandem mass spectrometry (MS/MS) [10], there are few reports on the pharmacological properties and therapeutical potential of its compounds. Cytotoxic effects of the crude saliva have been demonstrated on melanoma cells (SK-MEL-28) and pancreatic adenocarcinoma cells (MIA PaCa-2), with no cytotoxicity in non-tumoral human fibroblasts [11]. Similarly, Sousa and colleagues[12] demonstrated the induction of apoptosis in breast cancer cell lines (MDA-MB-123 and MCF-7), but not in the non-tumor breast lineage MCF-10A. Data obtained recently by our research group demonstrated that *A. sculptum* saliva has high cytotoxicity and anti-proliferative effect, involving cell cycle arrest and cytoskeleton rearrangement in cells derived from leukemia (U937) and neuroblastoma (IMR-32 and CHLA-20) [13].

Therefore, the saliva from the tick *A. sculptum* may be an example of the potential pharmaceutical application of natural sources, affecting tumors such as neuroblastoma, often resistant to conventional chemotherapy. The findings gathered here during my thesis show that *A. sculptum* saliva contains small compounds that activates the intrinsic apoptosis pathway through the loss of mitochondrial outer membrane potential and caspases cleavage. Apoptosis is a complex process involving many molecules, organelles and processes regulated by the balance between anti- and pro-apoptotic proteins. These mechanisms are detailed in this work highlighting the way by which *A. sculptum* saliva may be affecting the fate of neuroblastoma cells.

2. JUSTIFICATION

Resistance to cell death is an early hallmark of developing cancer, therefore the specific induction of cell death has been proposed as the primary strategy to improve clinical treatment in malignant neoplasms. Programmed cell death involves many molecules, organelles, and processes regulated by different intracellular pathways, carefully regulated by the balance between anti- and pro-apoptotic proteins, and other signaling pathways that exert mutual regulation, promoting or inhibiting cell death according to the conditions in which the cells are found.

Although other targeting strategies such as biological or immune-modulating therapies are improving fast and resulting in promising outcomes, their combination with cell death-inducing drugs generally enhances their efficiency. Especially for tumors such as neuroblastoma that are not significantly associated with somatic mutations, cell-death inducing drugs with selectivity for cancer cells are among the most promising strategies. However, the development of resistance to the existing drugs available by certain types of tumors opens a need to search for new molecules capable of bypassing the resistance developed by cancer cells.

Venoms and other animal secretions are rich sources of bioactive compounds, mainly peptides. They interfere with cellular pathways such as programmed cell death, proliferation, cell cycle, immune activation, adhesion, cytoskeleton organization, and organelle function. The complete understanding of how those toxins trigger cell death pathways in cancer cells and if their use is safe is fundamental to the development of new drugs. Thousands of toxins were identified by modern science, and some are already being applied as therapeutic drugs.

However, few have gone on to clinical exploitation due to a lack of description of their mechanisms of action.

The crude saliva from the tick *Amblyomma sculptum* has proven to be an example of the potential of pharmaceutical application of Brazilian biodiversity; as it refers to a mixture of biologically active compounds that have been shown to selectively affect viability of cancer cells, inhibiting their proliferation, migration, and angiogenesis of endothelial cells. However, the specific mechanisms by which it selectively affects cancer cells have never been fully elucidated. Therefore, this investigation has significant potential for innovation and the screening of new drugs, looking for favoring patients that may benefit from our findings.

3. BIBLIOGRAPHICAL REVIEW

3.1. Cancer

Cancer represents one of the most challenging public health problems in the world and one of the main causes of early death in most countries. According to the International Agency for Research on Cancer, an estimated 19.3 million incidence and almost 10.0 million deaths occurred worldwide by 2020 [14]. In Brazil, it was estimated over 600 thousand new cases of cancer between 2020 and 2022. Of those, over 8.000 cases occurred in infants with up to one year old [15]. Pediatric cancer mainly includes leukemias, brain cancers, lymphomas, and solid tumors, such as neuroblastoma and Wilms tumors [17].

The term "cancer" is given to a collection of related diseases, classically defined as when abnormal cells grow uncontrollably and spread into surrounding tissues [18]. During carcinogenesis, normal cells accumulate epigenetic and genetic alterations, leading to activation of oncogenes and inhibition of tumor suppressor genes [19]. Cancer transformation induces the development of capabilities during the multistep tumorigenesis, called the Hallmarks of Cancer, including sustaining proliferative signaling, evading growth suppressors, resisting cell death, enabling replicative immortality, inducing angiogenesis, activating invasion and metastasis, reprogramming of energy metabolism, and evading immune destruction [20]. Cancer therapy strategies capable of overcoming those cell capabilities can be challenging [21]. Among those, chemotherapy is the most used treatment for most cancers, and essentially aims inducing programmed cell death in tumor cells [22].

3.2. Neuroblastoma

Neuroblastoma (NB) is the most frequent solid tumor in infants up to one year old and comprehends 8 to 10% of all pediatric cancers [2]. In Brazil, there is an estimative of about 7% incidence over the total number of childhood tumors, although NB-specific statistics are difficult to be evaluated in Brazil due to the lack of specific records about the disease [23]. According to the American Cancer Society, in children aged 18 months or older, it is often expressed as an unresectable or metastatic tumor that requires intensive multimodal therapy and is associated with survival rates below 50% [24]. Metastases are present in about 50% of patients at diagnosis, with bone marrow corresponding to 80% of cases, along with metastasis in bones, regional lymph nodes, and occasionally in the central nervous system or lungs [25].

NB is a cancer from immature nerve cells, that arise around the adrenal glands. It is considered a development disorder, as it originates from cells derived from the neural crest, likely Schwann Cell Precursor (SCP) cells [26,27]. During a normal embryonic development, the SCP cells are progenitors of sympathoadrenal cells that differentiate to sympathetic ganglion and adrenal catecholamine-secreting chromaffin cells. But during the establishment of a NB tumor, such differentiation processes are not properly completed [28].

Different stages of differentiation reflect on the heterogeneity of tumors, composed of distinct cellular phenotypes. Mesenchymal (MES) and adrenergic (ADR) phenotype populations were described in primary tumors by transcriptional and phenotypic analysis [29,30]. MES was associated with the presence of fewer tumorigenic cells and higher sensitivity to chemotherapy, but also higher senescence and metastasis, while ADR phenotypes are more proliferating and resistant to treatment. *In vitro*, ADR phenotypes are

28

known as N-type cells and MES as S-type cells as they resemble Schwann cells. A third population is described *in vitro* as I-type cells, that resemble cancer stem cells, and can transdifferentiate between N-type and S-type cells [26]. Cells with different phenotypes have distinct tumorigenic properties and it has been shown that the poorly differentiated or undifferentiated histology is associated with the worst prognosis [31,32].

As a heterogeneous disease, prognosis is based on clinical factors such as tumor stage and the patient's age at diagnosis, biological features of the tumor such as histology and DNA index or ploidy, cytogenetic factors, including amplification of the proto-oncogene *MYCN*, neurotrophin receptors index, and chromosomal alterations [33]. The International Neuroblastoma Staging System (INSS) classifies tumors into six categories according to the patient's age and clinical presentation, including surgical excision, lymph node involvement and metastatic sites [34] (figure 1). Stages 3 and 4 are considered the high-risk groups, which are metastatic and often refractory to conventional chemotherapy or resistant to secondary treatment [35]. As the INSS was intended for postsurgical staging, patients with localized disease, not undergoing surgery, could not be properly staged. Therefore, in 2009, the International Neuroblastoma Risk Group Staging System (INRGSS) was published as a new way to stratify patients before surgical intervention, based on clinical criteria and image-defined risk factors, not including surgical results or tumor spread to lymph nodes [36]. This system is now used in parallel with INSS (figure 1).

International Neuroblastoma Staging System (INSS)		International Neuroblastoma Risk Group Staging System (INRGSS)	
Stage	Definition	Stage	Definition
1	Localized tumor with complete gross excision, with or without microscopic residual disease; ipsilateral lymph nodes negative for tumor microscopically.	L1	Localized tumor not involving vital structures as defined by the list of image-defined risk factors and confined to one body compartment.
2A	Localized tumor with incomplete gross excision; nonadherent ipsilateral lymph nodes negative for tumor microscopically.	L2	Localized tumor with the presence of one or more image-defined risk factors (IDRFs).
2B	Localized tumor with or without complete gross excision; with ipsilateral nonadherent lymph nodes positive for tumor.	M	Metastatic disease (except stage MS).
3	Unresectable unilateral tumor infiltrating across the midline, with or without regional lymph node involvement; localized unilateral tumor with contralateral regional lymph node involvement; or midline tumor with bilateral extension by infiltration or by lymph node involvement.	MS	Metastatic disease in children younger than 18 months of age at diagnosis with metastases limited to the skin, liver, and/or bone marrow.
4	Any primary tumor with dissemination to distant lymph nodes, bone, bone marrow, liver, skin and/or other organs (except as defined for stage 4S).		
4S	Localized primary tumor (as defined for stage 1, 2A or 2B), with dissemination limited to skin, liver, and/or bone marrow (limited to infants).		

Figure 1-Neuroblastoma staging systems. Adapted from Whittle, S. B 2017 [37].

Treatment for NB is based on accurate diagnosis and prognostication, with treatment strategies based on known risk factors. Children with low- and intermediate-risk neuroblastoma show over 90% long-term event-free survival rates to less than 50% for those with the high-risk disease [37]. For the low and intermediate risk patients, treatment strategies include observation alone, surgical resection or moderate doses of chemotherapy with surgical resections [38]. Treatment of patients with high-risk and relapsed NB, on the other hand, remains a challenge. It requires intensive multimodality treatment that may include (1) induction chemotherapy, to reduce the primary and metastatic tumors and facilitate successful surgery; (2) surgical resection, a complete excision of the primary tumor; (3) high-dose chemotherapy with autologous stem cell rescue; (4) radiation therapy, (5) maintenance

treatment with 13-cis-retinoic, a differentiation inducing drug, and (6) immunotherapy [3,39]. Many chemotherapy drugs and various combinations of cyclophosphamide, doxorubicin, cisplatin, carboplatin, etoposide, topotecan and vincristine have been developed in the last 20 years for high-risk NB [40]; however, so far, overall survival rates in this population did not improve significantly [41].

3.3. Programmed Cell Death (PCD)

The induction of tumor cells death has long been the main strategy to improve cancer clinical treatment. The concept of programmed cell death (PCD) is applied to any pathological event mediated by an intracellular programmed mechanism and it is a fundamental process that maintains tissue homeostasis, removes unwanted or damaged cells, and ensures the recycling of cellular constituents [4].

According to the latest recommendations of the Nomenclature Committee on Cell Death, PCD can be divided into three major groups: (1) type I cell death or apoptosis, which shows cytoplasmic shrinkage, chromatin condensation, nuclear fragmentation and plasma membrane blebbing, leading to the formation of apoptotic bodies, that are efficiently degraded within lysosomes after phagocytic uptake; (2) type II cell death or autophagy, an extensive cytoplasmic vacuolization that also leads to phagocytic uptake and consequent lysosomal degradation; and (3) type III cell death or necrosis, which do not involve phagocytic and lysosomal degradation of cell corpses [42].

3.3.1. Apoptosis

The term apoptosis was first presented to describe the morphological processes leading to ordered cellular self-destruction [43]. It is the most investigated, selective, and controlled

cell process, being involved in cell development, differentiation, normal cell turnover and, most importantly, the removal of damaged/stressed or harmful cells in a genetically determined manner [44]. Apoptosis represents the major type of cell death that occurs when DNA damage is irreparable and involves the activation of proteolytic cascade mediated by caspases.

Caspases are a family of conserved proteases known for their role in controlling cell death and inflammation. They are characterized for a cysteine residue in their active site and an unusual specificity for aspartic acid residues. When active, caspases are composed by an amino-terminal domain, followed by large and small catalytic subunits that form the protease domain [45]. Initiator caspases initiate the apoptosis signal while the executioner caspases carry out the massive proteolysis that leads to apoptosis. A caspase recruitment domain (CARD) or a death effector domain (DEC) are present in initiator caspases, promoting their recruitment and activation in multiprotein complexes (figure 2). The initiator caspases can be activated by dimerization and directly binding to other molecules in the cell. The executioner caspases on the other hand, have an extended amino-terminal pro-domain and require cleavage by initiator caspases for their activation, which occurs when the large and small subunits are separated [45,46]. Caspases-2, -8, -9 and -10 are initiator caspases, while caspases-3, -6 and -7 are executioner caspases. Caspases -1, -4, -5, and -12, are human proteases associated to inflammation control, and eventually linked to inflammation-induced apoptosis [45]. However, those and many new caspases are still under investigation, such as caspase-14 and other variations of caspase-12.
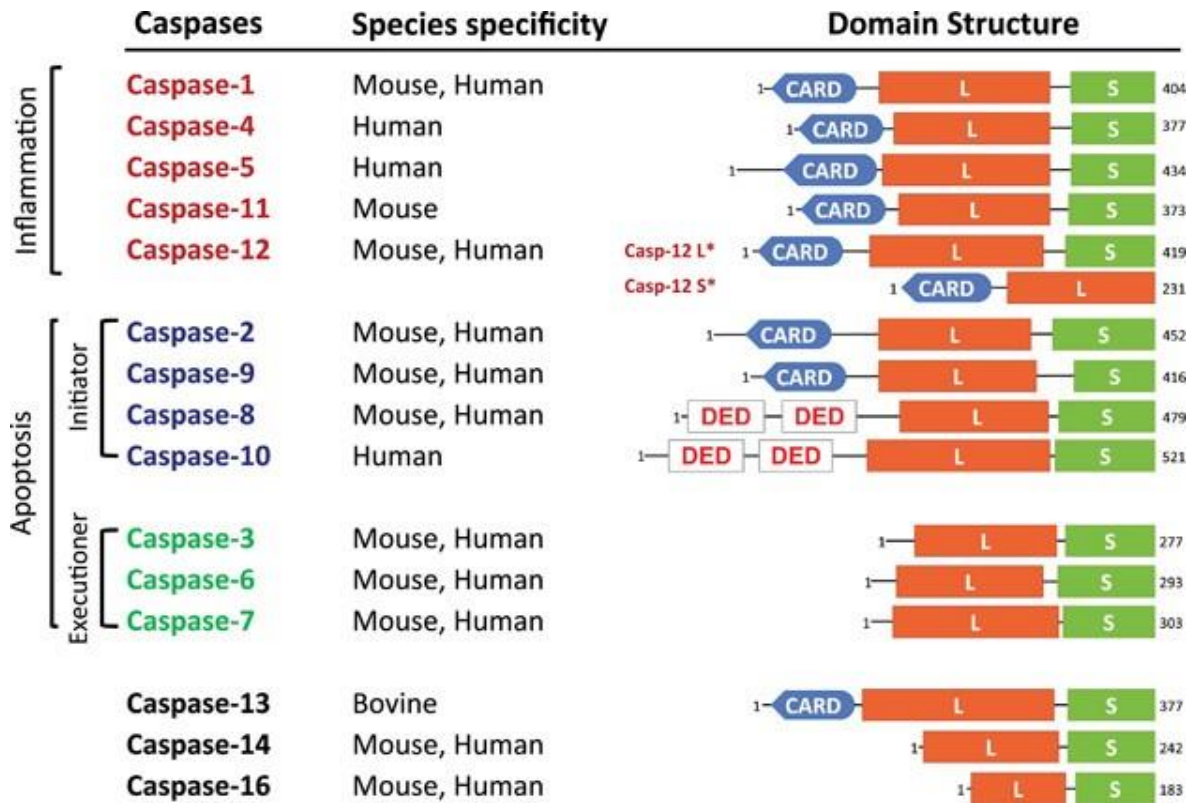
Figure 2 – Caspases domains and specificities.

Caspase-mediated cleavage is not exclusive for apoptotic pathways, as it has been described to be associated to differentiation of myeloid cells [47,48]. Although, their main role is associated and essential during apoptotic cell death, which can be specifically regulated by two different signaling pathways: the intrinsic or mitochondrial pathway and the extrinsic or death receptor pathway (figure 3) [4]. The extrinsic pathway is triggered, as its name implies, when death ligands bind to death receptors in the cellular surface. Although several death receptors have been described, the best known are the type 1 TNF receptor (TNFR1), Fas (CD95), and TRAIL receptors (DR4 and DR5), that bind to their respective ligands, TNF-α, Fas ligand (FasL) and TRAIL ligand. When ligands activate receptors at the cell surface, receptor intracellular domains recruit adapter proteins, such as TNF receptor-associated death domain (TRADD) or Fas-associated death domain (FADD) [49]. The

adapter proteins then recruit and interact with the initiator pro-caspase-8 or pro-caspase-10, forming the death-inducing signaling complex (DISC). Although, there are a few singularities with TNFR1 activation, as it mediates apoptosis in two sequential signaling complexes, what is well described by Micheau and Tschopp 2003 [50]. When DISC formation is succeeded by the activation of any death receptor pathway, the initiating caspases are activated, starting the cascade by cleaving other downstream proteins and executioner caspases [51,52].

In contrast, the intrinsic pathway of apoptosis is induced by several factors, such as cellular stress inducers (such as hypoxia, oxidative stress or high concentrations of cytosolic Ca2+), irreparable genetic damage or deprivation of growth factors [42]. But regardless of the initial stimulus, all those initiating factors generate the permeabilization of the mitochondrial outer membrane throughout the activation of Bcl-2 family of pro-apoptotic proteins, such as Bax and Bak [53]. In healthy mitochondria, cations are accumulated due to a strong transmembrane negative potential formed during normal oxidative metabolism. However, apoptotic inducing factors that regulate the opening of mitochondrial membrane pores lead to an electrochemical potential collapse, in which ions, proteins and metabolites are released from the mitochondria, along with mitochondrion loss of function [54].

The mitochondrial permeabilization, therefore, leads to the release of pro-apoptotic molecules into the cytoplasm, such as cytochrome C. Cytochrome-C is a heme protein normally located at the external face of the inner mitochondrion membrane, where it works as an electron transporter at the electron transport chain [54]. But when in the cytoplasm, cytochrome-C binds to the **a**poptotic protease activating factor-1 (APAF-1), which recruits the pro-caspase-9 and forms a complex called apoptosome [4,55]. Consequently, caspase-9 is cleaved and activated, followed by the cleavage of downstream executioner caspases.

34
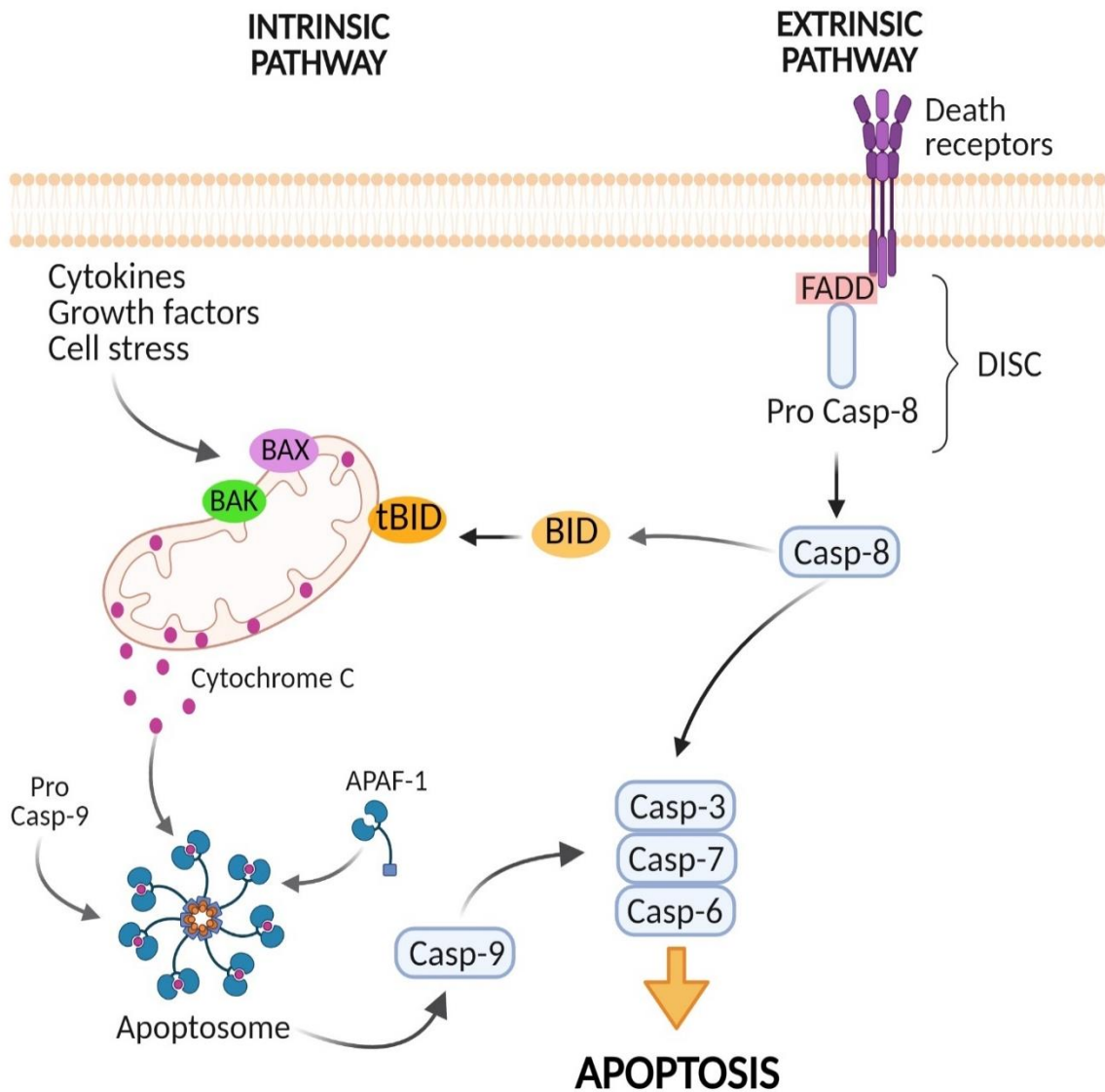
Figure 3 – Apoptotic signaling - Intrinsic and extrinsic pathways.

The extrinsic pathway might also activate the intrinsic mechanisms, which is mainly coordinated by the pro-apoptotic Bid protein. This protein is one of the targets downstream of caspase-8, which phosphorylates Bid and generates its truncated form (tBid), promoting mitochondrial potential loss and permeabilization by activation of Bax and Bak [56]. These are pro-apoptotic proteins members of the BCL-2 family, responsible for coordinating the formation of pores in mitochondrial outer membrane [57].

When any of the apoptotic pathways is triggered and the executioner caspases are activated, they start to cleave essential nuclear components that maintain cell function and viability, such as lamins, DNA fragmentation factor 45 (DFF45), poly-ADP-ribose polymerase (PARP-1), α-Fodrin (Asp1185), among others, leading to DNA fragmentation, nuclear disintegration and condensation of chromatin [58]. PARP-1 is associated to the regulation of membrane structures, cell viability, cell division and the actin cytoskeleton, and is possibly the best characterized proteolytic substrate of executioner caspases [59]. Caspase-3 and caspase-7 are the primarily responsible for PARP-1 cleavage during apoptosis. Although, other caspases, including caspases-2, -4, -6, -8, -9 and -10, can also cleave PARP when at high concentrations [60]. Lamins, major structural proteins of the nuclear envelope, on the other hand, are primarily cleaved by caspase-6 and caspase-3, that become activated both by the intrinsic and extrinsic pathway of apoptosis, also leading to nuclear and cellular damage [61]. Thus, as the executioner caspases start to act, the apoptotic cells then start to shrink and develop membrane blebbing, forming vesicles that are known as apoptotic bodies. These are then rapidly phagocytosed by macrophages and efficiently degraded within their lysosomes [53]. Therefore, the biochemical and morphological changes associated with apoptosis are dependent on the activation of the executioner caspases, which is considered a decision switch between life and death for both normal and cancer cells.

3.3.1.1 BCL-2 PROTEIN FAMILY

Proteins of the Bcl-2 family are known as regulators of apoptosis, as they control cell death primarily by direct binding interactions that regulate mitochondrial outer membrane permeabilization (MOMP) [57]. This protein family is represented by both pro and

antiapoptotic members. Antiapoptotic proteins are often exploited by tumor cells to avoid their death, thus playing an important role in carcinogenesis and in acquisition of resistance to various therapeutic agents. On the other hand, proapoptotic proteins are often down regulated in tumor cells, as they would act in the activation of intrinsic apoptotic pathways [62].
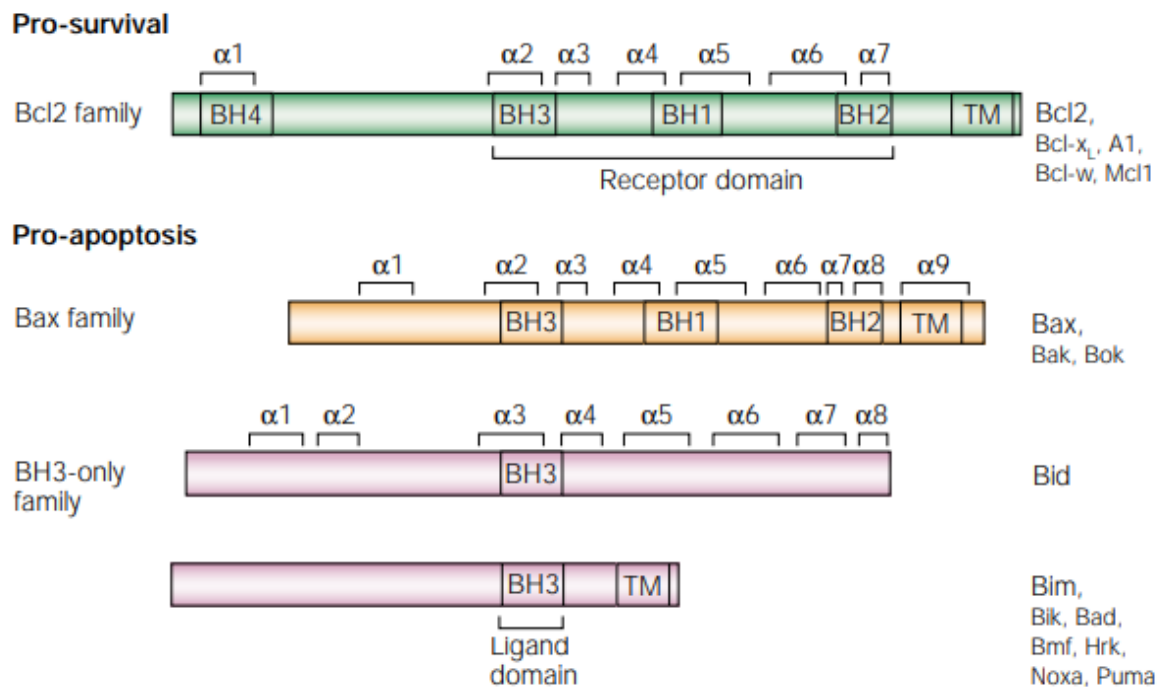
Figure 4 – Subfamilies of Bcl-2 proteins. Adapted from Cory, S. & Adams, J. M, 2002 [63].

Proteins of this family have homologue regions known as BH domains (figure 4). The family is divided in three groups. The first, comprises the anti-apoptotic proteins that contain 4 BH domains and include Bcl-2, Bcl-XL, Mcl-1 and Bcl-W, which interact and inhibit pro-apoptotic proteins. The second group comprehends pro-apoptotic proteins with 3 BH domains, including Bax, Bak and Bok, responsible for mitochondrial permeabilization regulation as they form pores into the mitochondrial outer membrane. Finally, the third group (BH3-only) are also composed by pro-apoptotic proteins, but by those that contain only one

BH domain and include Bid, Bim, Puma, Noxa, Bad, Bmf, Hrk and Bik; being responsible for initiating apoptotic signals and controlling mitochondrial membrane permeability by interacting and activating Bax, Bak and Bok, or also by inhibiting anti-apoptotic proteins. [57,63].

3.3.1.2   ENDOPLASMIC RETICULUM INDUCED INTRINSIC APOPTOSIS

Stress of the endoplasmic reticulum (ER) can also trigger intrinsic apoptosis mediated by MOMP [64]. ER is a eukaryotic cell organelle responsible for protein synthesis and calcium (Ca2+) signaling, also providing a suitable environment for lipid, steroid, and cholesterol biosynthesis [65]. Secretory and transmembrane proteins are translocated to the ER lumen to fold into their native conformation and undergo posttranslational modifications important for their activity and structure. However, extra-cellular environmental changes, such as reactive oxygen species (ROS), hypoxia, and nutrients deprivation could induce disturbance in cellular redox regulation of ER, leading to an imbalance in homeostasis and consequent accumulation of unfolded proteins, establishing the "ER stress" condition [64]. To keep a protein control, the unfolded protein response (UPR) system is needed to rebalance the protein-folding homeostasis. But if cells fail to recover from ER stress, UPR switches from pro-survival to pro-apoptotic condition [66].

Three ER-localized transmembrane signal-transducers of UPR can detect accumulation of unfolded proteins and lead to ER-stress induced apoptosis: (1) the inositol-requiring enzyme (IRE-1), (2) the protein kinase RNA-like ER kinase (PERK) and (3) the activating transcription factor 6 (ATF6) (figure 5). Activated IRE-1 recruits the TNF receptor-associated factor-2 (TRAF2) and apoptosis signal-regulating kinase 1 (ASK1), leading to activation of caspase-12, phosphorylation of c-Jun-N terminal kinase (JNK) and CHOP upregulation. Consequently, leading to MOMP through activation of Bim, Bak and Bax,

inducing the release of pro-apoptotic proteins and caspase cleavage [67–69]. Activation of

PERK and ATF6, on the other hand, lead to direct up-regulation of CHOP, activating Bim,

Bak and Bax [70]. Also, ER stress generates ROS and Ca2+ release into cytosol, facilitating

the accumulation of unfolded proteins and depolarization of the inner mitochondrial

membrane [64]. Additionally, ER stress was also described to activate DR5, leading to

TRAIL induced apoptosis [71,72].
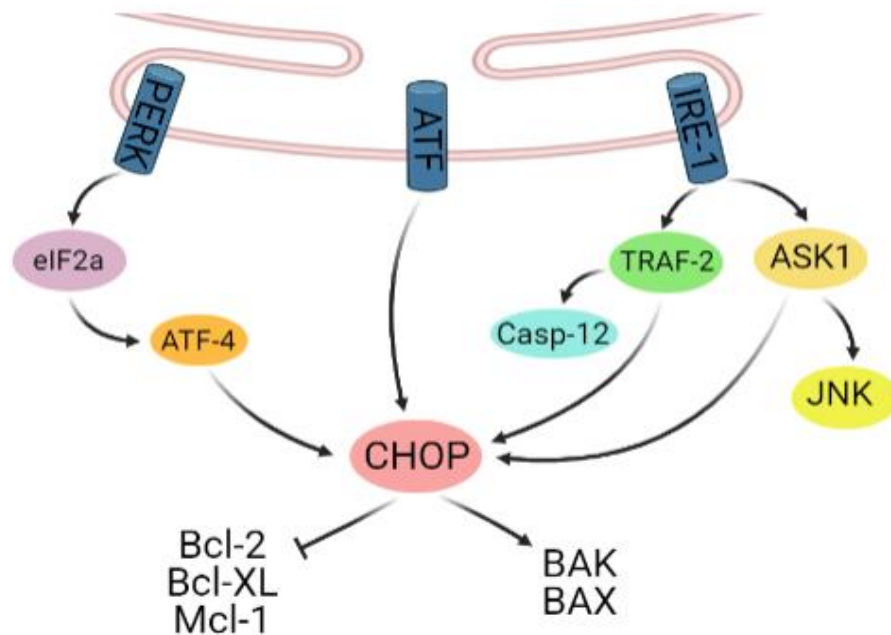
Figure 5- ER stress induction of pro-apoptotic proteins.

3.3.1.3.   JNK INDUCED INTRINSIC APOPTOSIS

Jun N-terminal kinase (JNK) is described for activating both extrinsic and intrinsic

pathways. JNK belongs to the superfamily of Mitogen Activated Protein (MAP) kinases, that

are involved in the regulation of cell proliferation, differentiation, and apoptosis [73]. The

JNK family of MAP kinases was initially identified as ultraviolet (UV)-responsive protein

kinases. Although, it has been described that it can also be activated by growth factors,

cytokines, stress factors and death receptors [74,75]. Activated JNK can be translocated to the nucleus or to the mitochondria, stimulating apoptotic pathways in many ways (figure 6).

When translocated to the nucleus, JNK phosphorylates several transcriptional factors, including JunD, ATFs, ELK, p53, RAR-α and c-Myc, but most importantly, JNK phosphorylates and transactivates c-Jun, a signal-transducing transcription factor of the AP-1 family. Which is involved in the transcription of a wide variety of proteins, including several pro-apoptotic ones, such as TNF-α, Fas-L and Bak [76,77]. JNK primarily contributes to the extrinsic pathway when activated by death receptors through AP-1 mediated increase expression of death receptor ligands and pro-apoptotic proteins [75,78]. JNK may also promote phosphorylation of Bid, which translocates to mitochondria and promotes the release of pro-apoptotic proteins, such as cytochrome-c, but also SMAC/DIABLO and OMI, mitochondrial intermembrane proteins that inhibit the anti-apoptotic protein XIAP [79,80]. When directly translocated to mitochondria, phosphorylated JNK phosphorylates the BH3-only family of Bcl2 proteins to antagonize their anti-apoptotic activity, especially thru inhibition of Bcl2 and Bcl-XL; along with phosphorylation of Bad and Bax, also leading to mitochondria membrane permeabilization [77].
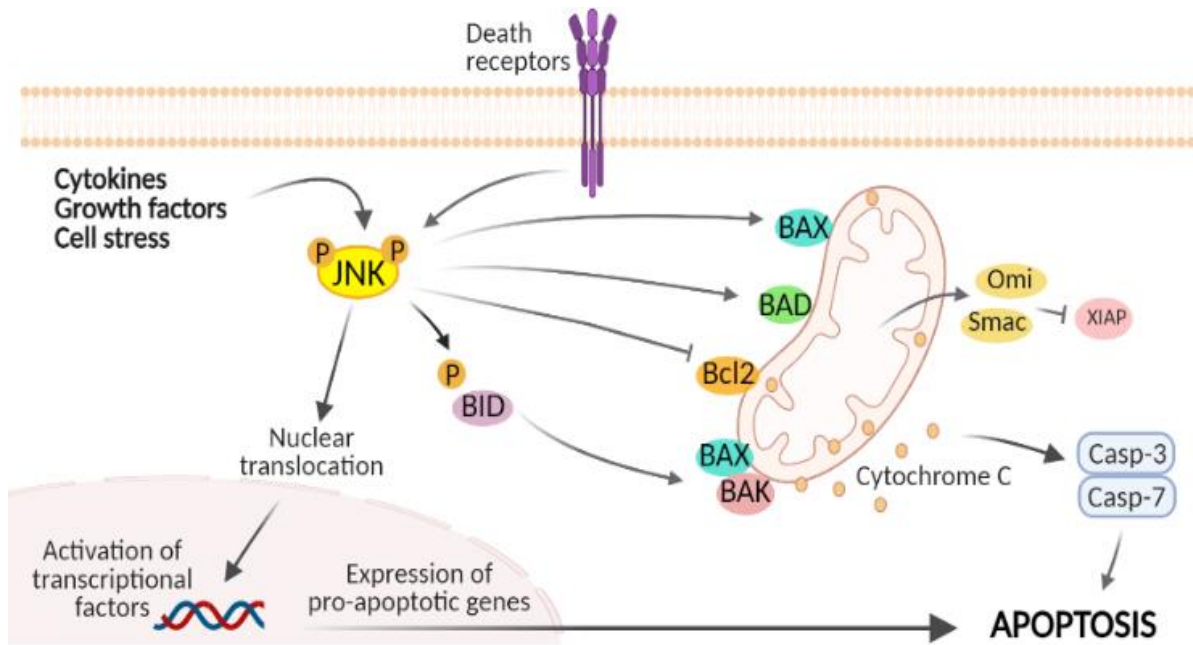
Figure 6 – JNK induced apoptosis.

3.3.1. Type-II and type-III programmed cell death pathways

Autophagy is a process of self-degradation that involves the destruction and recycling of cell constituents by lysosomal degradation, considered the type-II programmed cell death pathway [81]. In response to cellular stress, such as nutrient starvation, growth factor withdrawal and energy depletion, autophagy induces degradation and recycling of cellular components, suppling a continual source of metabolic building blocks to overcome the cellular deficiency [82]. Therefore, autophagy also plays a key role in maintenance of cell homeostasis, function, and development. In certain circumstances, however, autophagy can lead to cell death. Which mainly happens after intense autophagy induction and a failed effort to mitigate cell damage [82].

Autophagy processes are mediated by evolutionarily conserved autophagy-related genes (ATG) (figure 7). The ATG proteins encoded by these genes are responsible for controlling specific stages of autophagosome initiation and formation, as well as its

elongation, fusion to lysosomes and recycling [83]. mTORC1 and Beclin-1 are the two mains autophagy-related inducers [84]. mTORC1 interacts with ATG13, phosphorylating it and reducing its affinity with the autophagy activating kinase (ULK1), which plays a major role in autophagy initiation, phosphorylating multiple downstream factors. Therefore, stress factors induce direct or AMPK mediated inhibition of mTORC1, enabling ATG13 to interact and activate ULK1 [85]. Once activated, ULK1 complex drives the formation of the phagophore, the initial autophagosomal precursor membrane structure, through direct activation of the VPS34 (vacuolar protein sorting 34) complex and by mediating trafficking of ATG9 [86]. Beclin-1, on the other hand, is mainly upregulated by the specific targeting of mitochondria to autophagy, known as mitophagy, owing to the failure of mitochondria-depleted cells to generate energy; along with activation by cytoplasmatic ROS, ER stress, oxidative stress, or NF-kB, TNFα and JNK pathways. Beclin-1 can also be inhibited by Bcl-2 and Bcl-XL proteins [84]. Similar to mTORC1, beclin-1 induces phagophore nucleation and autophagy initiation by VSP34 activation and ATG9 recruitment. To complete autophagosome formation, a cytosolic form of the microtubule-associated protein light chain 3 (LC3-I) is recruited to autophagosomal membranes and converted to LC3-II by ATG4, along with ATG7, responsible for the activation of LC3-I and elongation of phagophore membrane [82]. LC3-II plays a key role as a receptor at the phagophore membrane and interacts with adaptor proteins present on protein aggregates and damaged mitochondria, thereby promoting their selective uptake and degradation. When the autophagosomes finally fuses with lysosomes to form autolysosomes, intra-autophagosomal components are degraded by lysosomal hydrolases, along with LC3-II and p62, considered markers for autophagy degradation [83]. Degradation and recycling of cell constituents will then provide

energy, biosynthesis, and damage mitigation, along with prevention of mitochondria damage, ER stress and inflammation.

However, cell death may result from extreme levels of autophagy activation, leading to overconsumption of cellular organelles and re-routing of cellular membrane sources to support autophagosome generation, to the point where cellular membrane homeostasis is disturbed [82]. A complex crosstalk between apoptotic and autophagic signaling pathways is also a subject of studies. Autophagic cell death has been described as a backup mechanism when apoptosis in blocked, deficient, or deregulated [87]. Caspase-8 might not only generate the truncated form of bid, but also activates beclin-1, acting in both pathways. Also, beclin-1 and ATG-4 are inhibited by anti-apoptotic proteins such as Bcl-2 and Bcl-XL, which may inhibit autophagy and enhance apoptosis under certain conditions. Upon TRAIL treatment, two autophagy proteins, ATG-7 and p62/SQSTM1, were described to be recruited to DISC and essential for TRAIL-induced Ca2+ influx and induced cell death on leukemia cells [88], which was associated to PIM kinases on glioblastoma cells [89].

On the other hand, autophagy may inhibit apoptosis by engulfing pro-apoptotic caspases, such as caspase-8, and damaged reactive mitochondria to prevent the release of cytochrome c [90]. Therefore, it is still difficult to define a single function for autophagy, as the process has different effects depending on cell stimuli and escape from apoptosis.

In cancer, it is difficult to stablish when autophagy protects survival or contributes to cell death. As a cell protective survival pathway, autophagy prevents chronic tissue damage that can lead to cancer initiation and progression, along with regulated cell death induction thru excessive activation or whenever apoptosis is blocked. On the contrary, in stablished tumors, cancer cells may upregulate basal autophagy, protecting cells from stress-inducing microenvironmental conditions such as low oxygen and nutrient deprivation, enhancing

survival in the hostile tumor microenvironment [91,92]. Therefore, as autophagy exerts its effects in multiple ways, the role of autophagy in tumorigenesis is still considered context-dependent.
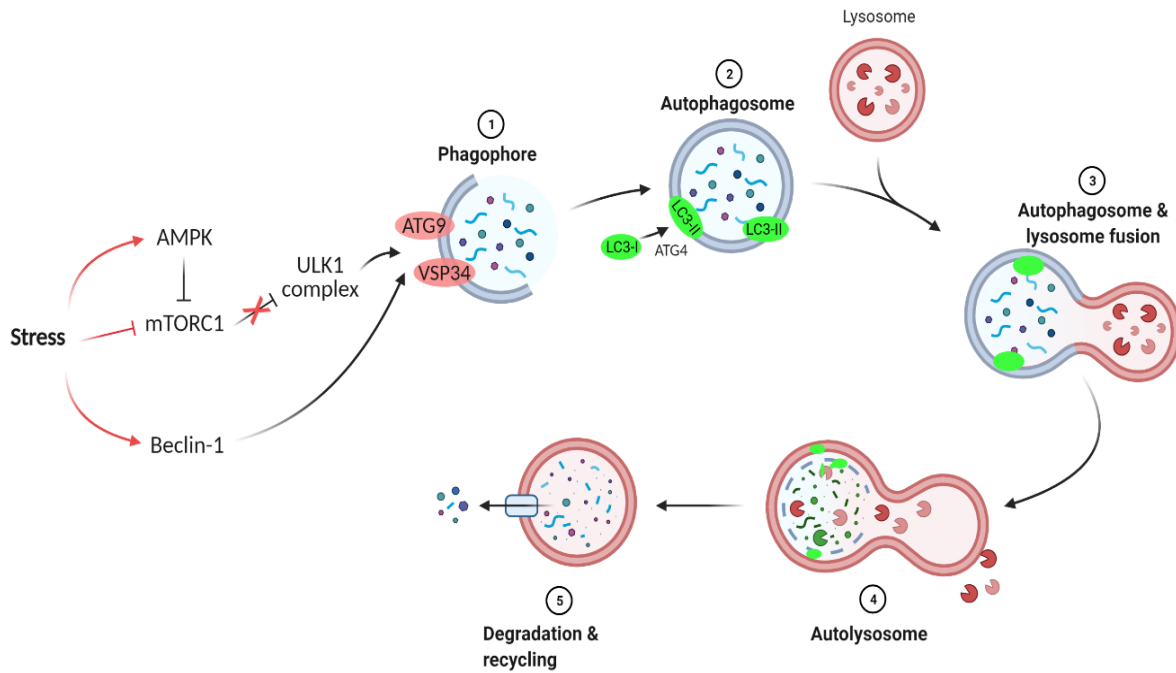
Figure 7- Autophagy pathway in mammalian cells

Besides autophagic and apoptotic cell death, another important programmed cell death pathway is programmed Necrosis, or type-III cell death, mainly consisting of Necroptosis and Pyroptosis pathways. Necrosis is basically characterized by the cytoplasmic granulation and organelle or cellular swelling that culminates in the leakage of intracellular contents from the cell. Necroptosis is a regulated cell death with such necrotic features, mainly controlled by tumor necrosis factors (TNF) [4]. Although, FAS activation was also described to induce necroptosis by activation of proteins of the receptor-interacting protein (RIP) family [93]. Necroptosis research is relatively new and was originated when small molecules termed necrostatins were shown to be able to suppress this necrotic form of cell death, previously understood as uncontrolled cell death pathway [94]. One of these molecules, necrostatin-1,

was subsequently found to inhibit receptor-interacting serine/threonine kinase 1 (RIP1), thus blocking the necrotic effect of TNF [95].

Necroptosis is activated in response to severe stress or blocked apoptosis and can be induced by inflammatory cytokines or chemotherapeutic drugs. Its activation is biochemically regulated by the activation of RIP family [96]. This family of kinases have emerged as essential sensors of cellular stress, that are associated to many different cellular pathways, such as activation of NF-kappaB and MAP kinases, but also to mediate apoptosis - by interacting with death receptors or inflammatory pathways - and necrosis [94]. Under TNF stimulation, RIP3 promotes the phosphorylation of RIP1, thus forming a necrosome complex. The mixed lineage kinase domain-like protein (MLKL) is then recruited to the complex, where it is phosphorylated and translocated to the plasma membrane, interacting with phospholipids, and compromising membrane integrity resulting in cell rupture [94]. MLKL may also promote generation of ROS and activation of JNK, leading to different cell death pathways as well [97,98]. Another crosstalk between programmed necrosis and apoptosis is the fact that RIP1 and RIP3 are inactivated by caspase-8, which leads to pro-apoptotic caspase activation cascade. But when caspase-8 is deleted, depleted, or inhibited, the ligation of TNFR1 results in necroptosis, demonstrating another possible route of programmed cell death when apoptosis is blocked [99].

Pyroptosis, on the other hand, is a caspase-1 dependent cell death pathway, which is characterized by a lytic form of cell death, triggered by various pathological stimulus and crucial for controlling infections [100]. Pathogen recognition receptors (PRR), such as Toll-like receptors (TLR), recognize pathogen associated molecular patters (PAMPs) or damage associated molecular patterns (DAMPs) and induce the assembly of associated speck-like

protein containing caspase recruitment domains (ASC), forming the complex known as inflammasome, that activates caspase-1 [101].

Once activated, caspase-1 cleaves gasdermin proteins (GSDM), pore-forming effector proteins that cause membrane permeabilization [102]. Along with GSDM cleavage, caspase-1 also activates and induces the release of cytokines such as IL-18 and IL-1β. The formation of pores, then, induces cell swelling, osmotic lysis, and chromosomal DNA cleavage by endonucleases. Differently than apoptotic pathways, however, pyroptosis does not involve effector caspase cleavage and nucleus fragmentation [100,101]. A non-canonical pathway triggered by the detection of Lipopolysaccharide (LPS), a major structural component of the outer membrane of Gram-negative bacteria, may also induce inflammatory pyroptosis thru activation of human caspase-4 and caspase-5 (or the murine homolog caspase-11), which also cleaves gasdermin proteins and induces plasmatic membrane pore formation [46]. Inflammation, therefore, may also promote programmed cell death pathways in tumoral cells, inhibiting cell proliferation, migration, and tumor growth. Thus, inflammasome factors are usually reduced in tumor cell lines and future studies towards the elucidation of pyroptosis mechanisms will contribute to the drug development targeting molecules that act as pyroptotic inflammasomes. As discussed by Kayagaki and colleagues in 2021 [103], such induced cell death is an active and well controlled event that may also be associated to several other diseases.
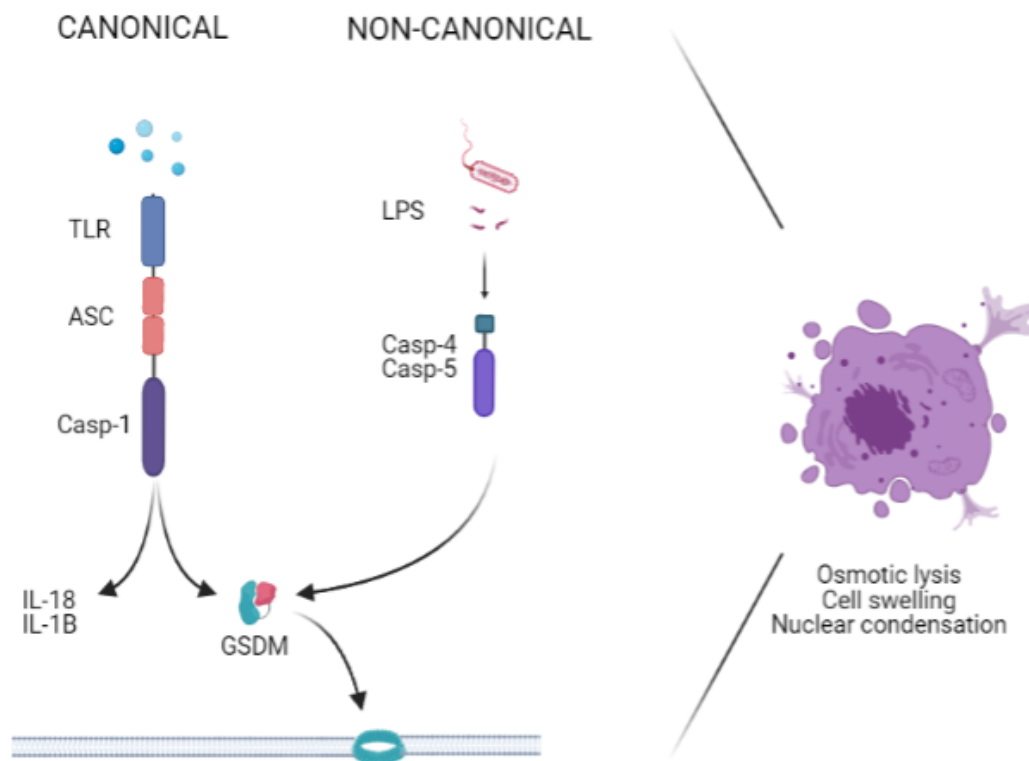
Figure 8- Canonical and non-canonical pathways of pyroptosis.

3.4. Natural compounds as new bioactive molecules sources for cancer therapy

Natural compounds from plants, microorganisms, and animal secretions are promising biologically active molecules to the development of new therapeutic drugs. In 2003, it was estimated that about 40% of the available medicines were developed from natural sources [104]. The first natural products to be described as medicine date centuries ago and include, for example, antibiotics formed in moldy soy curd, used by Chinese populations to treat infections and tetracycline antibiotics produced by *Streptomyces*, present in beer consumed by old African civilizations [105]. The anesthetic properties of opium were also well known throughout history when Friedrich Serturner, in 1804, isolated morphine from its resin. It was

first distributed only in 1817 and started to be commercialized by Heinrich Merck only in 1827, more than a century before the foundation of the modern Food and Drug Administration agency (FDA) in the United States, or the Brazilian National Health Surveillance Agency (Anvisa) [106].

More recently, due to new investments and technological advances, new drugs derived from animal secretions and isolated toxins have been developed and approved by the FDA. The observation that patients envenomated by the lethal Brazilian *Bothrops jararaca* suffered from hypotension and severe intestinal contractions led to the first animal toxin-derived drug, called Captopril, an angiotensin-converting enzyme (ACE) inhibitor that is used to treat hypertension [107]. Other examples include the pain reliever Ziconotide (commercial name: Prialt), derived from the venom of *Conus magus* cone snail and is considered over 100 times more powerful than morphine, and the glycemia regulator Exenatide (commercial name: Byetta®), obtained from the saliva of the North American lizard *Heloderma suspectum* [108]. Over half of all natural products approved by 2015 by the FDA were derived from animal sources [105].

The development of new therapeuticals from natural sources requires significant investments, not only in resources, but also in time; mainly due to the effort required to isolate and identify these therapeutical compounds. Consequently, the pharmaceutical industry has progressively moved away from natural products towards synthetic compounds [109]. However, natural products are combinations of structures and molecules selected by evolutionary pressures to interact with a wide variety of proteins and other biological targets for specific purposes, giving them a diversity and efficiency that is hardly achievable in synthetic ways [110,111].

Efforts to expand the impact of natural chemical diversity on the drug discovery process follows two main paths: (1) characterization of crude mixtures to create fractional libraries of natural compounds; and (2) combinatorial synthesis from natural products, to amplify the structural context in which the unique characteristics of natural products are expressed [109,112]. This, together with advances in genomics, metabolic engineering, and synthetic chemistry, offers new possibilities for exploring the remarkable biochemical diversity of nature's "small molecules".

Animal venoms are mixtures of cytotoxic and modulating components, selective and potent to vital physiological processes in prey animals [113–115]. Snakes and arthropods toxin-derived compounds have already been described for their highly selective toxicity on a variety of cancer cells [115,116]. Chlorotoxin, for example, is a toxin derived from scorpion venom with affinity for chloride channels, affecting ion conductance. It specifically and selectively interacts with metalloproteinase-2 (MMP-2) isoforms, which are specifically upregulated in gliomas and related cancers, but are not normally expressed in normal brain cells [117]. Crotamine is a snake venom peptide with high specificity for proliferating cells that act on cell membrane's sodium channels. It is slightly analgesic and myotoxic, as it penetrates muscles cells promoting necrosis [118]. Cardiotoxins are also derived from snake venoms, acting as membrane active proteins inducing apoptosis thru lysosomal activation pathways [119]. Similarly, Melittin is a honeybee toxin derived peptide that induces strong pore formation on tumor cell membranes, also known for causing the release of inflammatory cytokines, sodium channels blockage, growth suppression and apoptosis induction [120,121].

Animal toxins have already been studied as agents to prevent the progression of cancer [122] (figure 9). Cancer initiation was impaired by Rhodostomin, a snake-derived desintegrin, which decreases superoxide production, and by Snake Venom L-Amino Acid

Oxidases (svLAAOs) flavorenzymes that enhance caspase-8 and caspase-9 gene expression. Similarly, metalloproteinases (svMPs) and svLAAOs from snake venom and arthropod-derived toxins may impact cancer promotion by apoptosis activation or ion channel blockage. Likewise, immune-modulating, anti-proliferative, and anti-metastatic peptides and proteins, with or without catalytic activity were found in snakes, spiders, scorpions, bees, frogs, and more recently, ticks [122].
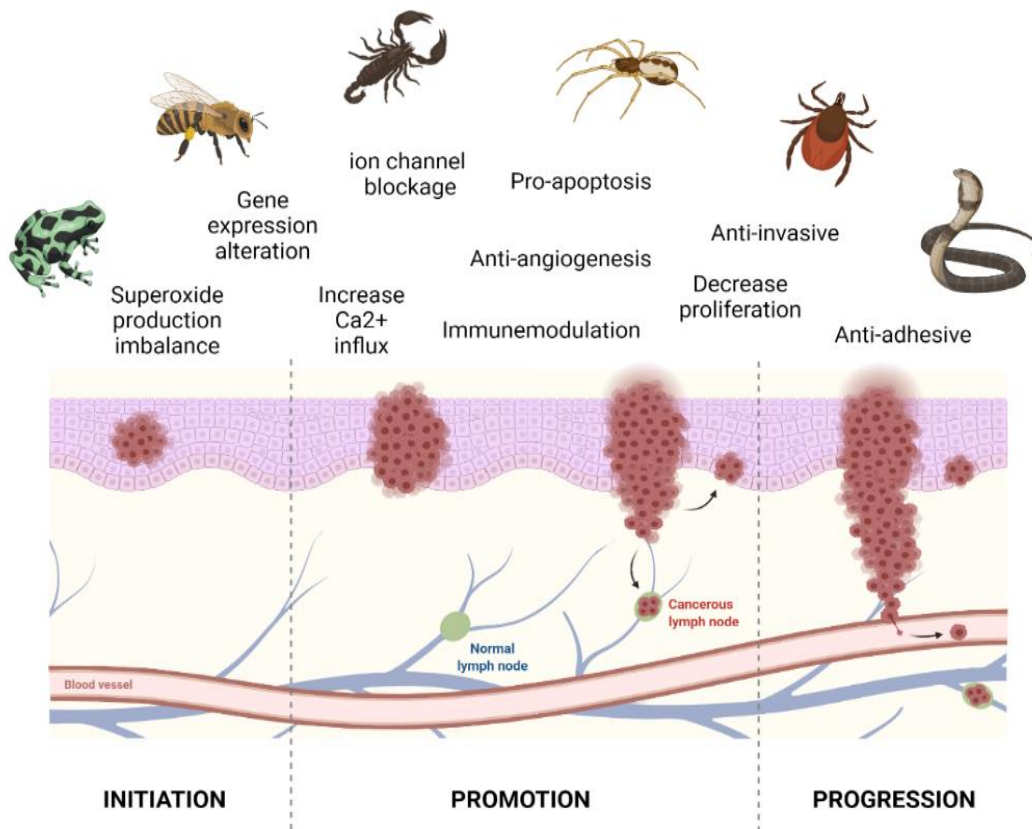
Figure 9 - Effects of animal venoms or toxins on the pathology of cancer development. Adapted from Chaisakul et al., 2016 [122].

3.5. Amblyomma sculptum

Ticks are hematophage ectoparasitic arthropods generally associated with high chances of dispersion and pathogen transmission, implicating a higher concern to global health [123].

. Ticks have four life stages (egg, larva, nymph and adulthood) and can be classified as soft ticks – *Argasidae* and hard ticks – *Ixodidae* [124], mainly differing in that hard ticks have a dorsal shield called scutum and their mouthparts are visible from above. Also, hard ticks tend to have a long attachment to the host that can last for up to 3 weeks [123].

Before blood consumption, saliva is pumped into the feeding site, starting alternate cycles of feeding and salivation [125] (figure 10). During feeding, the tick hypostome penetrates the host dermis and gets in contact with host nerve endings, blood, and lymphatic vessels, fibroblasts, dendritic cells, macrophages, mast cells, natural killer (NK) cells, T lymphocytes, along with soluble mediators such as cytokines, chemokines, and lectins that contribute to the host local and systemic immune responses [126].
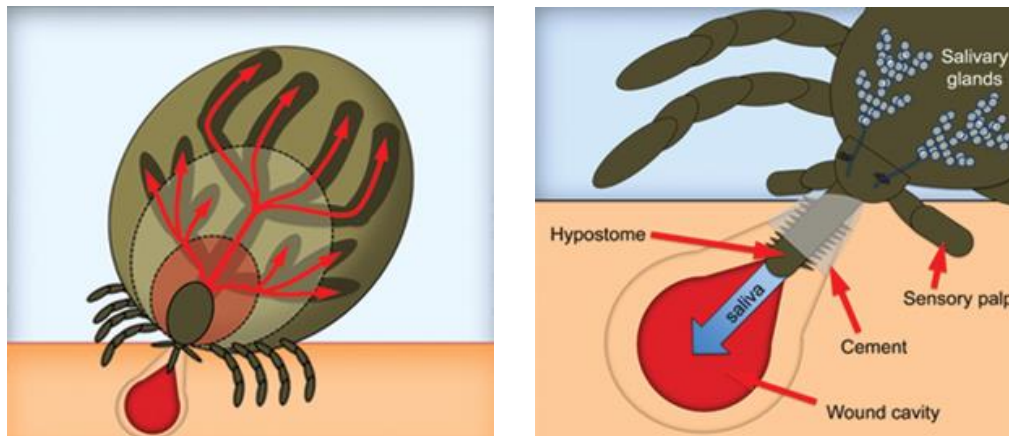
Figure 10 – Tick feeding structures and mechanisms. Adapted from Chmelar et al., 2016 [127].

As blood is the only nutritious source, adaptation to blood-feeding must include a complex cocktail of salivary components that help the parasite to overcome hosts' defenses against (1) hemostasis, which depends on the triad of blood coagulation, platelet aggregation, and vasoconstriction; (2) inflammation at the feeding site, which can produce itching or pain and, thus, initiates defensive behavior in their hosts; and (3) immunity, involving cellular and humoral responses [126,128]. Recent progress in transcriptome research has revealed that

hard ticks have hundreds of different small peptides and proteins expressed in their salivary secretion and glands, most of them still with unknown functions [128]. Currently, over 30.000 protein sequences deposited on GenBank are assigned to tick saliva or tick salivary glands. As reviewed by Nuttall P. in 2019 [129], small non-peptide or protein molecules may include endogenous nucleoside adenosine, arachidonic acid derivatives, endocannabinoids, amides, and microRNAs.

Amblyomma cajennense is a complex of hard tick species from the Americas. It includes six species, with *Amblyomma sculptum* and *Amblyomma cajennense sensu stricto (s.s.)* (Fabricius, 1787) present in Brazil [130]. *Amblyomma cajennense s.s.* is associated with the Amazon region and its equatorial climate, with no evidence of disease transmission. On the other hand, *A. sculptum* (figure 11 A) occurs in the biomes Cerrado, Atlantic Forest, Pantanal and Caatinga (in areas of tropical climate) [131]. In these habitats, it represents the most common human parasitic tick and the main vector of *Rickettsia rickettsii*, which causes the Brazilian spotted fever, the most serious tick-borne zoonosis in the New World [132]. Both species can be found in the transition areas between the Cerrado and Amazon biomes (figure 11 B), which commonly generates identification errors [133].
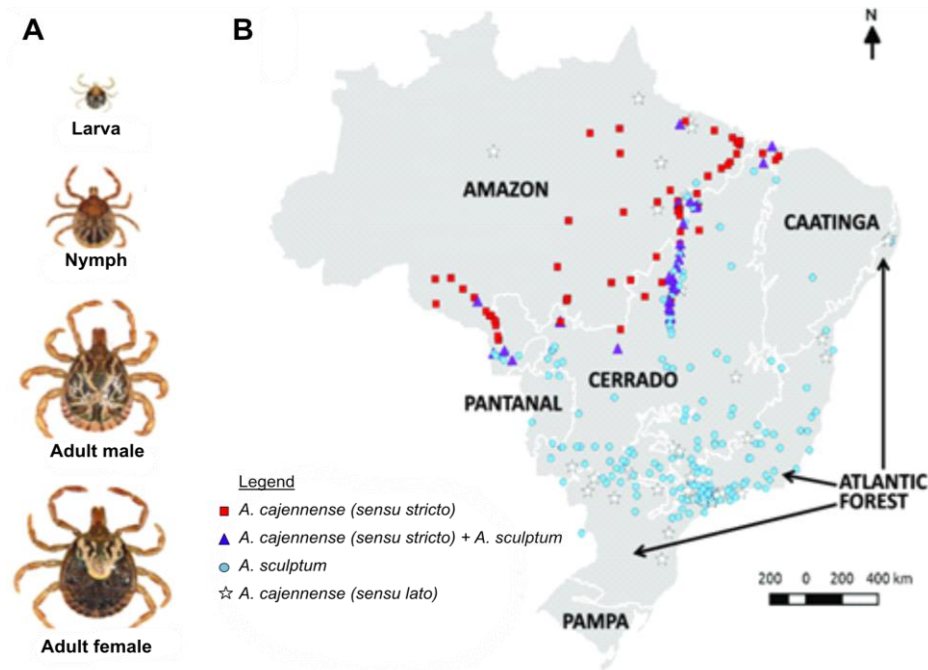
Figure 11 – A. sculptum *life stages (A) and distribution in Brazil (B). Adapted from Martins & Menezes 2017 [131].*

The literature already presents some data on the composition of *A. sculptum* saliva [9], but there are few reports over the pharmacological potential of its salivary secretion. A cDNA library of the salivary glands of *A. sculptum* demonstrated a series of genes encoding compounds that affect the host's hemostatic system [134]. From this library, it was possible to develop a series of clones and recombinant proteins involved with the hemostatic system, such as Amblyomin-X [136]. Both are inhibitors of the tissue factor pathway (or TFPI), single-chain polypeptides that can inhibit Factor Xa (FXa), responsible for the formation of thrombin and consequent blood clot formation. The crude saliva has shown to present similar effect, with inhibition of platelet aggregation and thrombin formation in melanoma and pancreas adenocarcinoma cell lines [11]. Also, *A. sculptum* infestations do not generate the acquisition of host resistance, modulating the host's immune response. It seems to inhibit the complement system significantly reducing the local inflammatory process [137,138] and

interferes in the differentiation and migration of dendritic cells, expression of stimulatory molecules, and production of cytokines [139].

As for anti-tumoral potential, many effects of the salivary secretion of *A. sculptum* have already been described. Cytotoxic effects of *A. sculptum*'s crude saliva have been demonstrated on melanoma cells (SK-MEL-28) and pancreatic adenocarcinoma cells (MIA PaCa-2), with no cytotoxicity observed in non-tumoral human fibroblasts [11]. Similarly, Sousa and collegues 2018 [12] demonstrated cytotoxicity and apoptosis induction in cells derived from breast tumors (MDA-MB-123 and MCF-7), but not in the non-tumor lineage MCF-10A. Previous findings from our research group demonstrated that *A. sculptum's* crude saliva has a high cytotoxicity and antiproliferative effect, involving the loss of mitochondrial potential and cytoskeleton rearrangement in cells derived from leukemia (U937) and neuroblastoma (IMR-22 and CHLA-20) [140]. However, little is known about the mechanisms of action associated to such cytotoxicity. Therefore, the present project brings data for the better comprehension of *A. sculptum*'s crude saliva cytotoxicity over neuroblastoma cell lines.

4. GENERAL AIM

The present project aims to describe the mechanisms involved in the cytotoxicity induced by *Amblyomma sculptum* crude saliva and its derived compounds on neuroblastoma cells.

4.1 SPECIFIC AIMS

- To identify the programmed cell death associated with the cytotoxicity of the crude saliva.

- To investigate the selectivity of the crude saliva cytotoxic effect to tumoral cells.

- To describe the modulation of cell death associated proteins by the saliva.

- To identify and isolate the bioactive compounds from the crude saliva that may be responsible for the observed anti-tumoral effect.

5. MATERIAL AND METHODS

5.1 Crude Saliva and fractions

Amblyomma sculptum ticks were collected by researchers from the Butantan Institute, SP, Brazil with the tick dragging technique [141] and maintained as described by Oliveira and colleagues 2012 [142]. As observed in figure 12, ticks were fed the blood of domestic rabbits (*Oryctolagus cuniculus*) without prior tick infestations. Ticks were placed inside a cotton chamber (10 cm x 15 cm) on the back of the rabbits until they reached 1.0 cm in width and 1.2 cm in length or after eight days of feeding. They were then removed by torsion from the rabbits' backs. Salivation was induced using the methodology described by Oliveira et al., 2012 [142] with minor modifications. Briefly, ticks were ventrally attached to a double-sided tape on a wood base, and 5-10 µl of a dopamine solution (Sigma-Aldrich, St. Louis, MO, USA; 5% w/v in 0.15 M NaCl) were injected into the dorsal region using a micrometric syringe. Saliva was collected for 4 h at room temperature in microcapillary tubes fastened to the wood base, with one end in contact with the tick's hypostome, as observed in figure 12.

Figure 12 – Amblyomma sculptum and their saliva collection by the research group of Dr. Simone Simons, from the Butantan Institute. Ticks were collected by dragging techniques on open fields of São Paulo state, Brazil (1). Tick were fed on *Oryctolagus cuniculus* domestic rabbits (2), salivation was induced by a dopamine stimulation and crude saliva (CS) was collected on microcapillary tubes (3) as described by Oliveira et al., 2012 [142].

The collected saliva was immediately frozen on dry ice. Saliva samples were pooled, filtered (0.22 µm), aliquoted, frozen on dry ice and ethanol, and kept at -80 °C until use. All experiments were carried out using protocols approved by the Ethics Committee for the Use of Animals of the Butantan Institute (CEUA No 1872100317). CS protein concentration was estimated using the Bradford protein assay [143]. The experimental investigations over CS induced cancer cell cytotoxicity were then performed as demonstrated on figure 13.
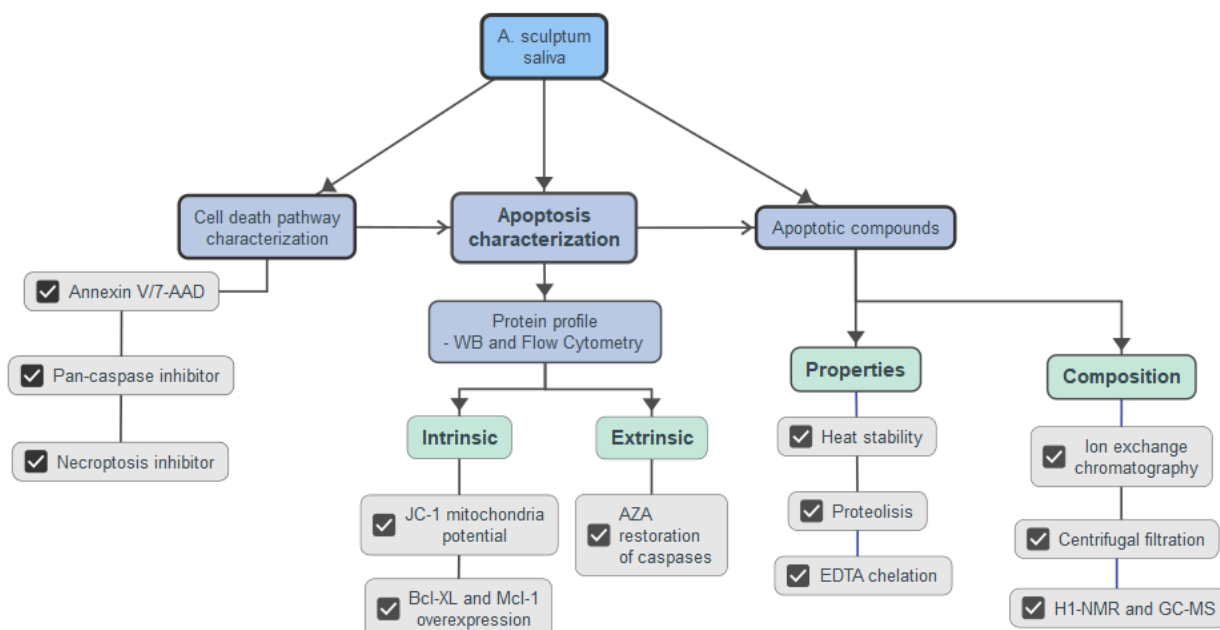
Figure 13 - Fluxogram of methods and approaches for the development of the study.

CS was fractionated by ion exchange chromatography in a Resource Q column (FPLC; AKTA Purifier; GE Healthcare), equilibrated with 20 mM Tris-HCl buffer, pH 8 (buffer A), and eluted with a linear gradient of NaCl in 20 mM Tris-HCL/500 mM NaCl buffer (buffer B). Fractions were pooled and concentrated by freeze-drying up to 10% of the initial volume and dialyzed against 3 mM NaCl (3.5 kDa cut-off; SnakeSkin Dialysis Tubing; Thermo Fisher). Protein concentration was determined by the Bradford method [144] and fractions were kept at -80 ºC until use. CS fractionation by centrifugal filtration was performed using a 10 kDa cut-off Vivaspin 6 (Sigma Aldrich, St. Louis, USA) and a 3 kDa cut-off Amicon Ultra-2 (Sigma Aldrich, Saint-Quentin-Fallavier, France), following the manufacturer's recommendations.

5.2 Cell lines and cellular edition

The neuroblastoma (NB) cell lines SH-SY5Y (ATCC® CRL-2266 ™), SK-N-SH (ATCC® HTB-11 ™), and Be (2)-M17 (ATCC® CRL-2267 ™) were obtained from

American Type Culture Collection (ATCC), as well as the colorectal adenocarcinoma cell line HCT-116 (ATCC® CCL-247EMT ™); the CHLA-20 NB lineage was obtained from the Children's Oncology Group Foundation (Philadelphia, PA, USA); and the MDA-MB-231 breast tumor derived cell line was kindly provided by Patrick Legembre (Rennes, France). Stem cells from human exfoliated deciduous teeth (SHED) were kindly donated by Dr. Alexandra Cristina Senegaglia from the Experimental Laboratory of Cell Culture, coordinated by Dr. Paulo Brofman, at PUCPR, Curitiba, PR, Brazil. All cell lines were maintained in Dubelcco's Modified Eagle's Medium (DMEM Ham's F12) culture medium containing 10% inactivated fetal bovine serum (GIBCO), with 100 IU/ml of penicillin and 0.1 mg/ml of streptomycin. Culture flasks were kept in an incubator with 5% CO_2, at 37°C, and observed daily under an optical microscope. All chemicals and reagents here described were purchased from Sigma Aldrich (St. Louis, MO, USA).

Bcl-XL and Mcl-1 overexpressing cells were generated using retroviral vectors encoding the full-length sequences of the gene of interest in the laboratory of Dr. Olivier Micheau (University of Burgundy - France), as described previously [145,146]. Bcl-XL full length (FL) was encoded the pBABE-Puro plasmid [147], allowing the selection of infected cells with puromycin selection at 2 µg/ml. Mcl-1 FL originally encoded by the pBabe-Flag-hMcl-1 vector, a generous gift from Roger Davis (Addgene plasmid 25371; https://www.addgene.org/25371/) was transferred into the pMIGR vector digested with HpaI using the following oligonucleotides OR277: 5'-AGA-TCT-atg-gat-tac-aag-gat-gac-gac-3' and OR278 5'-GTC-GAC-cta-tct-tat-tag-ata-tgc-c, after amplification using the Pfu DNA polymerase (Promega) and ligation with the T4 DNA ligase (Promega) [148]. After infection, Mcl-1 overexpressing cells were selected based on their GFP positivity by sorting using the BD FACSMelody Cell Sorter [149]. Briefly, GP2-293 cells (ATCC) were plated and used at

40% confluency for retroviral production using 1.5 µg pVSV-G (Clontech, Fitchburg, United States) and 10 µg corresponding plasmids, as described above. Transfections were performed with polyethyleneimine (PEI) as described by Ehrhardt et al., 2006 [149]. NaCl (150 mM) and 4 µg of PEI, along with the plasmids and retroviral vector as described above, were directly added to the GP2-293 cells and incubated for 8 to 16 hours. Cells were next washed with HBSS, fresh DMEM medium, and 10 mM sodium butyrate was added for 12 hours, to enhance retroviral production. Subsequently, GP2-293 was washed with fresh medium and the supernatant containing viruses was collected after 24 and 48 h to infect NB SH-SY5Y and Be (2)-M17 cell lines. Cells were allowed to recover for 24 to 48 hours and selected with puromycin or cell sorted before characterization, generally 1 or 2 weeks after infection, by analysis of protein expression by western blot. TRAIL-receptor-deficient HCT116 (DKO) cells were generated using the TALEN approach as described by Dufour et al., 2017 [150]. Caspase-8-deficient HCT116 cells were generated by CRISPR-mediated gene deletion as described by Elmallah et al., 2020 [151], using the pLC-RFP657-CASP8 plasmid, a kind gift from Dr. Beat Bornhauser (Addgene plasmid # 75164; http://n2t.net/addgene:75164 ; RRID:Addgene_75164) [152].

5.3 Treatments with tick salivary secretion and fractions

In every assay, the crude saliva (CS) was tested with a 10% dilution (SL10), incubated for 72 hours, as standardized in a previous study [13]. Fractions obtained from the CS were reconstituted to the initial volume of CS before fractionation and then a 10% dilution was used to evaluate the effect of each obtained fraction, the same way performed to the CS. The chemotherapy drug Camptothecin (CMPT; Sigma Aldrich, St. Louis, USA) was used at 10 µg/ml, as a positive control for apoptosis in some assays. Similarly, a cocktail of 1 uM

doxorubicin (Merck - Sigma Aldrich, USA) and 1ug/ml topotecan (Merck - Sigma Aldrich, São Paulo, Brazil) was also used as a positive control for cell death.

The involvement of caspases in saliva's effect was assessed by pre-treating cells for 60 minutes with 20 µM Q-VD-Oph (QVD; Selleckchem, Houston, United States) before adding the saliva extract. Q-VD-Oph is a pan-caspase inhibitor which highly inhibits caspase-1, caspase-3, caspase-7, caspase-8, caspase-9 and caspase-10. To evaluate the role of necroptosis cells were treated with 15 mM Necrostatin-1 (NEC; Tocris, Bristol, United Kingdom) for 1 hour before stimulation. This compound blocks non-apoptotic cell death by inhibiting the receptor-interacting protein kinase 1 (RIPK1). 5-Aza-2-deoxycytidine (AZA) (Sigma Aldrich, Saint-Quentin-Fallavier, France) at 10 µM was used to reconstitute the expression of caspase-8 in NB cell lines before treatment with SL10. AZA, widely used as an anticancer drug, is a DNA demethylating agent known for increasing activity of caspase-3, caspase-8 and caspase-9 [153].

For protein denaturation, CS was boiled at 95° C in a thermoblock for 5 minutes prior to stimulation of the cells. The serine protease proteinase K was used to cleave proteins and peptides present in saliva; 0.5 mg/ml of proteinase K was incubated with CS for 1 hour at 37°C, followed by enzyme inactivation for 5 minutes at 95°C, and only then it was added to the cells. The proteinase K concentration was confirmed by acrylamide gel to be sufficient to cleave high concentrated proteins (not shown).

To investigate if the cytotoxic activity of the CS was dependent of the presence of divalent ions, CS was treated with Ethylenediamine tetraacetic acid (EDTA). CS presents approximately 8 mM calcium (Ca^{+2}) and 1.5 mM magnesium (Mg^{2+}) [9]. EDTA is a chelating agent capable of chelating a series of ions, including Ca^{+2} and Mg^{2+} at high concentrations. EDTA at different dilutions, ranging from 0.01 mM to 20 mM, were added to the medium of

SH-SY5Y cells to find the highest concentration that would not significantly impair their viability for up to 72 hours. SL10 was incubated with 0.4 mM EDTA for 12 hours at 4°C before incubation with cells as previously described, following evaluation of induced cell death.

5.4 Cell death and apoptosis

Cell death was determined using the Annexin V-APC and 7-AAD labeling to detect the externalization of phosphatidylserine and cell membrane permeability, respectively. Analyzes were performed using BD FACSCanto II and BD LSR II flow cytometers (BD Becton-Dickinson, Franklin Lake, NJ, USA). Dying cells are presented as the percentage of positively stained cells compared to untreated cells as a control. Each experiment was performed independently at least three times. Cells were seeded at a density of 50.000 cells/well in 12-well plates overnight in complete medium. Following stimulation, cells were trypsinized and transferred to cytometer tubes, along with their supernatant. Tubes were then centrifuged at 300 rcf for 5 min and cells were washed with PBS 1X. Staining was performed in Binding Buffer containing Annexin V-APC and 7-Aminoactinomycin D (7AAD) (BD Pharmigen, France), according to the manufacturer's instructions. Single or double-positive stained cells were considered dying cells and the results are expressed in percentage of positively stained cells. The acquisition included a minimum of 10.000 cells per tube.

5.5 Cell viability

Cytotoxicity and cell viability were assessed by the Methylene Blue test [154]. Cells were plated at 30.000 cells/well density in 96-well plates. After treatments, cells were fixed with 99% methanol and stained with 0.05% Methylene Blue dye (Merck, Darmstadt,

Germany) aqueous solution for 10 minutes. Repeated washes were performed with running water to remove the excess of dye that could interfere with the result. Plates were left to dry overnight. Then 0.1 M HCl was added to each well, left in a plate shaker for 5 minutes in the dark, and reading was performed in a plate reader at 630 nm. The percentage of cell viability was calculated as follow: Cell viability (%) = (abs treated cells/abs untreated cells) x 100

5.6 Mitochondrial permeabilization

Mitochondrial potential was verified by JC-1 staining (Fisher Scientific,France). JC-1 is a membrane-permeable dye that enters and accumulates in energized mitochondria, changing stained mitochondria from green (fluorescence emission of 530±15 nm) to red-orange (fluorescence emission 590±17.5 nm) as the membrane's potential increases. Cells were plated at a density of 50.000 cells/well in 12-well plates and treated as described previously, and transferred to cytometer tubes, along with their supernatant. Cells were then stained with 2.5 µg/ml of JC-1 for 30 minutes in an incubator at 37°C, following washes with 1X PBS to remove any excess staining solution. Analyzes were performed in a BD FACSCanto II cytometer in channels B575/25 nm and B530/20 nm.

5.7 Western blot and protein expression analysis

Protein levels were evaluated by immunoblotting. Cells were plated in 6-well plates at 500.000 cells/well and treated as described previously or directly collected from culture flasks. Lysis was further performed with 1% NP-40, Tris-HCl, 3 M NaCl and 5% glycerol. Protein content of lysates were measured by Lowry (Bio-Rad, Marnes-la-Coquette, France). Proteins were resolved by electrophoresis in sodium dodecyl sulfate-polyacrylamide gels (SDS-PAGE) containing 12% of SDS, 30% of acrylamide, 1% of Ammonium persulfate and

2% of N,N,N′,N′-tetramethylethylene-diamine (TEMED) in a Tris-Hcl (1.5 M, pH 8.8) buffer. After electrophoresis, proteins were transferred to polyvinylidene difluoride (PVDF) membranes (Thermo Fisher Scientific, GE Healthcare Life Sciences Amersham, UK) in a borate transfer buffer (3 g of boric acid in Tris-HCl buffer). Nonspecific binding sites were blocked by incubation in PBS containing 0.5% Tween 20 (PBST) and 5% powdered milk, for 30 minutes at room temperature. Membranes were incubated overnight with a specific primary antibody described at Table 1, washed four times in PBST and incubated for 1 hour with a horseradish peroxidase (HRP)-conjugated secondary antibody. Secondary antibodies HRP-conjugated anti-rabbit were obtained from Jackson ImmunoResearch (Interchim, Montluçon, France) and HRP-conjugated anti-mouse IgG1-, Ig2a- and Ig2b-specific antibodies were from Southern Biotech (Clinisciences, Nanterre, France). Blots were revealed using the Covalight Xtra ECL enhanced chemiluminescence reagent according to the manufacturer's protocol (Covalab, France) and visualized on Bio-Rad's ChemiDoc XRS[+] Imaging System.

Table - 1 – Primary protein antibodies used for Western Blot.

PROTEIN	SIZE	PROVIDER	Ref./clone N°	DILUTION
HSC-70	70	Santa Cruz, Germany	SC-7298	1:1000
Caspase-3	17	Cell Signaling, Netherlands	SA15	1:1000
PARP-1	89-116	Santa Cruz, Germany	SC-25780	1:500
p-JNK	46	Cell Signaling, Netherlands	4668S	1:1000
Lamin A+C	41-50	Abcam, United Kingdom	AB133269	1:1000
Caspase-9	37-46	MBL, United States	M0543	1:1000
Mcl-1	40	Santa Cruz, Germany	SC-12756	1:500
GAPDH	35	Santa Cruz, Germany	SC-47724	1:500
IRE1	110	Cell Signaling, Netherlands	14C10	1:1000
Bcl-2	25	Santa Cruz, Germany	SC-16323	1:1000
Bcl-XL	27	Cell Signaling, Netherlands	54H6	1:1000

DR5	40-55	Abcam, United Kingdom	AB16955	1:1000
DR4	40-55	Abcam, United Kingdom	AB16942	1:1000
Caspase-7	45-55	Cell Signaling, Netherlands	D5H1	1:1000
Caspase-2	35-51	Santa Cruz, Germany	SC-53928	1:1000
Caspase-3	32	Cell Signaling, Netherlands	8610	1:1000
FAS	45-55	Santa Cruz, Germany	SC-74540	1:1000
Caspase-10	27-55	MBL, United States	M059-3	1:1000
Caspase-8	35-55	MBL, United States	M032-3	1:1000
Bid	22	Cell Signaling, Netherlands	3C5	1:1000
Bax	25	Santa Cruz, Germany	SC-20067	1:500
Rip	76	Cell Signaling, Netherlands	D94C12	1:1000
Survivin	17	Cell Signaling, Netherlands	71G4B7	1:500
GSDMD	35-50	Abcam, United Kingdom	AB210070	1:1000
GSDME	35-55	Abcam, United Kingdom	AB215191	1:1000

5.8 Flow cytometry and protein expression analyses

Cleavage of caspase-3 was also evaluated by flow cytometry. Cells (50.000 cells/well) were seeded in 12-well plates and treated as previously described with CS or fractions. Following incubation, cells and the supernatants were collected and transferred to cytometry tubes. Cells were then washed with PBS 1X and permeabilized with 0.5% saponin in 3% BSA for 10 minutes, saturated with 3% BSA for 20 minutes, and finally stained with the final dilution of 1:800 of primary antibody to cleaved caspase-3 (Cell signaling, Leiden, Netherlands), for 20 minutes. Subsequently, cells were washed twice with 1x PBS and stained with the secondary anti-rabbit antibody conjugated to Alexa Fluor 680 for 15 minutes in BSA 3%, washed twice with 1x PBS, and analyzed by cytometry on the BD FACSCanto II or LSR II BD cytometer on channels 712/21 nm and 720/13 nm, respectively.

To check the basal extracellular expression of death receptors for TRAIL and FAS in NB cells and control lineage MDA-MB-231, cells were collected and 50.000 cells were

transferred to cytometry tubes. Then washed with PBS 1X and saturated with 3% BSA for 30 minutes. Subsequently marked for 45 minutes with mouse antibodies anti-FAS (BD Biosciences, France) and anti-DR4 and anti-DR5, that were both generated by Dr. Agathe Dubuisson and colleagues, as demonstrated previously [155], in collaboration to CovalAb (Villeur-banne, France). As a negative signal control, the IgG1 isotype antibody (New Englang BioLabs, France) was used. Cells were then washed again and incubated with the secondary anti-mouse antibody conjugated to Alexa Fluor 680 (Jackson ImmunoResearch, United States) for 30 minutes. Finally, cells were analyzed in BD FACSCanto II cytometer in channel 712/21 nm.

5.9 Chemical characterization of the low molecular weight fraction

Chemical characterization of the <10 kDa fraction were performed by our collaborator professor Guilherme Sassaki at the Nuclear Magnetic Resonance Center, Department of Biochemistry and Molecular Biology, Biological Sciences Sector at the Federal University of Paraná, Curitiba-PR, Brazil.

Gas chromatography–mass spectrometry (GC-MS) was performed on Shimadzu Nexis QP2020-MS equipment containing a 25 m capillary column (VF5-MS). The temperature program was defined for the separation of methyl ester derivatives, methyl glycosides and acetylated derivatives. Derivatives were eluted in the CP-Sil-5CB capillary column as follows: injector 250∘C, oven start at 50∘C (hold 2 minutes) to 90∘C (hold 1 minute), 280 ∘C (hold for 2 minutes) and up to 310 ∘C held for 5 minutes. Electronic impact (EI) spectra were obtained at 70 eV. Derivatization of the samples followed the protocol described by Sassaki and colleagues 2008 [156]. The amino acids and carbohydrates were esterified and

glycosidated using a 0.6M MeOH solution, temperature of 80◦C for 20 h. After drying over nitrogen gas, the residue was acetylated using pyridine–MeOH–Ac2O (100 µl, 1:1:4, v/v) at 100◦C for 60 minutes and subjected to GC-MS analysis for the identification.

Nuclear Magnetic Resonance (NMR) spectras were obtained using Bruker Ascend 600 MHz equipment with a TCI cryoprobe (Bruker Biospin, Massachusetts, EUA). Lyophilized <10 kDa fraction was resuspended using 640 µL of D2O (Cambridge Isotope Laboratories) and 10 µL of TSP-d 4 (tetradeuterated sodium trimethylsilylpropionate, Cambridge Isotope Laboratories), centrifuged at 10.000 rpm for 10 minutes and supernatants was transferred into a 5 mm NMR tube. NMR spectra of the 1H NMR were acquired under a controlled temperature of 298.15 K, number of transients (NS) of 64, the 90º pulse was calculated for each sample, waiting time between acquisition (d1) equal to 10 seconds, number of acquisition points (TD) equal to 64k and spectral window of 25 ppm (SW). Spectra were acquired using NOESYPR1D pulse sequence with solvent pre-saturation (HOD) signal. Bruker TopSpin® program (version 3.1) was used for data processing, with phase and baseline corrected and calibrated through the signal relative to the TSP-d 4 at δ 0.00. NMR experiments of Heteronuclear Single Quantum Coherence (HSQC), TOCSY, diffusion measurement, and 2D-DOSY followed protocols previously described by Sassaki and colleagues 2011 [157].

5.10 Statistical analysis

Statistical analyses were performed for flow cytometry quantitative results using parametric T-test for comparisons between two treatments or control, or variance two-way ANOVA, with Tukey's or Sidak's test for multiple comparisons. Sidak was used when

comparing several variables within a single cell line and Tukey when comparing variables within different cell lines that were also correlated. GraphPad Prism software version 6 was used for all analyses. Data were expressed as mean ± SD and p-value *p<0.05, **p<0.01, ***p<0.001, and ****p<0.0001 were considered significant.

6. RESULTS

6.1 Amblyomma sculptum's crude saliva cytotoxicity is independent of caspase-8 or death receptors activation.

To identify the intracellular mechanisms associated with the cytotoxicity previously described for the crude saliva (CS), its effect was initially evaluated over the triple negative breast cancer cell line MDA-MB-231, the colorectal adenocarcinoma cell line HCT116 and the neuroblastoma (NB) cell line SH-SY5Y, by annexin-V and 7-AAD staining after 72 hours stimulation as previously standardized [13]. As demonstrated in figure 14A, all cell lines were susceptible to CS, with the highest sensitivity shown by SH-SY5Y cells, and this effect was significantly prevented by treatment with the pan-caspase inhibitor QVD.

After demonstrating that CS's cytotoxicity was dependent on the cleavage of caspases, the basal level of proteins related to programmed cell death was analyzed in four NB cell lines (SH-SY5Y, CHLA-20, Be(2)-M17, and SK-N-SH), and MDA-MB-231 and HCT116 cell lines (Figure 14B). As observed, whereas slight differences were observed for caspase-2, caspase-3 and caspase-9 protein levels in these cell lines, NB cells were devoid of caspase-10 and caspase-8, as expected [161], but also devoid of DR4, Bcl-XL, Mcl-1 and gasdermin D (GSDMD). Gasdermin E (GSDME) was highly present in MDA-MB-23 and Be(2)-M17 cells. Bcl-2 and IκBα levels are relatively the same for all cell lines, except for SH-SY5Y that shows some higher levels. On the other hand, RIP and BID protein levels are only low for SH-SY5Y (figure 14 B).

The observation that death receptors were absent in NB cells was confirmed by flow cytometry analysis (Figure 14 C). No or little membrane surface expression of death

receptors FAS, DR4 and DR5 was detected on SH-SY5Y cell line, as opposed to MDA-MB-231 which expresses a significant amount of these receptors.

To investigate if cell death on NB cells could be enhanced with the presence of initiator caspases, we have evaluated the impact of the demethylating agent AZA, that acts as a DNA methyltransferase inhibitor and has been found to restore caspase-8 and caspase-10 mRNAs and protein expressions [158]. SK-N-SH was the only NB lineage that significantly restored caspase-8 expression (figure 14 D), but it did not affect the amount of cell death after SL10 treatment (figure 14 E). Similarly, caspase-8 knockdown HCT116 cells were also evaluated, but differently than SK-N-SH cells, there was a slight reduction in SL10 induced cell death on the HCT116 cells without caspase-8 expression compared to the wild-type cells. The DKO HCT116 cells, that don't express TRAIL death receptors, on the other hand, showed the same sensibility to the CS as the wild type HCT116 cells. QVD significantly prevented cell death upon SL10 treatment on every cell line evaluated (figure 14 E).

Together, those findings demonstrate that CS-induced cell death was independent of death receptor activation or extrinsic apoptotic pathways on NB cells, which does not exclude the possibility of different mechanisms of action for other tumor cells. Along with that, low or absent levels of the anti-apoptotic proteins such as Mcl-1 and Bcl-XL (figure 14 B), related to the regulation of mitochondrial membrane permeabilization, suggests that these NB cell lines may be not only resistant to receptor-induced apoptotic pathways but also easily prone to intrinsic apoptosis.
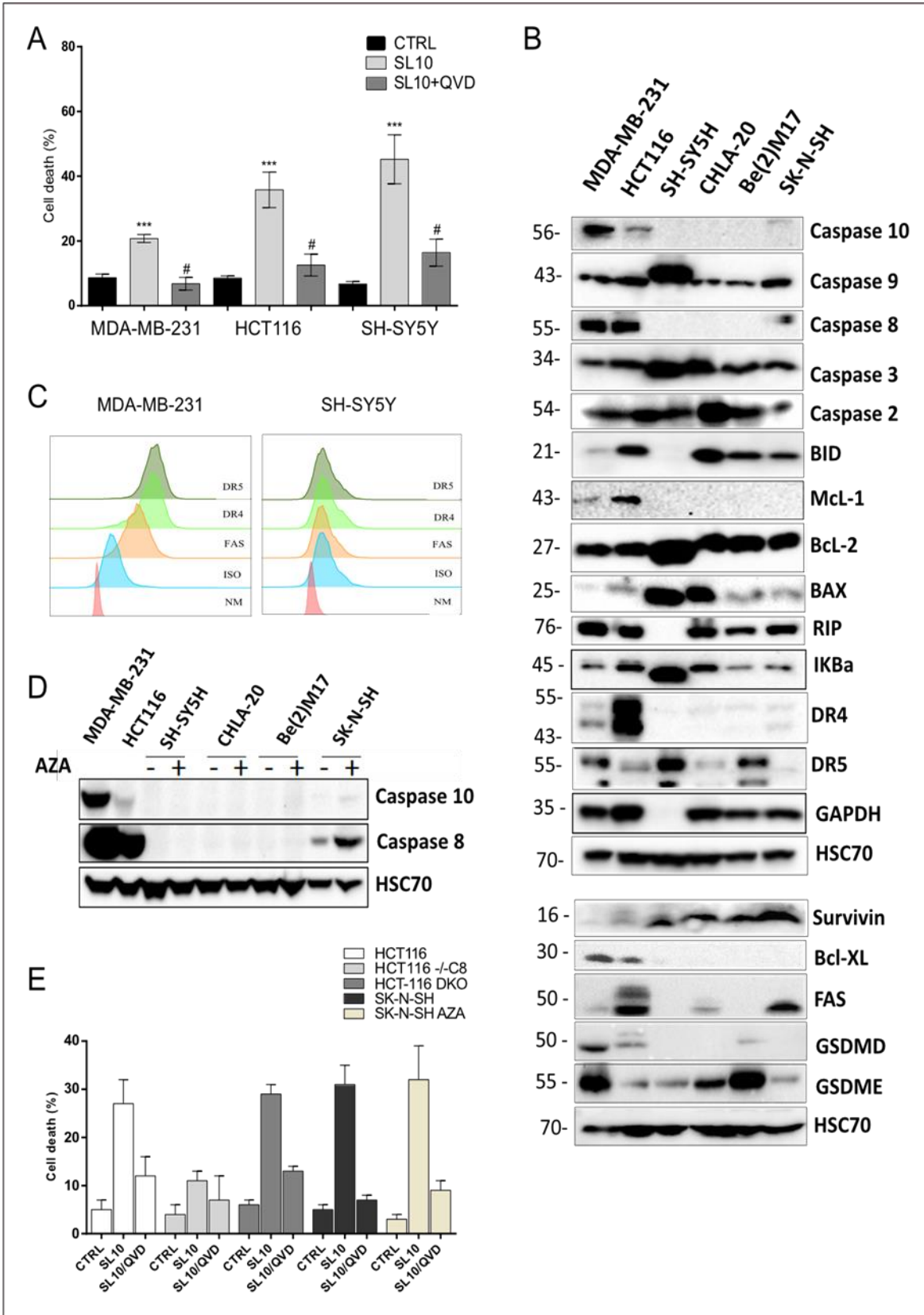
Figure 14 - *A. sculptum's* saliva induces cell death in tumor cells independently of death receptors activation. Breast cancer (MDA-MB-231), colon rectal adenocarcinoma (HCT116) and NB (SH-SY5Y) cell lines were treated with 10% of the crude saliva of A. *sculptum* for 72 hours alone or in addition to QVD, cell death was then assessed with annexin V and 7AAD staining by flow cytometry (A). T-test statistics were applied to compare each cells control group to its respective treatment, results expressed as the mean ± SD with P ≤ 0.001 (***) were considered significant. (#) represents the statistical difference between SL10 and SL10 with QVD treatment, with mean ± SD with P ≤ 0.05. Basal expression of cell death associated proteins were analyzed by western blot in colon rectal (HCT-116), neuroblastoma (SH-SY5Y, CHLA-20, Be(2)M-17 and SK-N-SH) and breast cancer cell lines (MDA-MB-231) (B). The cell surface expression of FAS, DR4 and DR5 death receptors was also assessed on MDA-MB-231 and SH-SY5Y cells by flow cytometry staining (C). 10 µM of AZA demethylating agent was used to restore caspase-8 expression on NB cell lines (D). Previously to SL stimulation, 10 µM of AZA was used on the SK-N-SH NB cell line and HCT116 wild type, caspase-8 deficient and DKO cells; after that, apoptosis was accessed again by annexin V and 7AAD staining (E).

6.2 *Amblyomma sculptum's* crude saliva induces apoptotic cell death in NB cells.

The time-dependent effect of CS induced cell death over the NB cell line SH-SY5Y was confirmed upon annexin-V staining after SL10 stimulation for 24, 48, and 72 hours. We demonstrate that cell death upon CS stimulation increased in a time-dependent manner, and became statistically significant only after 72 hours (figure 15 A). Consistently, cleavage of caspase-3, lamin A and C, and loss of the proform of PARP-1 were observed after 72 hours by WB (figure 15 B). Those basically characterize apoptotic activated pathways, but it could not be excluded that in addition to apoptosis, CS could also trigger late necroptosis. For that, we used the necroptosis inhibitor Necrostatin-1 (NEC) in two NB cell lines, SH-SY5Y and Be(2)-M17. The inhibitor, however, did not significantly affect the CS's effect over NB cells (figure 15 C). Also, the combined treatment of QVD and NEC did not show any significant

difference when QVD was used alone, suggesting triggering of apoptosis is in fact the main cell death pathway induced by CS.
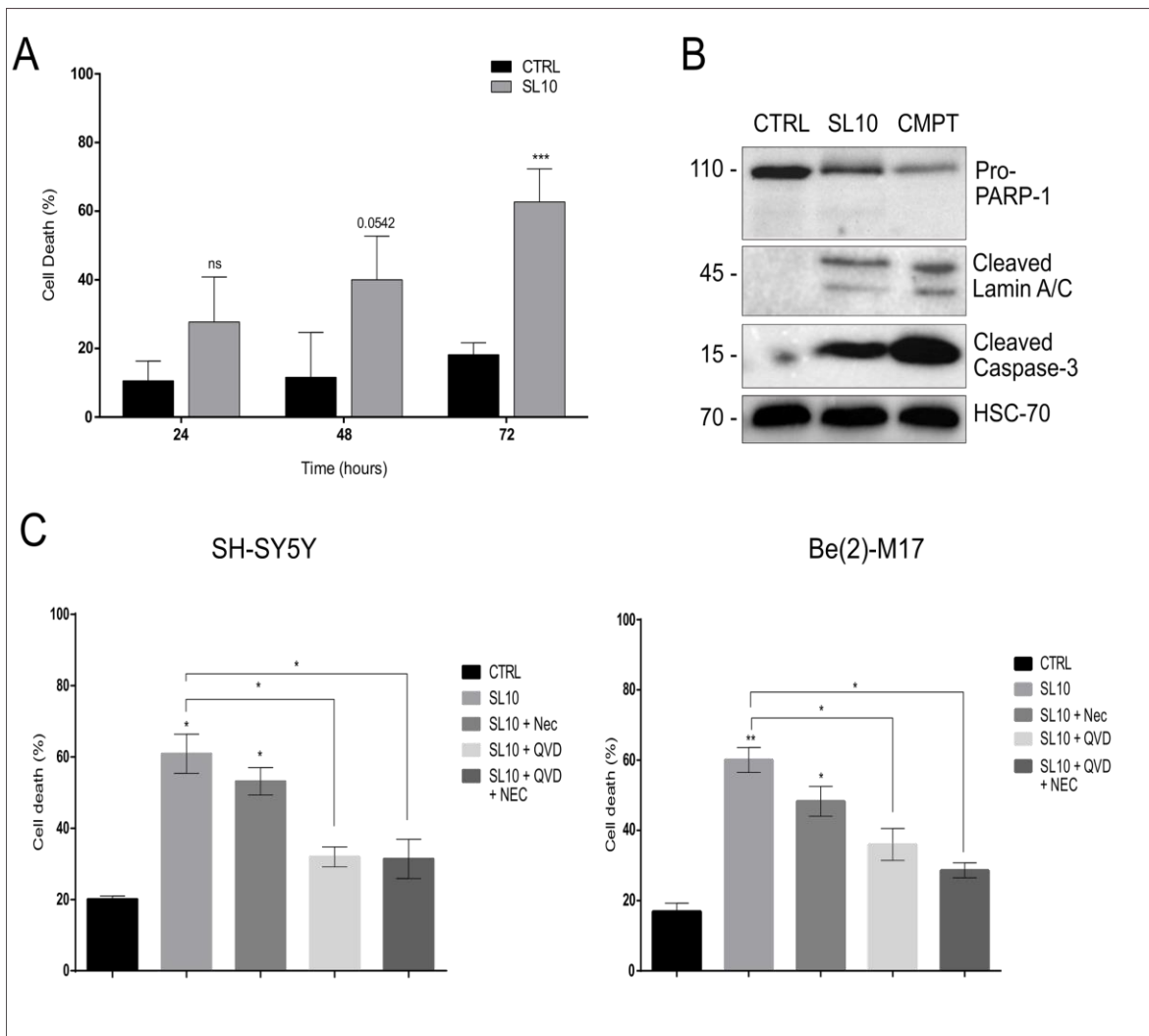
Figure 15 - *A. sculptum* saliva induces apoptosis in NB cell lines. SH-SY5Y cell line was stimulated for 24, 48 and 72 hours with SL and 10ug/ml of CMPT, cell death was then accessed by annexin V and 7AAD staining (A). Cleavage of PARP-1, Lamins and caspase-3 were verified by western blot analysis (B). SH-SY5Y and Be(2)-M17 cell lines were treated with 15 mM of necrostatin-1 (NEC) necrosis inhibitor and 20 µM of QVD apoptosis inhibitor previously to the SL10 stimulation (C). Cell death was then stained by annexin V and 7AAD staining. T-test statistics were applied to compare each cells control group to its respective treatment (A) and ANOVA with Tukey analysis for multiple group comparison (C), results expressed as the mean ± SD with $P \leq$ 0.05 (*), $P \leq$ 0.01 (**) and $P \leq$ 0.001 (***) were considered significant.

6.3 Anti-apoptotic proteins of the intrinsic pathway prevent saliva-induced mitochondrial potential loss and cell death.

Considering the cytotoxicity of the CS is mainly associated with apoptosis, but in an independent manner of extrinsic pathways, the intrinsic pathway was investigated. We first overexpressed Bcl-XL and Mcl-1 anti-apoptotic proteins, responsible for inhibiting mitochondria outer membrane permeabilization (MOMP), in SH-SY5Y and Be(2)-M17 NB cells (figure 16 A). CMPT treatment was used as a positive control for the induction of intrinsic cell death, which is inhibited by Bcl-XL and Mcl-1 anti-apoptotic proteins. The SL10 treatment was also evaluated on those cells. Bcl-XL overexpression alone could inhibit most apoptotic death induced by SL10 and CMTP for both cell lines. As for Mcl-1 alone, little protective effect was observed. However, when both proteins BclXL/Mcl-1 were overexpressed together (BclXL/Mcl-1-OE), the percentage of cell death induced by SL10 was lower than 17% on SH-SY5Y and 37% for Be(2)-M17 (figure 16 B). Statistical analysis showed that after overexpression of the antiapoptotic proteins, neither SL10 nor CMPT were able to induce significant cell death on SH-SY5Y cells. As for Be(2)-M17, SL10 was still able to induce significant cell death, but with about 20% reduction compared to the mock cells (figure 16 C).
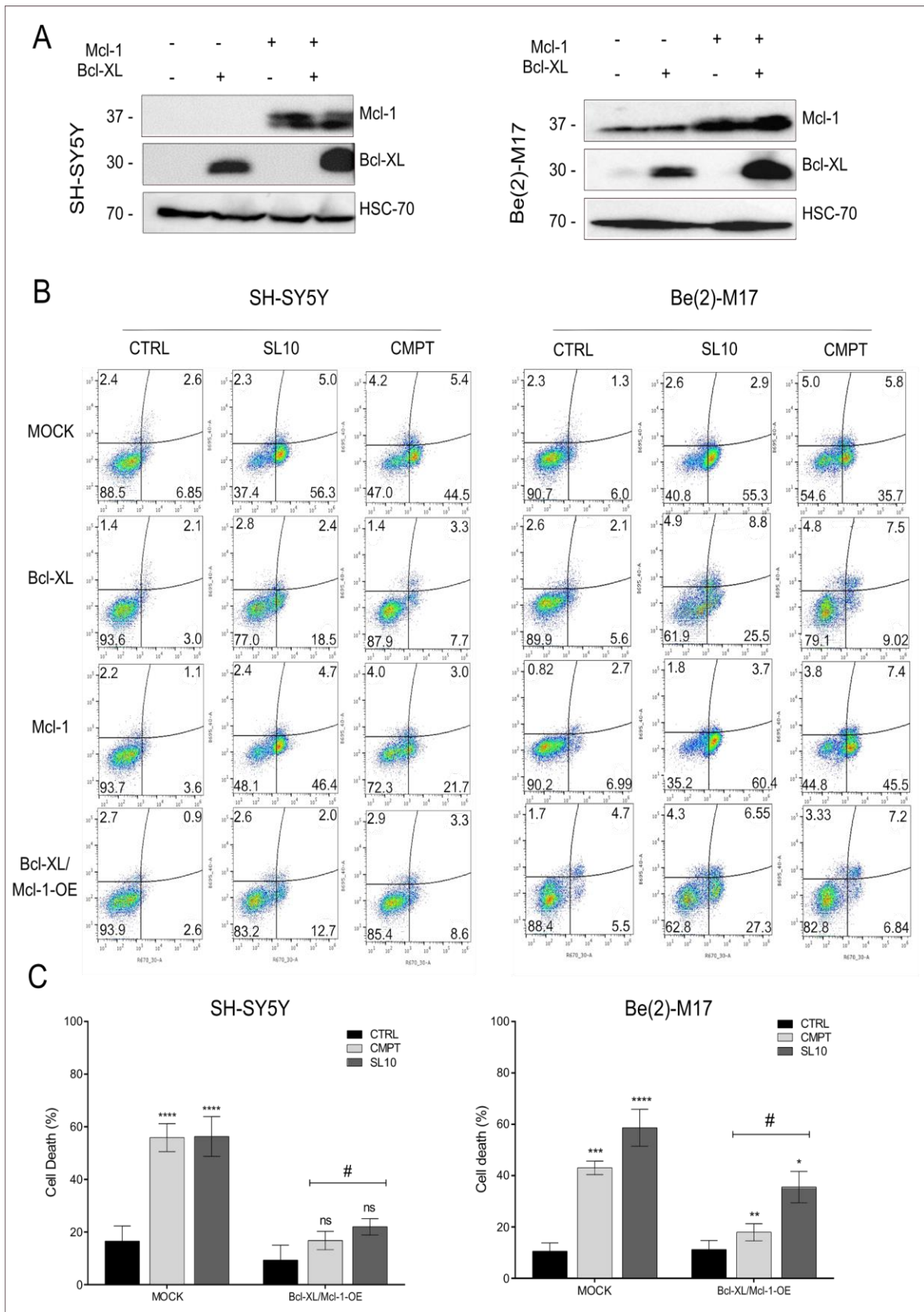
Figure 16 - Expression of Mcl-1-OE and Bcl-XL-OE proteins inhibits the cytotoxic effect of the SL. SH-SY5Y and BE(2)-M17 cell lines overexpressing Mcl-1 and Bcl-XL protein plasmids were generated from lentiviral infections and their levels were confirmed by WB analysis (A). Single transfected and double positive cells for both anti-apoptotic proteins (BclXL/Mcl-1-OE) and the control cells transfected with mock plasmids (MOCK) were stimulated with 10% of the SL for 72 hours; cell death was accessed by the percentage of annexin V (horizontal) and 7AAD (vertical) staining (B). Statistical analyses were performed and results are expressed as the mean ± SD. P ≤ 0.05 (*), p ≤ 0.01 (**) and p ≤ 0.001 (***) were considered significant and represent statistical comparisons between each cell's control group. Statistical difference between mock and BclXL/Mcl-1-OE cells with the same respective treatment are represented by bars and (#) represents P ≤ 0.05 (C). 10ug/ml of camptothecin (CMPT) was used as a positive control for intrinsic apoptotic triggering.

MOMP was then verified by JC-1 staining, which accumulates in mitochondria and generates a red fluorescence. If mitochondria is depolarized, the fluorescence ratio decreases. JC-1 staining showed over 60% of mitochondrial potential loss for SH-SY5Y and Be(2)-M17 treated with SL10. However, the double over-expression of Mcl-1 and Bcl-XL significantly prevented mitochondrial permeabilization induced by SL10 in both cell lines, as well as for the positive control with CMPT (figure 17). Therefore, the overexpression of Mcl-1 and Bcl-XL allowed us to demonstrate that cell death induced by the saliva occurs through mitochondrial membrane-potential loss.
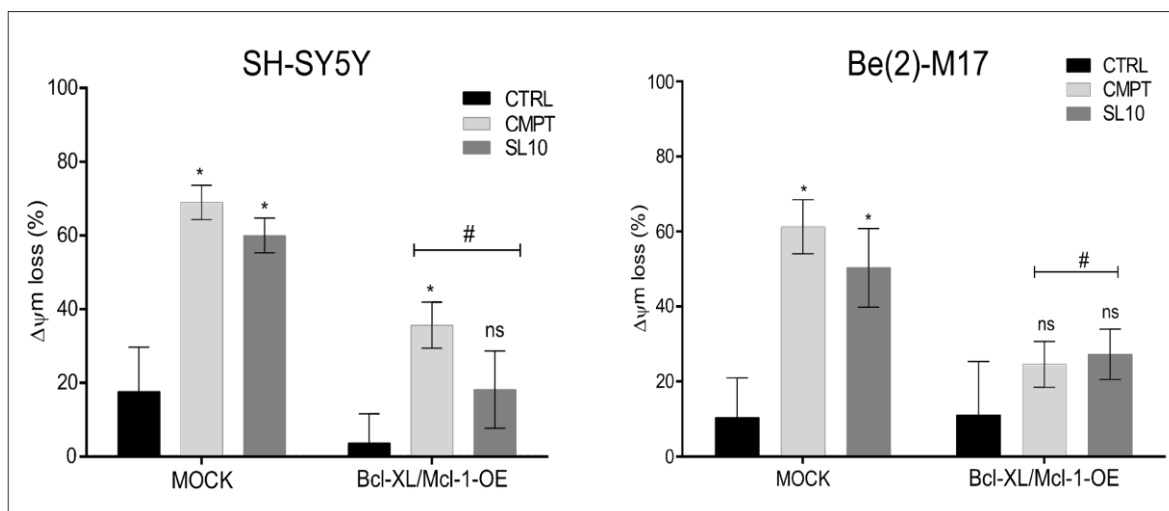
Figure 17 – SL10 induces mitochondrial potential loss on NB cell lines. SH-SY5Y and Be(2)-M17 double positive cells for Mcl-1-OE and Bcl-XL-OE chimeric proteins (BclXL/Mcl-1-OE) and the control cells transfected with mock plasmids (MOCK) were stimulated with 10% of the SL for 72 hours and mitochondrial potential by JC-1 staining was then evaluated by flow cytometry. Results are expressed as the mean ± SD. (*) represents statistical difference with p ≤ 0.05 comparing treatments with each cell's control group (black) and (ns) represents no statistical difference. Bars represent comparisons between MOCK and BclXL/Mcl-1-OE cells with the same respective applied treatment and (#) represents P ≤ 0.05. 10ug/ml of camptothecin (CMPT) was used as a positive control for intrinsic apoptotic triggering.

6.4 CS´s pro-apoptotic activity is induced by small non-protein compounds.

To identify and isolate the bioactive compounds from the CS that may be responsible for the observed anti-tumoral effect, CS was submitted to fractionation by two different procedures. Ion-exchange chromatography (IEC) was performed in a Resource Q column equilibrated with 20 mM Tris-HCl buffer and a linear 0-500 mM NaCl gradient. Chromatographic profile using an UV detector (216 and 280 nm) showed several peaks reunited in seven pools (figure 18 A). Before testing for specific activity, each pool was

dialyzed in a 3.5 kDa cut-off membrane to clean residue buffer and NaCl. Cell viability (figure 18 B) and morphology (figure 18 C) analysis showed that none of them had any effect on cells.
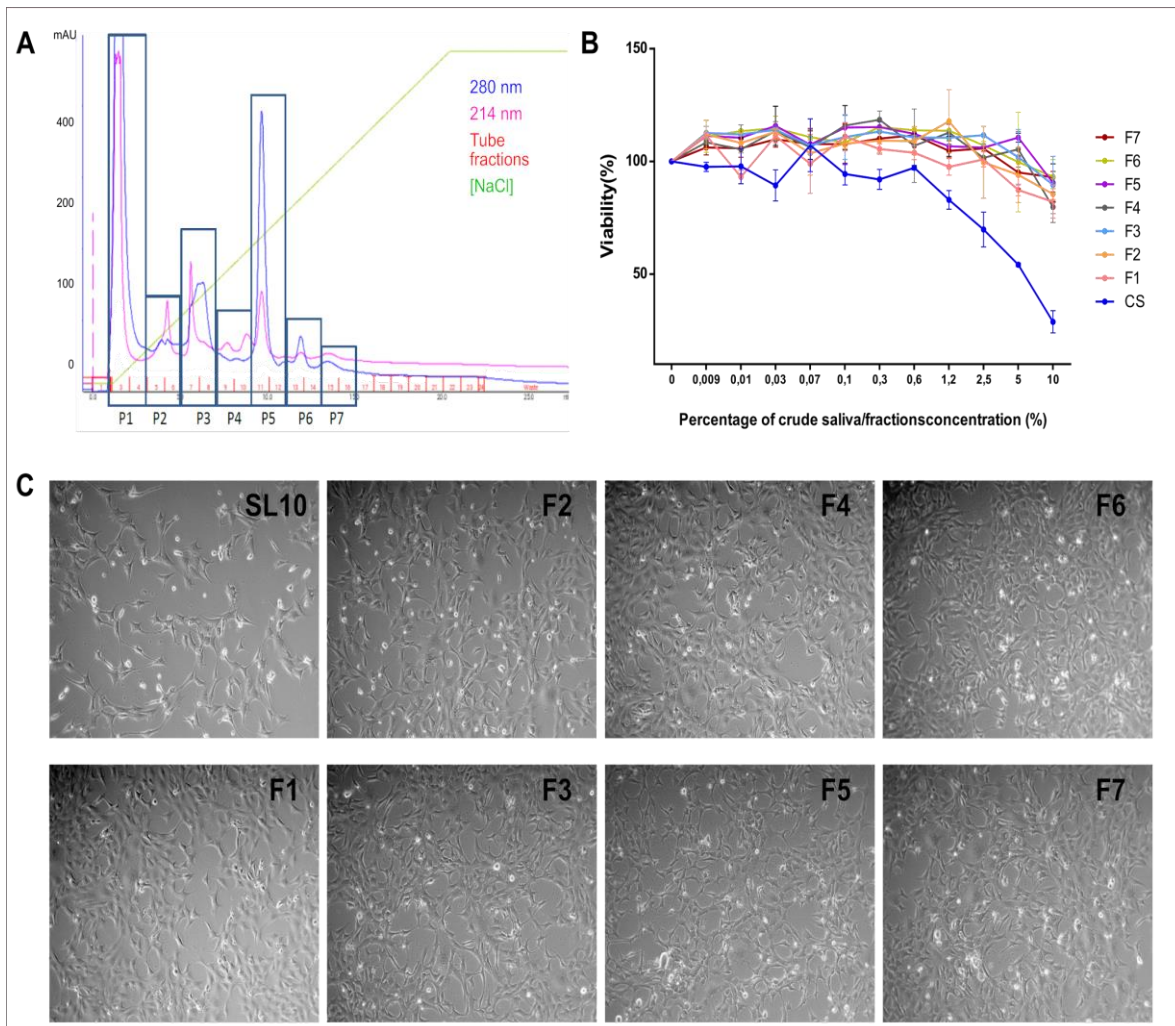
Figure 18 - Ion exchange chromatography (IEC) fractionation of *A. sculptum's* CS. Seven pool fractions (P1 – P7) obtained in the Resource Q column at the FPLC (AKTA Purifier - GE Healthcare), as previously described by Simons et al., 2011 [159] (A). Cell viability evaluated by methylene blue assay after 72 hours stimulation with the salivary fractions obtained by IEC in a series dilution starting at 10% concentration (B); tests were performed in three independent tests and absorbance at 630 nm was normalized to percentage of viability. Optical microscopy imaging after 72 hours stimulation with 10% of each fraction and CS (C).

As most compounds found within animal toxins are amino-acid based [159] and based on previous findings from our group that the CS of *A. sculptum* is rich in peptides and proteins [10,160], we had in mind that pro-apoptotic compounds within CS would have a protein nature. To further investigate if CS's activity would rely on protein components, it was boiled at the denaturant temperature of 95 °C. However, no significant difference was observed compared to the native saliva (figure 19 A). CS was also treated with proteinase K (protK), a broad-spectrum serine protease, resulting in a slight, though significant, reduction in cell death (Figure 19 B). Additionally, no significant decrease was observed for caspase-3 cleavage after protK treatment (Figure 19 C). Of note, SL10 treated with protK was also boiled to enzyme inactivation before cellular assay. As a negative control, to assure protK was not toxic at high concentrations, PBS and protK alone were added to the cells at the same conditions.
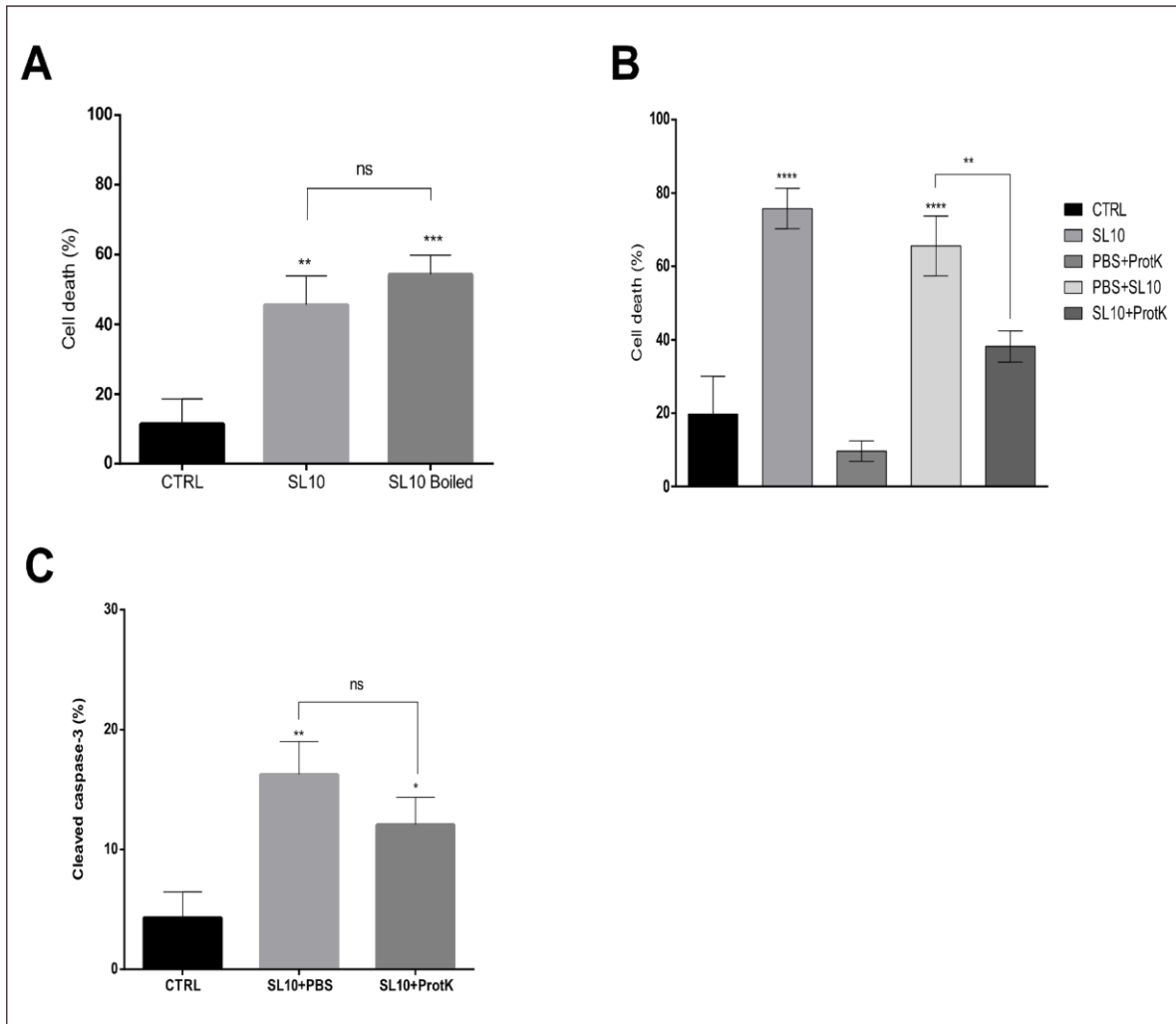
Figure 19 - Pro-apoptotic effect of CS is within compounds resistant to boiling. CS was boiled at 95 ℃ for 5 minutes before stimulation on SH-SY5Y and cell death was then accessed by annexin V and 7AAD staining (A). CS was treated with proteinase K (ProtK) for 1 hour at 37 ℃ before stimulation on SH-SY5Y following cell death assessment by annexin V and 7AAD staining . Prot K was inactivated by boiling at 95 ℃ before cell treatment. PBS 1x was used as a manipulation control (B). Caspase-3 cleavage was verified by flow cytometry upon stimulation with CS after proteinase k treatment (C). Results are expressed as mean ± SD. $P \leq 0.05$ (*), $p \leq 0.01$ (**) and $p \leq 0.001$ (***) compared to each cell's control group were considered significant. Bars represent comparisons between groups.

To investigate if the cytotoxic activity of the tick saliva was dependent of the presence of divalent ions, which mainly includes small protein-based compounds such as lectins or

proteases, the chelating agent EDTA was used to chelate Ca^{2+} and Mg^{2+} within the CS. EDTA cytotoxicity was tested previously (figure 20 A), to find the proper concentration of EDTA that would not impair cell viability, and then incubated with SL10 before cell stimulation. At a concentration of 0.4 mM, EDTA failed to prevent CS-induced apoptosis in SH-SY5Y cells (figure 20 B), suggesting that divalent cations present in the saliva are not significantly involved in the cytotoxic effect of SL10 over NB cells. It must be stressed though that we have not demonstrated that the amount of EDTA used was sufficient to chelate all ions within the saliva.
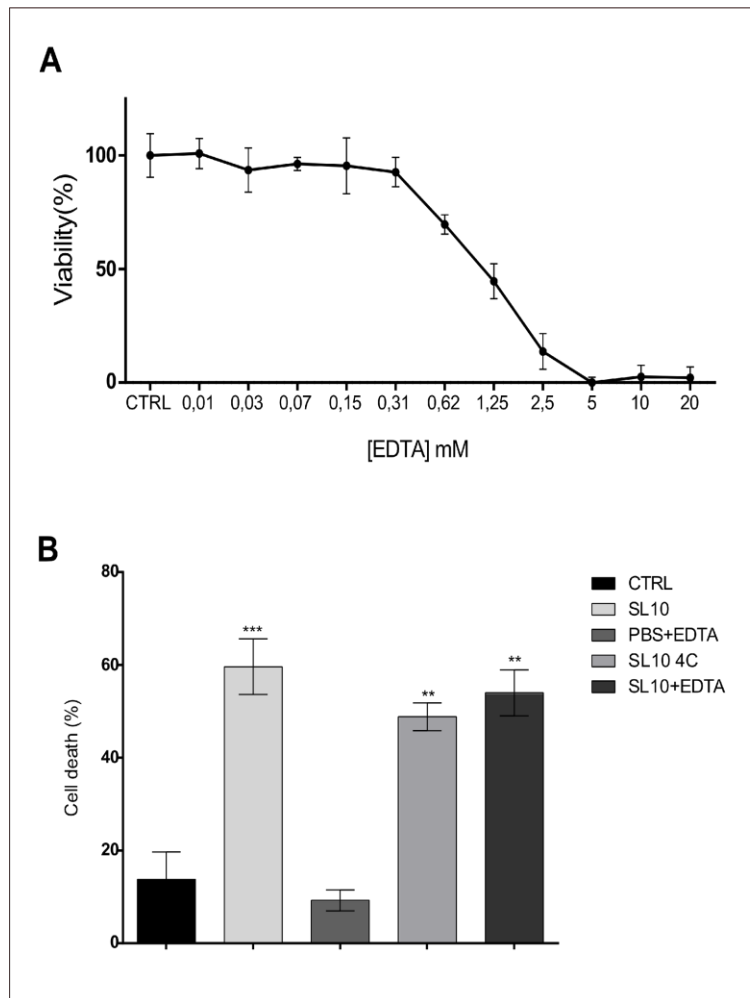
Figure 20- EDTA chelation of ions did not affect SL10 cytotoxicity. Cell viability by methylene blue assay with different concentrations of EDTA on SH-SY5Y cell line (A). Cell death was accessed by annexin V and

7AAD staining after stimulation with 10% of the crude saliva (SL10) and saliva previously treated with 0.4 mM of EDTA for 12 hours at 4°C before it was added to the cells. PBS 1x treatment the same way with EDTA was used as a negative control for EDTA cytotoxicity (PBS+EDTA). The crude saliva was also incubated for 12 hours at 4°C as a control for its cytotoxic activity (SL10 4C). Results are expressed as mean ± SD with $P \leq$ 0.01 (**) and $p \leq 0.001$ (***) compared to the control group considered significant.

Taken together, our results made us conclude that the induction of apoptosis by CS does not rely on folded proteins. If amino-acid-based, it would likely be small peptides, which are usually molecules with some resistance to proteolysis and heat denaturation. Thus, we tested the hypothesis that small molecules, which could have been lost in dialysis during chromatography fractionation, would be responsible for the tumor cell death. Therefore, centrifugal filtration was performed, as illustrated in figure 21A.

As observed, the active effect is fully present in <10 kDa fractions (figure 21 B). Such activity was maintained when fractions were boiled (figure 21 C). That led us to the discovery that the pro-apoptotic potential of the CS is within small molecules that are highly stable and resistant to proteolysis induced by proteinase K and denaturation by high temperatures. To evaluate if such fraction was also selectively impairing only cancer cells, like it is described for the CS [13], non-tumoral stem cells from human exfoliated deciduous teeth (SHED) were treated with the fraction (figure 21 D). As expected, SHED cells were not significantly sensitive to the fraction as well.
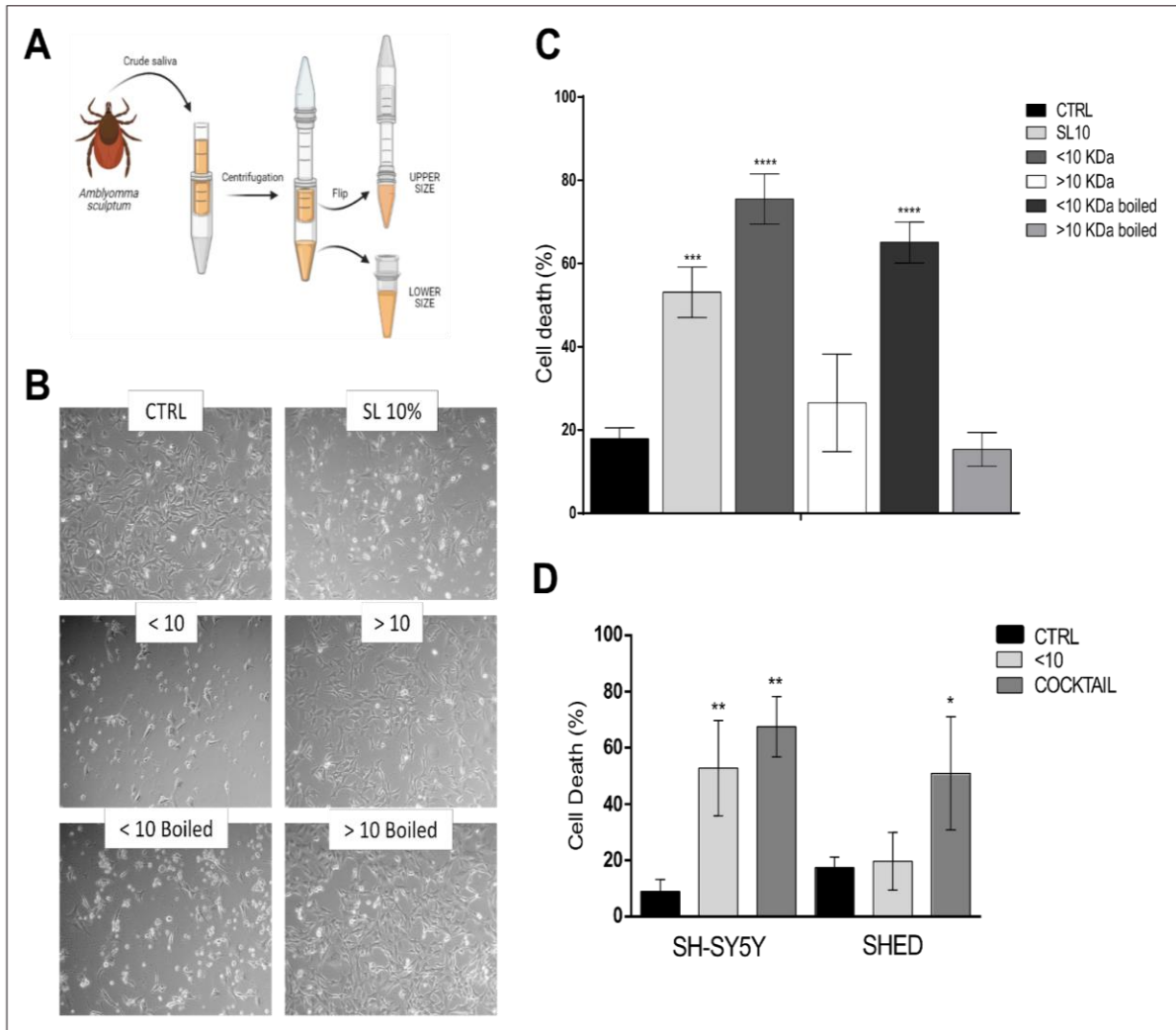
Figure 21 -The activity of the CS is within compounds smaller than 10 kDa. CS was fractionated by molar mass using Vivaspin 6 with 10 kDa cut-off and cells were then stimulated with the fractions smaller (<10) and bigger (>10) than 10 kDa (A) within the saliva, with and without boiling for 5 minutes at 95 ℃. The activity of the different fractions was observed by optical microscopy (B) and annexin V and 7AAD staining (C). Stem cells from human exfoliated deciduous teeth (SHED) and SH-SY5Y were also stimulated with the <10 and the cocktail of chemotherapy drugs (1 uM doxorubicin and 1ug/ml topotocan) as a positive control, followed by cell death detection by annexin V and 7AAD staining (D). Statistics compared to each cells control group. Results are expressed as mean ± SD. P ≤ 0.05 (*), p ≤ 0.01 (**) and p ≤ 0.001 (***) were considered significant.

6.5 **Active fraction induces strong intrinsic apoptosis.**

Another dialysis fractionation was applied to the CS, with a cut-off of 3 kDa. It revealed that saliva's cytotoxic effect was within the <3 kDa fraction (figure 22 A). Differently than observed in SL10, however, the protK was not sufficient to significantly reduce cell death induced by <3 kDa fraction (figure 22 B). Both SL10 and <3 kDa treatments induced cleavage of caspase-9 and caspase-3. However, the <3 kDa active fraction, like the positive control with CMPT, induced significantly higher amounts of cleaved caspase-3 than SL10 (figure 22 C).

Over-expression of Bcl-XL and Mcl-1 prevented caspase-3 cleavage induced by both the active <3 kDa fraction and SL10 (figures 22 D and 22 E). Consistently, inhibiting the intrinsic pathway by over-expressing Bcl-XL and Mcl-1 in these cells impaired appearance of caspase-9 and lamin A and C cleaved products after stimulation with CS and <3 kDa fraction. Similarly, phosphorylation of Jun N-terminal kinase (JNK) was also reduced by the double expression of anti-apoptotic proteins. Caspase-7 might be slightly cleaved, but further investigations are necessary for confirmation. While IRE-1 expression was not impaired (figure F 22).
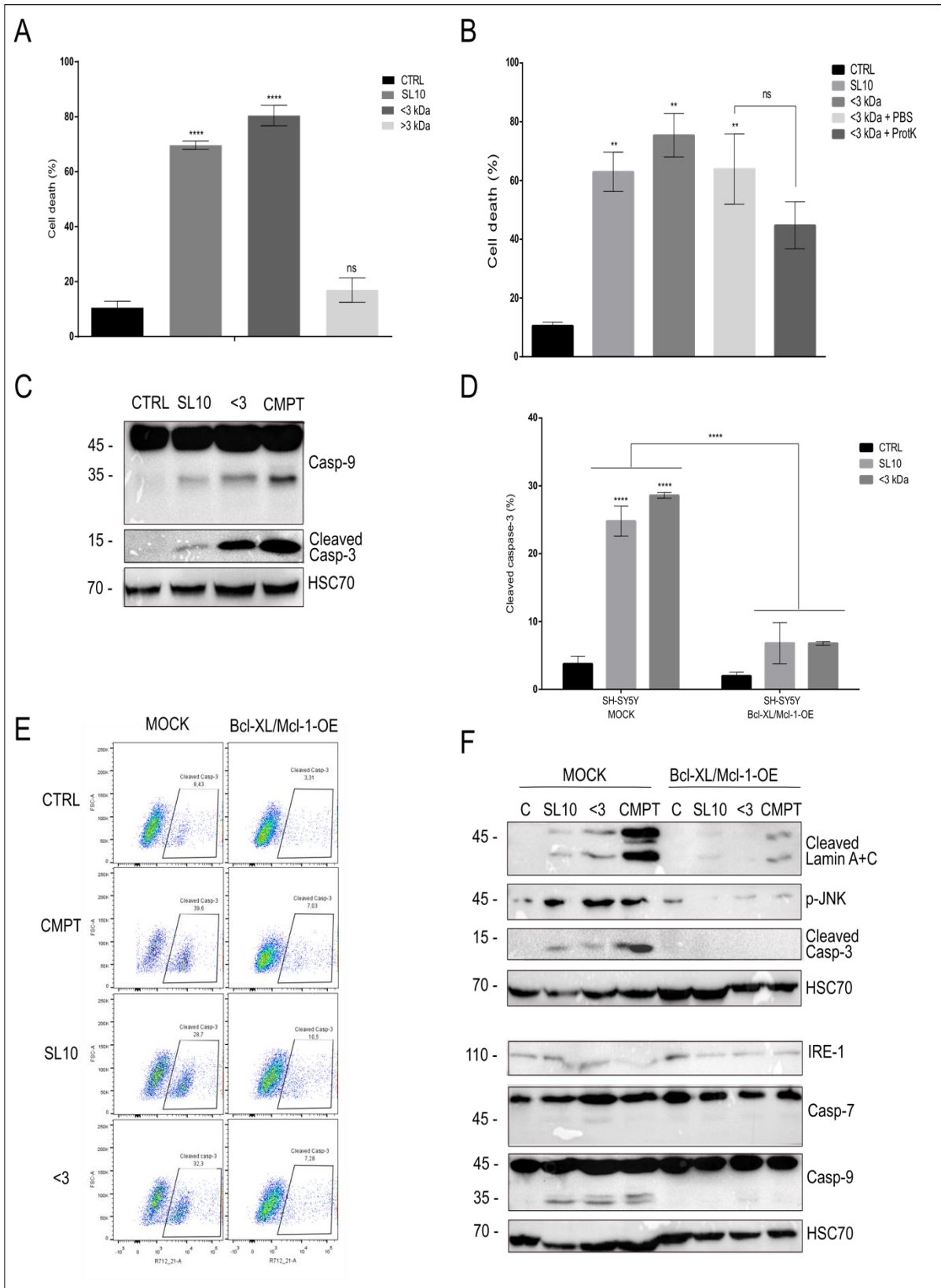
Figure 22 - Lower than 3 kDa fraction from *A. sculptum* saliva induces intrinsic apoptosis in NB cells. SH-SY5Y were treated with SL10 and the lower than 3 kDa fraction (<3), cell death was then accessed by Annexin V and 7AAD staining (A). Lower than <3 kDa fraction was treated with 0,5 mg/ml of proteinase K (ProtK) for 1 hour at 37℃ before stimulation on SH-SY5Y and cell death assessed by annexin V and 7AAD staining. Prot K within the saliva fraction was inactivated by boiling at 95℃ before cell treatment. PBS 1x was used as a manipulation control (B). Cleavage of caspase-3 and caspase-9 were verified by Western Blot (C) and flow cytometry (D/E). Cleavage of lamins, caspase-3 and caspase-9 were analyzed by western blot after treatment with SL10, <3 kDa fraction and CMPT on SH-SY5Y with BclXL/Mcl-1-OE and without (mock) overexpression of Mcl-1 and Bcl-XL (F). Results are expressed as mean ± SD. P ≤ 0.05 (*), p ≤ 0.01 (**) and p ≤ 0.001 (***) were considered significant. (*) Represent comparisons with each cell's control group and bars represent comparisons between groups.

6.1 **Chemical characterization of the low molecular weight fraction from CS**

The low molecular weight fraction was subjected to gas chromatography–mass spectrometry (GC-MS) and nuclear magnetic resonance spectroscopy (H1-NMR) analysis. As observed on table 2, GC-MS analysis showed the presence of different amino acids such as Valine, Leucine, Glycine, Aspartic acid, Glutamic acid, Phenylalanine and N-Acetil Lysine. High glycine presence was mainly attributed to residues from the Vivaspin 6 ultrafiltration devices used for the fractionation of CS by molecular weight. We also detected the presence of sugars such as Mannose, Galactose, Glucose and Galactosamine; along with other organic compounds such as myo-inositol and imizadol. Finally, fatty acid methyl esters (FAME) of 16 and 18 carbons were also identified. Preliminary data (not shown) of MNR also suggest the presence of aliphatic and aromatic peptides. Similarly, HSQC results based

on the spectra at the shifts of 1H confirm the presence of side chains compatible with Alanine, Leucine, Valine, Glutamate, Glutamine, Phenylalanine and Tyrosine.

Table 2 – Compounds found within the <10 kDa fraction by GC-MS analysis.

Amino Acids	%
Valine	0,98
Leucine	1,07
Aspartic acid	6,9
Glutamic acid	1,98
Phenylalanine	3,43
N-Acetil lysine	1,29
Sugars	
Manp	0,44
Galp	0,31
Glcp	3,1
GalNp	0,82
Other organic compounds	
Acetamideacrilate	0,15
Myo-inositol	2,58
Imidazol	2,83
Glycerol-3-acetylated	74,12
Fatty Acid Methyl Esters (FAME)	%
C16:0	23,61
C18:2	19
C18:1	27,53
C18:0	29,93

GC–MS analysis on CP-Sil-5CB capillary column and samples acetylated using pyridine – MeOH–Ac2O.

Manp=Mannose or Mannopyranose, Galp= Galactose or Galactopyranose, Glcp=Glucose or Glucopyranose, GalNp=Galactosamine or Galactosamine pyranose.

7. DISCUSSION

Since it started to be studied in 2011, *A. sculptum* CS has demonstrated high anti-tumoral potential. It induced proliferation rate reduction on melanoma and pancreas adenocarcinoma cells, which was not seen in normal fibroblasts [161]. The cytotoxic activity was also described in breast cancer cell lines, with no cytotoxicity reported in normal breast gland cells [12]. CS was also able to impair endothelial cell proliferation and migration, which was associated with disintegrins and cathepsin-L in the saliva [10]. In addition, coagulation inhibitors derived from CS or salivary glands have also been shown to significantly reduce angiogenic processes through the inhibition of VEGF-A, cell adhesion, and migration [135,162]. Recently, our group demonstrated loss of viability of up to 80% in five NB cell lines (SH-SY5Y, SK-N-SH, CHLA-20, IMR-32, and Be(2)M-17), after 72 hours of incubation with CS, which was associated with cell cycle arrest and cytoskeleton disarrangement [13]. However, the cell death pathways involved had never been studied in detail. In the present study, we investigate how the CS from *A. sculptum* triggers programmed cell death (PCD) in tumoral cell lines in a selective way and the possible compounds present in the CS that would be associated with such cytotoxicity.

We show that CS induces significant cell death in breast cancer, colorectal adenocarcinoma and NB cells (figure 14A). Cell death induced by SL10 was inhibited in all tumor cell lines evaluated by the pan-caspase inhibitor QVD, demonstrating that its effect is dependent on the activation of caspases. NB cells showed intense susceptibility that may be conflicting, at first, with the low or absent levels of initiator caspase-10 or caspase-8 and TRAILR1/DR4. Only SH-SY5Y and Be(2)M17 cells presented TRAILR2/DR5, while only SK-N-SH showed APO-1/FAS receptors, as revealed by blotting analysis (figure 14B), while

the extracellular surface expression of all those receptors, was absent in the SH-SY5Y NB cell line (figure 14C). However, initiator caspase deficiency has been reported before and seems to be a common aspect in neuroblastoma cells [163–165]. A previous study showed that 13 out of 18 NB cell lines presented abnormal DNA methylation, and inactivation of caspase-8 that was correlated to tumor severity and resistance to death receptor-induced apoptosis [166–168]. As for TRAIL receptors, other studies have also demonstrated the absence of TRAILR1/DR4 in the NB cell line evaluated, with some protein level for TRAILR2/DR5 and resistance to TRAIL ligand induced apoptosis [169,170]. Those cells that did show some sensitivity to TRAIL also showed DR5 and caspase-8 expression, or had their caspase-8 expression recovered by demethylating agents [170].

AZA, 5-Aza-2-deoxycytidine (decitabine) or 5-azacytidine (Vidaza), are demethylating agents used for the treatment of several types of cancer, known to recover caspase-8 and caspase-10 expression in many cancer cells [158,171]. In the present study, NB cells were treated with AZA previously to SL10 stimulation. SK-N-SH was the only cell line that significantly responded to AZA with caspase-8 restoration (figure 14D), even though this treatment did not affect the SL10 induced cell death (figure 14E). In contrast, treatment with the pan-caspase inhibitor entirely prevented cell death induced by CS in SK-N-SH cells, either treated or not with AZA.

The proteolytic cascade mediated by caspase activation is associated with many PCD pathways, but their role is essential and mostly related to apoptotic cell death [44]. Cleavage of essential nuclear components to cell function and viability, such as PARP-1 and Lamin A/C, was evidenced after SL10 stimulation on the SH-SY5Y cell line (figure 14B). PARP is possibly the best characterized proteolytic substrate of executioner caspases, mainly caspase-3 and caspase-7 [59]. At the same time, lamins are major structural proteins of the

89

nuclear envelope primarily cleaved by caspase-6 and caspase-3 [61]. Caspase-3, cleaved by many different substrates during apoptotic pathways and largely used as an apoptosis indicator, was also cleaved upon SL10 stimulation on NB cells (figure 14B). In a previous study, CS from *A. sculptum* was also found to induce caspase-3 cleavage in breast cancer cell lines [12].

Deletion, depletion or inhibition of initiator caspases may result in necroptosis triggering upon receptors activation, as a cell death escape route if apoptosis is blocked [99], which is mainly regulated by the activation of proteins of the RIP family [96]. In our study, however, the necroptosis inhibitor NEC did not affect SL10 induced apoptosis over NB cells. On the other hand, the pan-caspase inhibitor QVD alone significantly inhibited cell death induction by SL10, and such inhibition was not increased upon combination of QVD and NEC (figure 17). Suggesting that the activation of extrinsic pathways of apoptosis is unlikely to be associated with the cytotoxicity of CS.

The intrinsic apoptosis pathway can be induced by several factors that generate mitochondria outer membrane permeabilization (MOMP) and consequent release of proapoptotic molecules into the cytoplasm, such as cytochrome C, that leads to activation of caspase-9, responsible for activating downstream executioner caspases, such as caspase-3 [55]. The involvement of MOMP in the proapoptotic activity of *A. sculptum's* saliva was evaluated in NB cell lines SH-SY5Y and Be(2)-M17 overexpressing Mcl-1 and Bcl-XL (figure 16A); since all NB cell lines tested in the present work were deficient for the expression of those proteins, as previously demonstrated in other NB cell lines [172]. Those are antiapoptotic proteins of the Bcl-2 family that interact with and inhibit proapoptotic proteins such as Bax and Bak [57]. The expression of Bcl-XL inhibited CMPT and SL10-

induced cell death, but not Mcl-1 overexpression alone. However, the combination of both increased the antiapoptotic effect compared to Bcl-XL alone (figure 16B).

The reconstitution of both Bcl-XL and Mcl-1 on NB cells prevented not only apoptosis, but also MOMP (figure 17). Suggesting that some pro-apoptotic proteins, such as Bak and Bax, may be activated. These effector pro-apoptotic proteins are mainly activated by BH3-only proteins, and among those, PUMA, BIM, BID and NOXA were described to be effectively sequestered by either Bcl-XL or Mcl-1 [173]. Several different factors are known for inducing BH3 proteins, which include hypoxia, proteasome inhibitors, radiation, ER stress, ischemia and deprivation of cytokines, growth factors and nutrients; that are mainly associated to transcription modulation of others such as p53, CHOP, FOXO3 and miRNAs, for example [174,175].

The possible induced activation of Bax and Bak proteins by CS's compounds may also be associated with ER stress. Upon ER stress, CHOP is up regulated and as a transcription factor, it regulates the expression of many pro-apoptotic genes, leading to activation of BIM, PUMA, NOXA and direct activation of BAK and BAX, and therefore leads to mitochondrial permeabilization [64]. CHOP also downregulates the expression of Bcl-2, Bcl-XL and Mcl-1 anti-apoptotic proteins [70]. Cell cycle arrest by suppression of p21 has also resulted from CHOP over activation [176]. Additionally, ER stress may also activate pro-apoptotic proteins thru IRE-1 activation. For the CS or <3 kDa fraction, however, no significant changes in IRE1 levels were observed (figure 22 F). IRE-1 binds to TNF receptor-associated factor 2 (TRAF2), triggering the activation of caspase-12 [177] and activation of ASK1, that subsequently promotes phosphorylation of JNK [178].

JNK may be activated not only by ER stress, but also by death receptors and reactive species of oxygen (ROS) [179,180]. Its phosphorylation may regulate not only programmed

cell death, but also proliferation and migration [97]. As previous studies have demonstrated along with cell death induced by the CS of *A. sculptum,* cell cycle arrest [13] and inhibition of migration [10], JNK phosphorylation might be a key event on the permeabilization of mitochondria and intrinsic apoptosis induced by compounds found within CS. We have demonstrated here that JNK is phosphorylated upon treatment of NB cells with the CS and fractions extracted from it, but not when Bcl-XL and Mcl-1 are overexpressed (figure 22F). Phosphorylated and active JNK are known as a transcription factor and associated to activation of pro-apoptotic proteins such as BAD, BAX and BID [74].

ROS are short-lived and highly reactive molecules that might, therefore, activate mitochondrial, death receptor and ER pathways of apoptosis [182]. Excessive ROS is mainly produced under stress conditions, such as ER stress or DNA damage, generating increased expression of several proteins, such as p53, PUMA, NOXA, BAX and JNK [183–185]. Excessive intracellular ROS may also affect caspase activity, as their catalytic site cysteins are susceptible to oxidation, which may eventually lead to their cleavage [186,187]. H_2O_2 was described to upregulate FasL, translocating FADD to the plasma membrane and activating caspase-8 [188]. Similarly, upregulation of TRAIL death receptors by ROS was also reported [189]. In mitochondria, ROS may cause hyperpolarization and a collapse in mitochondrial membrane potential and membrane translocation of BAX and BAK [190,191]. Finally, oxidative stress and mitochondrial Ca^{2+} accumulation can trigger opening of mitochondrial permeability transition pores (mPTP) [192].

The function of Ca^{2+} in intrinsic apoptosis is also a complex subject that might involve redox systems and ER stress [193]. The overload of Ca^{2+} influx or its full blockage leads to the opening mPTP and consequently, MOMP [194]. As Bcl-XL has also been reported to block Ca^{2+} induced apoptosis and such pathway may also involve caspase cleavage [195], it

is possible that CS's compounds induce intracellular Ca^{2+} overload. Along with that, the increase of cytoplasmic Ca^{2+} may also be due to its release from the ER lumen thru ER stress or IP3 receptor and such release was also described to be blocked by Bcl-XL and Bcl-2 [196], suggesting another possible involvement of the ER stress on the cytotoxicity of CS, but mediated by the Ca^{2+} overload. Altogether, how mitochondria or effector pro-apoptotic proteins are first activated by CS is still to be further investigated.

Many animal-derived compounds and toxins are known for their anti-tumoral effect associated with mitochondria potential loss [197,198]. Venoms and toxins from snakes, bees, wasps, scorpions, and marine animals have been highly investigated for their activity on cancer immunomodulation, anti-invasive, anti-adhesive, anti-proliferation, and inhibition of metastasis on different cancer cells [199]. Tick saliva is often left aside. However, lectins, proteinases, phospholipases, hyaluronidases, neurotoxins, thrombin inhibitors, Kunitz-like inhibitors, and antimicrobial proteins and peptides are just a few examples of molecules commonly present in the saliva of ticks [199]. Even then, so far, there are no clinical studies involving the use of substances isolated from tick saliva nor drugs available for therapeutic purposes [200].

To identify the nature of CS components that would impair NB cell survival, we performed fractionation by liquid chromatography (figure 18A), similar to what was done by Simons and col. (2011) [160]. Fractions were collected by protein detection and associated in seven pools based on NaCl gradient. Most of the components in arachnid saliva and other arthropods' secretions are proteins [199]; and also, a rich source of bioactive peptides with antitumoral potential [115,159]. Several animal peptides have been found to exert their effects intracellularly, including by causing mitochondrial membrane disruption and mitochondrial-dependent apoptosis [159], as observed with the salivary secretion of *A.*

sculptum. However, none of the fractions showed the same cytotoxic effect as the CS over NB cells (figure 18 B/C). Therefore, it was considered that some could have been degraded, lost, or split during the fractionation process or storage.

Peptide bonds are formed by molecular reactions of dehydration synthesis, which may be resistant to heating but may be effectively cleaved by trypsin or proteases, such as proteinase K [201]. With that in mind, CS was boiled to induce protein denaturation or was treated with proteinase K. Results showed that boiling had no effect on the SL10-induced cell death (figure 19 A), eliminating folded proteins as the source of cytotoxicity. While proteinase K treatment did reduce the efficiency of SL10-induced cell death on SH-SY5Y NB cells (figure 19B), which could suggest the presence of pro-apoptotic peptides within the CS. However, proteinase K did not significantly reduce the cleavage of caspase-3 (figure 19C). We also evaluated if the CS cytotoxicity was dependent on the presence of Ca^{2+} and Mg^{2+} divalent cations by treating the saliva with EDTA chelating agent before cell stimulation (figure 20). But no apparent changes were observed.

CS was then fractionated by molar mass with centrifugation systems to investigate the size of the active compounds (figure 21 A). Even after boiling, the < 10kDa fraction presented cytotoxic activity against the NB cells (figure 21). At the same time, the non-tumoral SHED cells were not significantly sensitive to such fractions (figure 21 D). Esteves and colleagues (2019) reached an active <3 kDa fraction from *A. sculptum´s* CS, associated with the modulation of dendritic cell behavior, allowing *Rickettsia rickettsia* infection in the tick's host [202]. Therefore, we fractionated the CS using centrifugation systems again, but with a cut-off of 3 KDa. In our results, such a fraction demonstrated the same cytotoxic effect as the CS or the < 10kDa fraction (figure 22 A). It significantly induced cleavage of caspase-

9 and caspase-3 (figure 22 C), which was reduced by the presence of Bcl-XL and Mcl-1 (figure 22 D/E), just like lamins cleavage (figure 22 F).

However, cell death was not significantly reduced when the <3 kDa fraction was treated with proteinase K (figure 22 B), which could be associated with a more substantial activity over cell death compared to the CS. But also, some peptides containing cystine knot motifs are frequently considered to have high levels of thermal, chemical, and enzymatic stability due to cross-bracing provided by the disulfide bonds, which could explain some resistance to proteinase K cleavage. Those peptides are largely found in arthropod venoms [203,204] and commonly target voltage-gated ion channels, show antibacterial, hemolytic and antiviral agents [205]. Because of their stability, they are becoming increasingly popular as protein engineering scaffolds targeting agents for chemotherapy [206]. For example, chlorotoxin (CTX) is a 4kDa cystine knot peptide that acts as a chloride channel inhibitor found in the *Leiurus quinquestriatus* scorpion venom that naturally targets tumors cells, including neuroblastoma [117]. Or the neurotoxin Huwentoxin from the Chinese spider *Selenocosmia huwena,* another cystine knot peptide that acts as a calcium channel blocker and has demonstrated potent antitumoral and analgesic properties [207].

Although little is specifically known about the compounds within tick saliva, phylogenomic analysis of nuclear protein-coding sequences from arthropod species suggests they share many similarities with other arthropod species [208] and should even be considered venomous animals as their salivary secretion share more molecular components with venomous than non-venomous animals [209]. Among arthropods, the mastoparan-L or analogues peptide isolated from wasp venoms [210], Bengalin isolated from the Indian black scorpion venom [211], linear α-helical [212] or Pancrastistatin [213] from spider venoms, are just a few examples of membrane interacting and penetrating peptides that selectively

lead cancer cells to mitochondria associated apoptosis. Besides peptides, the saliva of ticks may also hold other small compounds, such as cysteine-rich secretory proteins, cystatin, defensins, hyaluronidases, lectins, metalloproteases, phospholipases, serine proteases and amides [214]. Our preliminary analyses of the chemical composition of the low molecular weight fraction from *A. sculptum's* saliva confirm the presence of several amino acids, along with aliphatic and aromatic peptides (table 2), and also the presence of sugars, fatty acid methyl esters and other organic compounds such as myo-inositol and imizadol. All of those may be candidates as the sources of anti-tumoral compounds within the saliva of *A. sculptum*.

Many low molecular weight compounds within tick saliva are still to be found. To reliably suggest the possible compounds within the <3kDa fraction from *A. sculptum* saliva responsible for the mitochondria dependent apoptotic induction in NB cells, further analysis of its biochemical composition are needed. So far, we confirm the strong potential that this fraction holds as a source for novel anticancer compounds, highly stable and capable of selectively inducing cancer cells to mitochondria dependent apoptosis in NB cells, and that such effect is considerably blocked by the overexpression of Bcl-XL and Mcl-1. How exactly mitochondria are first affected, however, still needs further investigations, we might only suggest some initial triggers, such as activation of BH3-only or JNK proteins, ER stress, excessive ROS production or Ca2+ influx unbalance (figure 23).
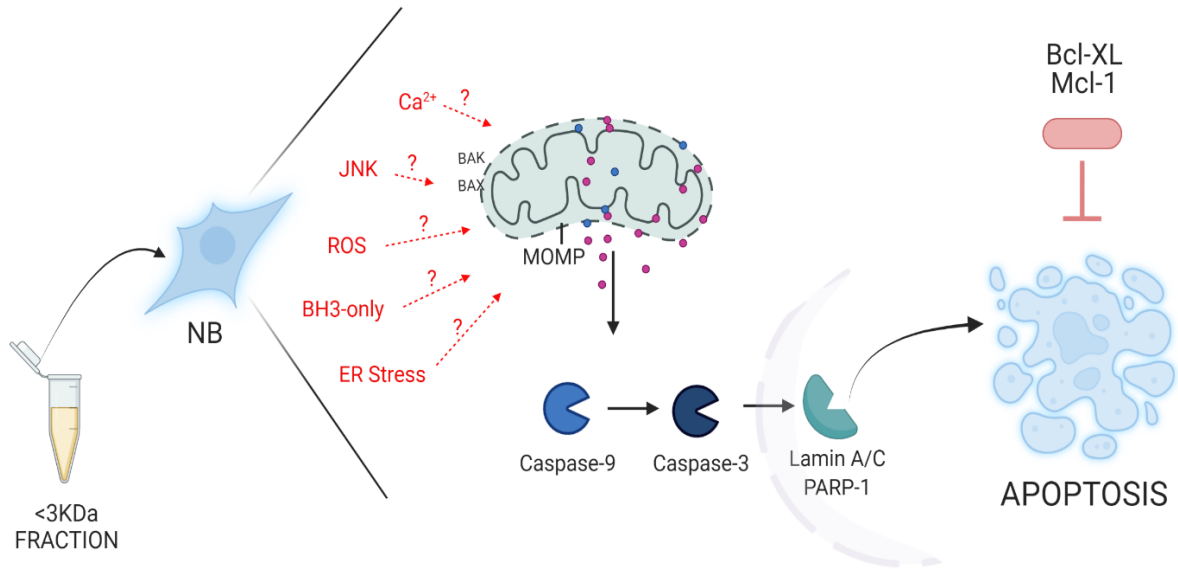
Figure 23 - Lower than 3KDa fraction from the crude saliva of the tick *Amblyomma sculptum* triggers intrinsic apoptosis in neuroblastoma (NB) cells. Red arrows indicate possible triggers for mitochondrial membrane permeabilization.

8. CONCLUSIONS

The programmed cell death pathways associated to the cytotoxic effect of the crude saliva of the tick *Amblyomma scultum* over cancer cells has, to date, never been fully elucidated. Here, we describe for the first time that its crude salivary secretion induces mitochondria membrane permeabilization on neuroblastoma cells, followed by cleavage of caspase-9 and caspase-3, along with cleavage of essential nuclear components that characterize intrinsic apoptosis induction. We also found that such activity is within molecules smaller than 3 kDa size, that are highly stable to denaturation and show some resistance to proteolysis. The pro-apoptotic effect of such salivary fraction is effectively inhibited by anti-apoptotic proteins such as Bcl-XL and Mcl-1, suggesting the involvement of Bak and/or Bax proteins, or direct depolarization of mitochondrial membrane by factors such as ROS or Ca^{2+} overload. Further analyses are still necessary to elucidate how mitochondria is first affected. Our initial analysis of compounds found within this low molecular weight fraction indicates the presence of many different nature of molecules, including peptides. But further investigation will also be necessary to characterize those potentially pro-apoptotic compounds. Altogether, our findings offer new, potentially useful information for further studies regarding the antitumoral potential within tick saliva that are required to extend our findings to additional conventional chemotherapeutic drug development.

9. FUTURE PERSPECTIVES

Further biochemical analysis regarding the investigation of the molecules and compounds found within the low molecular weight fraction of *A scultum's* saliva are already been caried out by gas chromatography–mass spectrometry (GC-MS) and Proton nuclear magnetic resonance (H+-NMR). In addition, in the coming months, we expect to investigate the mechanism by which the mitochondria are first affected by this salivary fraction. For that, BAX/BAK channel blockers will be used to treat the cells previously to the saliva treatment. ROS production will be evaluated by fluorogenic dyes. And new analysis of apoptotic protein levels, as well as ER stress proteins, upon treatment with the salivary fraction will also be necessary.

10. STUDY LIMITATIONS

The present study has some limitations. Its main limitation is regarding the acquisition of CS. We need about 100 female ticks to obtain only about 1 ml of saliva; collection and maintenance of ticks, as well as the collection of saliva itself are time consuming. Therefore, analysis such as the ion exchange chromatography, GC-MS or H+-NMR that need very high amounts of sample, need a long time to be performed, as it is necessary to accumulate a large amount of saliva. That, together with eventual issues on the transportation of the CS from the Butantan Institute to PUCPR and Burgundy University has significantly delayed our chronograms. Because of such limitation, the biochemical analysis regarding the investigation of the CS or <3 KDa fraction chemical characterization are still inconclusive and more time will be needed for those to be completed. Without such information, it is not yet possible to identify the specific source of the antitumoral activity. Also, those analysis of chromatography and spectrometry could not be performed in our own laboratories, as we do not own the necessary equipment, and relied on other collaborators.

Additionally, further studies are still necessary to fully elucidate how the compounds found with the active fraction first induce MOMP, leading to apoptotic cell death. We were able to describe that apoptosis is triggered thru the mitochondria permeabilization on NB cells, but it is still not yet clear if BAX and BAK are involved, and if so, what leads to its activation. Along with that, the CS possibly has different mechanisms of action for different tumor cells, such as HCT-116, and further studies are necessary to investigate such possible mechanisms in other cell models.

11.FINANCIAL SUPPORT

12.SUPPLEMENTARY ACTIVITIES

Along with the development of the project presented in this report, other studies were also carried out during the doctorate program under the supervision of Dra. Selene Elifio Esposito and Dr. Olivier Micheau. Those that have already generated publications on scientific journals are shown in Annex I.

13.REFERENCES

1. Huber, K.; Janoueix-lerosey, I.; Kummer, W.; Rohrer, H.; Tischler, A.S.; Janoueix-lerosey, I.; Rohrer, H. The Sympathetic Nervous System : Malignancy , Disease , and Novel Functions. **2018**, 163–170, doi:10.1007/s00441-018-2831-0.
2. Wolden, S.L.; Roberts, S.S. *Neuroblastoma*; Fourth Edi.; Elsevier Inc., 2016;
3. Berlanga, P.; Cañete, A.; Castel, V. Advances in Emerging Drugs for the Treatment of Neuroblastoma. *Expert Opinion on Emerging Drugs* **2017**, *22*, 63–75, doi:10.1080/14728214.2017.1294159.
4. Ouyang, L.; Shi, Z.; Zhao, S.; Wang, F.T.; Zhou, T.T.; Liu, B.; Bao, J.K. Programmed Cell Death Pathways in Cancer: A Review of Apoptosis, Autophagy and Programmed Necrosis. *Cell Proliferation* **2012**, *45*, 487–498, doi:10.1111/j.1365-2184.2012.00845.x.
5. Newman, D.J.; Cragg, G.M. Natural Products as Sources of New Drugs over the Nearly Four Decades from 01/1981 to 09/2019. *Journal of Natural Products* 2020, *83*, 770–803.
6. Aounallah, H.; Bensaoud, C.; M'ghirbi, Y.; Faria, F.; Chmelař, J.; Kotsyfakis, M. Tick Salivary Compounds for Targeted Immunomodulatory Therapy. *Frontiers in Immunology* 2020, *11*.
7. Chmelar, J.; Kotál, J.; Kovaríková, A.; Kotsyfakis, M. The Use of Tick Salivary Proteins as Novel Therapeutics. *Frontiers in Physiology* 2019, *10*.
8. Martins, T.F.; Barbieri, A.R.M.; Costa, F.B.; Terassini, F.A.; Camargo, L.M.A.; Peterka, C.R.L.; de C Pacheco, R.; Dias, R.A.; Nunes, P.H.; Marcili, A.; et al. Geographical Distribution of Amblyomma Cajennense (Sensu Lato) Ticks (Parasitiformes: Ixodidae) in Brazil, with Description of the Nymph of A. Cajennense (Sensu Stricto). *Parasites and Vectors* **2016**, *9*, doi:10.1186/s13071-016-1460-2.
9. Oliveira, D.G.L.; Simons, S.M.; Chudzinski-Tavassi, A.M.; Zamboni, C.B. Analysis of Saliva from Amblyomma Cajennense (Acari: Ixodidae) Species from Brazil by NAA. *Journal of Radioanalytical and Nuclear Chemistry* **2012**, *291*, 385–388, doi:10.1007/s10967-011-1265-x.
10. de Sá Junior, P.L.; Dias Câmara, D.A.; Sciani, J.M.; Porcacchia, A.S.; Moreira Fonseca, P.M.; Mendonça, R.Z.; Elifio-Esposito, S.; Simons, S.M. Antiproliferative and Antiangiogenic Effect of Amblyomma Sculptum (Acari: Ixodidae) Crude Saliva in Endothelial Cells in Vitro. *Biomedicine and Pharmacotherapy* **2019**, *110*, 353–361, doi:10.1016/j.biopha.2018.11.107.
11. Simons, S.M.; Júnior, P.L. de S.; Faria, F.; Batista, I. de F.C.; Barros-Battesti, D.M.; Labruna, M.B.; Chudzinski-Tavassi, A.M. The Action of Amblyomma Cajennense Tick Saliva in Compounds of the Hemostatic System and Cytotoxicity in Tumor Cell Lines. *Biomedicine and Pharmacotherapy* **2011**, *65*, 443–450, doi:10.1016/j.biopha.2011.04.030.
12. Sousa, A.C.P.; Oliveira, C.J.F.; Szabó, M.P.J.; Silva, M.J.B. Anti-Neoplastic Activity of Amblyomma Sculptum, Amblyomma Parvum and Rhipicephalus Sanguineus Tick Saliva on Breast Tumor Cell Lines. *Toxicon* **2018**, *148*, 165–171, doi:10.1016/j.toxicon.2018.04.024.

13. Nascimento, T.G. do; Vieira, P.S.; Cogo, S.C.; Dias-Netipanyj, M.F.; França Junior, N. de; Câmara, D.A.D.; Porcacchia, A.S.; Mendonça, R.Z.; Moreno-Amaral, A.N.; Sá Junior, P.L. de; et al. Antitumoral Effects of Amblyomma Sculptum Berlese Saliva in Neuroblastoma Cell Lines Involve Cytoskeletal Deconstruction and Cell Cycle Arrest. *Revista Brasileira de Parasitologia Veterinaria* **2019**, *28*, 126–133, doi:10.1590/s1984-296120180098.

14. Sung, H.; Ferlay, J.; Siegel, R.L.; Laversanne, M.; Soerjomataram, I.; Jemal, A.; Bray, F. Global Cancer Statistics 2020: GLOBOCAN Estimates of Incidence and Mortality Worldwide for 36 Cancers in 185 Countries. *CA: A Cancer Journal for Clinicians* **2021**, *71*, 209–249, doi:10.3322/caac.21660.

15. INCA Estimativa - Incidência Do Câncer No Brasil Available online: https://www.inca.gov.br/sites/ufu.sti.inca.local/files//media/document//estimativa-2020-incidencia-de-cancer-no-brasil.pdf (accessed on 20 January 2021).

16. Siegel, R.L.; Miller, K.D.; Fuchs, H.E.; Jemal, A. Cancer Statistics, 2021. *CA: A Cancer Journal for Clinicians* **2021**, *71*, 7–33, doi:10.3322/caac.21654.

17. Organization, W.H. WHO Global Initiative for Childhood Cancer. *Pediatric Hematology Oncology Journal* **2020**, *5*, 145–150, doi:10.1016/j.phoj.2020.06.005.

18. National Cancer Institute What Is Cancer? Available online: https://www.cancer.gov/about-cancer/understanding/what-is-cancer (accessed on 23 February 2021).

19. Peters, J.M.; Gonzalez, F.J. The Evolution of Carcinogenesis. *Toxicological Sciences* 2018, *165*, 272–276.

20. Hanahan, D.; Weinberg, R.A. Hallmarks of Cancer: The next Generation. *Cell* 2011, *144*, 646–674.

21. Miller, K.D.; Siegel, R.L.; Lin, C.C.; Mariotto, A.B.; Kramer, J.L.; Rowland, J.H.; Stein, K.D.; Alteri, R.; Jemal, A. Cancer Treatment and Survivorship Statistics, 2016. *CA: A Cancer Journal for Clinicians* **2016**, *66*, 271–289, doi:10.3322/caac.21349.

22. DeVita, V.T.; Chu, E. A History of Cancer Chemotherapy. *Cancer Research* 2008, *68*, 8643–8653.

23. Instituto Nacional do Câncer - INCA *Câncer Na Criança e Adolescente No Brasil: Dados Dos Registros de Base Populacional e de Mortalidade*; Rio de Janeiro, 2008; ISBN 9788573181395.

24. American Cancer Society Neuroblastoma Survival Rates by Risk Group Available online: https://www.cancer.org/cancer/neuroblastoma/detection-diagnosis-staging/survival-rates.html (accessed on 11 November 2021).

25. Morgenstern, D.A.; London, W.B.; Stephens, D.; Volchenboum, S.L.; Simon, T.; Nakagawara, A.; Shimada, H.; Schleiermacher, G.; Matthay, K.K.; Cohn, S.L.; et al. Prognostic Significance of Pattern and Burden of Metastatic Disease in Patients with Stage 4 Neuroblastoma: A Study from the International Neuroblastoma Risk Group Database. *European Journal of Cancer* **2016**, *65*, 1–10, doi:10.1016/j.ejca.2016.06.005.

26. Olsen, T.; Otte, J.; Mei, S.; Kameneva, P.; Björklund, Å.; Kryukov, E.; Hou, Z.; Johansson, A.; Sundström, E.; Martinsson, T.; et al. Malignant Schwann Cell Precursors Mediate Intratumoral Plasticity in Human Neuroblastoma. *bioRxiv* **2020**, 2020.05.04.077057, doi:10.1101/2020.05.04.077057.

27.   Johnsen, J.I.; Dyberg, C.; Wickström, M. Neuroblastoma—A Neural Crest Derived Embryonal Malignancy. *Frontiers in Molecular Neuroscience* 2019, *12*.

28.   Kameneva, P.; Kastriti, M.E.; Adameyko, I. Neuronal Lineages Derived from the Nerve-Associated Schwann Cell Precursors. *Cellular and Molecular Life Sciences* 2020, *78*, 513–529.

29.   Gartlgruber, M.; Sharma, A.K.; Quintero, A.; Dreidax, D.; Jansky, S.; Park, Y.G.; Kreth, S.; Meder, J.; Doncevic, D.; Saary, P.; et al. Super Enhancers Define Regulatory Subtypes and Cell Identity in Neuroblastoma. *Nature Cancer* **2021**, *2*, 114–128, doi:10.1038/s43018-020-00145-w.

30.   Veschi, V.; Verona, F.; Thiele, C.J. Cancer Stem Cells and Neuroblastoma: Characteristics and Therapeutic Targeting Options. *Frontiers in Endocrinology* **2019**, *10*, 1–10, doi:10.3389/fendo.2019.00782.

31.   Olsen, T.K.; Otte, J.; Mei, S.; Kameneva, P.; Björklund, Å.; Kryukov, E.; Hou, Z.; Johansson, A.; Sundström, E.; Martinsson, T.; et al. Malignant Schwann Cell Precursors Mediate Intratumoral Plasticity in Human Neuroblastoma. *bioRxiv* **2020**, doi:10.1101/2020.05.04.077057.

32.   Campos Cogo, S.; Gradowski Farias da Costa do Nascimento, T.; de Almeida Brehm Pinhatti, F.; de França Junior, N.; Santos Rodrigues, B.; Regina Cavalli, L.; Elifio-Esposito, S. An Overview of Neuroblastoma Cell Lineage Phenotypes and in Vitro Models. *Experimental Biology and Medicine* **2020**, *245*, 1637–1647, doi:10.1177/1535370220949237.

33.   American Cancer Society Neuroblastoma Stages and Prognostic Markers Available online: https://www.cancer.org/cancer/neuroblastoma/detection-diagnosis-staging/staging.html.

34.   Brodeur, G.M.; Pritchard, J.; Berthold, F.; Carlsen, N.L.; Castel, V.; Castelberry, R.P.; de Bernardi, B.; Evans, A.E.; Favrot, M.; Hedborg, F. Revisions of the International Criteria for Neuroblastoma Diagnosis, Staging, and Response to Treatment. *Journal of Clinical Oncology* **1993**, *11*, 1466–1477, doi:10.1200/JCO.1993.11.8.1466.

35.   Wylie, L.; Philpott, A. Neuroblastoma Progress on Many Fronts: The Neuroblastoma Research Symposium. *Pediatric Blood and Cancer* **2012**, *58*, 649–651, doi:10.1002/pbc.23329.

36.   Cohn, S.L.; Pearson, A.D.J.; London, W.B.; Monclair, T.; Ambros, P.F.; Brodeur, G.M.; Faldum, A.; Hero, B.; Iehara, T.; Machin, D.; et al. The International Neuroblastoma Risk Group (INRG) Classification System: An INRG Task Force Report. *Journal of Clinical Oncology* **2009**, *27*, 289–297, doi:10.1200/JCO.2008.16.6785.

37.   Whittle, S.B.; Smith, V.; Doherty, E.; Zhao, S.; McCarty, S.; Zage, P.E. Overview and Recent Advances in the Treatment of Neuroblastoma. *Expert Review of Anticancer Therapy* 2017, *17*, 369–386.

38.   Anderson, S.: J.; Elliott, M.; Gaze, M.; Gray, J.; Makin, G.; Squire, R.; Ramanujachar, R.; Tweddle, D.; Wheeler, K. *CHILDREN'S CANCER AND LEUKAEMIA GROUP (CCLG) NEUROBLASTOMA SPECIAL INTEREST GROUP Treatment of Patients with Low/Intermediate Risk Neuroblastoma On Behalf of CCLG Neuroblastoma*; 2015;

39.   Smith, V.; Foster, J. High-Risk Neuroblastoma Treatment Review. *Children* **2018**, *5*, 114, doi:10.3390/children5090114.

40. Modak, S.; Cheung, N.K. v. Neuroblastoma: Therapeutic Strategies for a Clinical Enigma. *Cancer Treatment Reviews* **2010**, *36*, 307–317, doi:10.1016/J.CTRV.2010.02.006.

41. Wagner, L.M.; Danks, M.K. New Therapeutic Targets for the Treatment of High-Risk Neuroblastoma. *Journal of Cellular Biochemistry* **2009**, *107*, 46–57, doi:10.1002/JCB.22094.

42. Galluzzi, L.; Vitale, I. Molecular Mechanisms of Cell Death: Recommendations of the Nomenclature Committee on Cell Death 2018. *Cell Death & Differentiation* **2018**, *25*, 486–541, doi:10.1038/s41418-017-0012-4.

43. Kerr, J.F.R.; Wyllie, A.H.; Currie, A.R. Apoptosis: A Basic Biological Phenomenon with Wide-Ranging Implications in Tissue Kinetics. *British Journal of Cancer* **1972**, *26*, 239–257, doi:10.1038/bjc.1972.33.

44. Mishra, A.P.; Salehi, B.; Sharifi-Rad, M.; Pezzani, R.; Kobarfard, F.; Sharifi-Rad, J.; Nigam, M. Programmed Cell Death, from a Cancer Perspective: An Overview. *Molecular Diagnosis and Therapy* 2018, *22*, 281–295.

45. Shalini, S.; Dorstyn, L.; Dawar, S.; Kumar, S. Old, New and Emerging Functions of Caspases. *Cell Death and Differentiation* 2015, *22*, 526–539.

46. van Opdenbosch, N.; Lamkanfi, M. Caspases in Cell Death, Inflammation, and Disease. *Immunity* 2019, *50*, 1352–1364.

47. Solier, S.; Fontenay, M.; Vainchenker, W.; Droin, N.; Solary, E. Non-Apoptotic Functions of Caspases in Myeloid Cell Differentiation. *Cell Death and Differentiation* **2017**, *24*, 1337–1347, doi:10.1038/cdd.2017.19.

48. Sordet, O.; Rébé, C.; Plenchette, S.; Zermati, Y.; Hermine, O.; Vainchenker, W.; Garrido, C.; Solary, E.; Dubrez-Daloz, L. Specific Involvement of Caspases in the Differentiation of Monocytes into Macrophages. *Blood* **2002**, *100*, 4446–4453, doi:10.1182/BLOOD-2002-06-1778.

49. Schneider, P.; Tschopp, J. Apoptosis Induced by Death Receptors. In Proceedings of the Pharmaceutica Acta Helvetiae; Pharm Acta Helv, March 2000; Vol. 74, pp. 281–286.

50. Micheau, O.; Tschopp, J. Induction of TNF Receptor I-Mediated Apoptosis via Two Sequential Signaling Complexes. *Cell* **2003**, *114*, 181–190, doi:10.1016/S0092-8674(03)00521-X.

51. Yang, A.; Wilson, N.S.; Ashkenazi, A. Proapoptotic DR4 and DR5 Signaling in Cancer Cells: Toward Clinical Translation. *Current Opinion in Cell Biology* 2010, *22*, 837–844.

52. Wong, R.S. Apoptosis in Cancer: From Pathogenesis to Treatment. *Journal of Experimental and Clinical Cancer Research* 2011, *30*.

53. Elmore, S. Apoptosis: A Review of Programmed Cell Death. *Toxicologic Pathology* **2007**, *35*, 495–516, doi:10.1080/01926230701320337.

54. Belizário, J.E.; Alves, I.; Occhiucci, J.M.; Garay-Malpartida, M.; Sesso, A. A Mechanistic View of Mitochondrial Death Decision Pores. *Brazilian Journal of Medical and Biological Research* 2007, *40*, 1011–1024.

55. Wong, R.S.Y. Apoptosis in Cancer: From Pathogenesis to Treatment. *Journal of Experimental and Clinical Cancer Research* **2011**, *30*, 1–14, doi:10.1186/1756-9966-30-87.

56. Burlacu, A. Regulation of Apoptosis by Bcl-2 Family Proteins. *Journal of Cellular and Molecular Medicine* **2003**, *7*, 249–257, doi:10.1111/j.1582-4934.2003.tb00225.x.

57. Kale, J.; Osterlund, E.J.; Andrews, D.W. BCL-2 Family Proteins: Changing Partners in the Dance towards Death. *Official journal of the Cell Death Differentiation Association* **2018**, *25*, 65–80, doi:10.1038/cdd.2017.186.

58. Kivinen, K.; Kallajoki, M.; Taimen, P. Caspase-3 Is Required in the Apoptotic Disintegration of the Nuclear Matrix. *Experimental Cell Research* **2005**, *311*, 62–73, doi:10.1016/j.yexcr.2005.08.006.

59. Vyas, S.; Chesarone-Cataldo, M.; Todorova, T.; Huang, Y.H.; Chang, P. A Systematic Analysis of the PARP Protein Family Identifies New Functions Critical for Cell Physiology. *Nature Communications* **2013**, *4*, doi:10.1038/ncomms3240.

60. Cohen, G.M. Caspases: The Executioners of Apoptosis. *Biochemical Journal* 1997, *326*, 1–16.

61. Broers, J.L.V.; Ramaekers, F.C.S. The Role of the Nuclear Lamina in Cancer and Apoptosis. *Advances in Experimental Medicine and Biology* **2014**, *773*, 27–48, doi:10.1007/978-1-4899-8032-8_2.

62. Senichkin, V. v.; Pervushin, N. v.; Zuev, A.P.; Zhivotovsky, B.; Kopeina, G.S. Targeting Bcl-2 Family Proteins: What, Where, When? *Biochemistry (Moscow)* 2020, *85*, 1210–1226.

63. Cory, S.; Adams, J.M. The BCL2 Family: Regulators of the Cellular Life-or-Death Switch. *Nature Reviews Cancer* 2002, *2*, 647–656.

64. Kim, C.; Kim, B. Anti-Cancer Natural Products and Their Bioactive Compounds Inducing ER Stress-Mediated Apoptosis: A Review. *Nutrients* 2018, *10*.

65. Schröder, M.; Kaufman, R.J. The Mammalian Unfolded Protein Response. *Annual Review of Biochemistry* 2005, *74*, 739–789.

66. Chen, Y.; Brandizzi, F. IRE1: ER Stress Sensor and Cell Fate Executor. *Trends in Cell Biology* **2013**, *23*, 547–555, doi:10.1016/j.tcb.2013.06.005.

67. Tabas, I.; Ron, D. Integrating the Mechanisms of Apoptosis Induced by Endoplasmic Reticulum Stress. *Nature Cell Biology* 2011, *13*, 184–190.

68. Shemorry, A.; Harnoss, J.M.; Guttman, O.; Marsters, S.A.; Kőműves, L.G.; Lawrence, D.A.; Ashkenazi, A. Caspase-Mediated Cleavage of IRE1 Controls Apoptotic Cell Commitment during Endoplasmic Reticulum Stress. *eLife* **2019**, *8*, doi:10.7554/eLife.47084.

69. Banerjee, A.; Ahmed, H.; Yang, P.; Czinn, S.J.; Blanchard, T.G. Endoplasmic Reticulum Stress and IRE-1 Signaling Cause Apoptosis in Colon Cancer Cells in Response to Andrographolide Treatment. *Oncotarget* **2016**, *7*, 41432–41444, doi:10.18632/oncotarget.9180.

70. Hu, H.; Tian, M.; Ding, C.; Yu, S. The C/EBP Homologous Protein (CHOP) Transcription Factor Functions in Endoplasmic Reticulum Stress-Induced Apoptosis and Microbial Infection. *Frontiers in Immunology* 2019, *10*, 3083.

71. Dufour, F.; Rattier, T.; Constantinescu, A.A.; Zischler, L.; Morlé, A.; Mabrouk, H. ben; Humblin, E.; Jacquemin, G.; Szegezdi, E.; Delacote, F.; et al. TRAIL Receptor Gene Editing Unveils TRAIL-R1 as a Master Player of Apoptosis Induced by TRAIL and ER Stress. *Oncotarget* **2017**, *8*, 9974–9985, doi:10.18632/ONCOTARGET.14285.

72. Lam, M.; Marsters, S.; Ashkenazi, A.; Walter, P. Misfolded Proteins Bind and Activate Death Receptor 5 to Trigger Apoptosis during Unresolved Endoplasmic Reticulum Stress. *eLife* **2020**, *9*, doi:10.7554/ELIFE.52291.

73. Sui, X.; Kong, N.; Ye, L.; Han, W.; Zhou, J.; Zhang, Q.; He, C.; Pan, H. P38 and JNK MAPK Pathways Control the Balance of Apoptosis and Autophagy in Response to Chemotherapeutic Agents. *Cancer Letters* 2014, *344*, 174–179.

74. Dhanasekaran, D.N.; Reddy, E.P. JNK Signaling in Apoptosis. *Oncogene* 2008, *27*, 6245–6251.

75. Chen, Y.J.; Liu, W.H.; Kao, P.H.; Wang, J.J.; Chang, L. sen Involvement of P38 MAPK- and JNK-Modulated Expression of Bcl-2 and Bax in Naja Nigricollis CMS-9-Induced Apoptosis of Human Leukemia K562 Cells. *Toxicon* **2010**, *55*, 1306–1316, doi:10.1016/j.toxicon.2010.01.024.

76. Ham, J.; Eilers, A.; Whitfield, J.; Neame, S.J.; Shah, B. C-Jun and the Transcriptional Control of Neuronal Apoptosis. *Biochemical Pharmacology* **2000**, *60*, 1015–1021, doi:10.1016/S0006-2952(00)00372-5.

77. Dhanasekaran, D.N.; Premkumar Reddy, E. JNK-Signaling: A Multiplexing Hub in Programmed Cell Death. *Genes and Cancer* 2017, *8*, 682–694.

78. Jin, H.O.; Park, I.C.; An, S.; Lee, H.C.; Woo, S.H.; Hong, Y.J.; Lee, S.J.; Park, M.J.; Yoo, D.H.; Rhee, C.H.; et al. Up-Regulation of Bak and Bim via JNK Downstream Pathway in the Response to Nitric Oxide in Human Glioblastoma Cells. *Journal of Cellular Physiology* **2006**, *206*, 477–486, doi:10.1002/jcp.20488.

79. Prakasam, A.; Ghose, S.; Oleinik, N. v.; Bethard, J.R.; Peterson, Y.K.; Krupenko, N.I.; Krupenko, S.A. JNK1/2 Regulate Bid by Direct Phosphorylation at Thr59 in Response to ALDH1L1. *Cell Death and Disease* **2014**, *5*, doi:10.1038/cddis.2014.316.

80. Deng, Y.; Ren, X.; Yang, L.; Lin, Y.; Wu, X. *A JNK-Dependent Pathway Is Required for TNF-Induced Apoptosis Induction of NF-B Has Been Shown to Inhibit TNF-Results Mediated JNK Activation and Blocking NF-B Results in Sustained Activation of JNK, Which May Directly Promote Mitochondria Pathway Is Crit*; 2003; Vol. 115;.

81. Mizushima, N. A Brief History of Autophagy from Cell Biology to Physiology and Disease. *Nature Cell Biology* **2018**, *20*, 521–527, doi:10.1038/s41556-018-0092-5.

82. Bialik, S.; Dasari, S.K.; Kimchi, A. Autophagy-Dependent Cell Death - Where, How and Why a Cell Eats Itself to Death. *Journal of Cell Science* **2018**, *131*, doi:10.1242/jcs.215152.

83. Levine, B.; Kroemer, G. Biological Functions of Autophagy Genes: A Disease Perspective. *Cell* 2019, *176*, 11–42.

84. Shi, B.; Ma, M.; Zheng, Y.; Pan, Y.; Lin, X. MTOR and Beclin1: Two Key Autophagy-Related Molecules and Their Roles in Myocardial Ischemia/Reperfusion Injury. *Journal of Cellular Physiology* 2019, *234*, 12562–12568.

85. Dossou, A.S.; Basu, A. The Emerging Roles of MTORC1 in Macromanaging Autophagy. *Cancers* 2019, *11*.

86. Zachari, M.; Ganley, I.G. The Mammalian ULK1 Complex and Autophagy Initiation. *Essays in Biochemistry* 2017, *61*, 585–596.

87. Arakawa, S.; Tsujioka, M.; Yoshida, T.; Tajima-Sakurai, H.; Nishida, Y.; Matsuoka, Y.; Yoshino, I.; Tsujimoto, Y.; Shimizu, S. Role of Atg5-Dependent Cell Death in

the Embryonic Development of Bax/Bak Double-Knockout Mice. *Cell Death and Differentiation* **2017**, *24*, 1598–1608, doi:10.1038/cdd.2017.84.

88.   Airiau, K.; Vacher, P.; Micheau, O.; Prouzet-Mauleon, V.; Kroemer, G.; Moosavi, M.A.; Djavaheri-Mergny, M. TRAIL Triggers CRAC-Dependent Calcium Influx and Apoptosis through the Recruitment of Autophagy Proteins to Death-Inducing Signaling Complex. *Cells* **2021**, *11*, doi:10.3390/CELLS11010057.

89.   Serrano-Saenz, S.; Palacios, C.; Delgado-Bellido, D.; López-Jiménez, L.; Garcia-Diaz, A.; Soto-Serrano, Y.; Casal, J.I.; Bartolomé, R.A.; Fernández-Luna, J.L.; López-Rivas, A.; et al. PIM Kinases Mediate Resistance of Glioblastoma Cells to TRAIL by a P62/SQSTM1-Dependent Mechanism. *Cell death & disease* **2019**, *10*, doi:10.1038/S41419-018-1293-3.

90.   Mukhopadhyay, S.; Panda, P.K.; Sinha, N.; Das, D.N.; Bhutia, S.K. Autophagy and Apoptosis: Where Do They Meet? *Apoptosis* **2014**, *19*, 555–566, doi:10.1007/s10495-014-0967-2.

91.   Chen, H.Y.; White, E. Role of Autophagy in Cancer Prevention. *Cancer Prevention Research* **2011**, *4*, 973–983, doi:10.1158/1940-6207.CAPR-10-0387.

92.   Turcotte, S.; Giaccia, A.J. Targeting Cancer Cells through Autophagy for Anticancer Therapy. *Current Opinion in Cell Biology* 2010, *22*, 246–251.

93.   Holler, N.; Zaru, R.; Micheau, O.; Thome, M.; Attinger, A.; Valitutti, S.; Bodmer, J.L.; Schneider, P.; Seed, B.; Tschopp, J. Fas Triggers an Alternative, Caspase-8-Independent Cell Death Pathway Using the Kinase RIP as Effector Molecule. *Nature immunology* **2000**, *1*, 489–495, doi:10.1038/82732.

94.   Degterev, A.; Hitomi, J.; Germscheid, M.; Ch'en, I.L.; Korkina, O.; Teng, X.; Abbott, D.; Cuny, G.D.; Yuan, C.; Wagner, G.; et al. Identification of RIP1 Kinase as a Specific Cellular Target of Necrostatins. *Nature Chemical Biology* **2008**, *4*, 313–321, doi:10.1038/nchembio.83.

95.   Conrad, M.; Angeli, J.P.F.; Vandenabeele, P.; Stockwell, B.R. Regulated Necrosis: Disease Relevance and Therapeutic Opportunities. *Nature Reviews Drug Discovery* **2016**, *15*, 348–366, doi:10.1038/nrd.2015.6.

96.   Linkermann, A.; Green, D.R. Necroptosis. *New England Journal of Medicine* 2014, *370*, 455–465.

97.   Dhanasekaran, D.N.; Premkumar Reddy, E. *JNK-Signaling: A Multiplexing Hub in Programmed Cell Death*; 2017; Vol. 8;.

98.   Chen, X.; Li, W.; Ren, J.; Huang, D.; He, W.T.; Song, Y.; Yang, C.; Li, W.; Zheng, X.; Chen, P.; et al. Translocation of Mixed Lineage Kinase Domain-like Protein to Plasma Membrane Leads to Necrotic Cell Death. *Cell Research* **2014**, *24*, 105–121, doi:10.1038/cr.2013.171.

99.   Nikoletopoulou, V.; Markaki, M.; Palikaras, K.; Tavernarakis, N. Crosstalk between Apoptosis, Necrosis and Autophagy. *Biochimica et Biophysica Acta - Molecular Cell Research* 2013, *1833*, 3448–3459.

100.   Bergsbaken, T.; Fink, S.L.; Cookson, B.T. Pyroptosis: Host Cell Death and Inflammation. *Nature Reviews Microbiology* **2009**, *7*, 99–109, doi:10.1038/nrmicro2070.

101.   Fang, Y.; Tian, S.; Pan, Y.; Li, W.; Wang, Q.; Tang, Y.; Yu, T.; Wu, X.; Shi, Y.; Ma, P.; et al. Pyroptosis: A New Frontier in Cancer. *Biomedicine and Pharmacotherapy* 2020, *121*.

102. Kovacs, S.B.; Miao, E.A. Gasdermins: Effectors of Pyroptosis Pyroptosis Defends against Intracellular Infection. **2018**, *27*, 673–684, doi:10.1016/j.tcb.2017.05.005.Gasdermins.

103. Newton, K.; Dixit, V.M.; Kayagaki, N. Dying Cells Fan the Flames of Inflammation. *Science (New York, N.Y.)* **2021**, *374*, doi:10.1126/SCIENCE.ABI5934.

104. Calixto, J.B.; Otuki, M.F.; Santos, A.R.S. Anti-Inflammatory Compounds of Plant Origin. Part I. Action on Arachidonic Acid Pathway, Nitric Oxide and Nuclear Factor κ B (NF-KB). *Planta Medica* 2003, *69*, 973–983.

105. Patridge, E.; Gareiss, P.; Kinch, M.S.; Hoyer, D. An Analysis of FDA-Approved Drugs: Natural Products and Their Derivatives. *Drug Discovery Today* 2016, *21*, 204–207.

106. Schiff, P.L. Opium and Its Alkaloids. *American Journal of Pharmaceutical Education* 2002, *66*, 186–194.

107. Cushman, D.W.; Ondetti, M.A. History of the Design of Captopril and Related Inhibitors of Angiotensin Converting Enzyme. *Hypertension* 1991, *17*, 589–592.

108. King, G.F. Venoms as a Platform for Human Drugs: Translating Toxins into Therapeutics. *Expert Opinion on Biological Therapy* 2011, *11*, 1469–1484.

109. Koehn, F.E.; Carter, G.T. The Evolving Role of Natural Products in Drug Discovery. *Nature Reviews Drug Discovery* 2005, *4*, 206–220.

110. Firn, R.D.; Jones, C.G. Natural Products - A Simple Model to Explain Chemical Diversity. *Natural Product Reports* 2003, *20*, 382–391.

111. Herzig, V.; Cristofori-Armstrong, B.; Israel, M.R.; Nixon, S.A.; Vetter, I.; King, G.F. Animal Toxins-Nature's Evolutionary-Refined Toolkit for Basic Research and Drug Discovery. **2020**, doi:10.1016/j.bcp.2020.114096.

112. Nicolaou, K.C.; Pfefferkorn, J.A.; Roecker, A.J.; Cao, G.Q.; Barluenga, S.; Mitchell, H.J. Natural Product-like Combinatorial Libraries Based on Privileged Structures. 1. General Principles and Solid-Phase Synthesis of Benzopyrans. *Journal of the American Chemical Society* **2000**, *122*, 9939–9953, doi:10.1021/ja002033k.

113. Khusro, A.; Aarti, C.; Barbabosa-Pliego, A.; Rivas-Cáceres, R.R.; Cipriano-Salazar, M. Venom as Therapeutic Weapon to Combat Dreadful Diseases of 21st Century: A Systematic Review on Cancer, TB, and HIV/AIDS. *Microbial Pathogenesis* 2018, *125*, 96–107.

114. Pal, P.; Roy, S.; Chattopadhyay, S.; Pal, T.K. Medicinal Value of Animal Venom for Treatment of Cancer in Humans - A Review. **2015**, *22*, 128–144.

115. Giribaldi, J.; Smith, J.J.; Schroeder, C.I. Recent Developments in Animal Venom Peptide Nanotherapeutics with Improved Selectivity for Cancer Cells. *Biotechnology Advances* 2021, *50*, 107769.

116. Khusro, A.; Aarti, C.; Barbabosa-Pliego, A.; Rivas-Cáceres, R.R.; Cipriano-Salazar, M. Venom as Therapeutic Weapon to Combat Dreadful Diseases of 21st Century: A Systematic Review on Cancer, TB, and HIV/AIDS. *Microbial Pathogenesis* **2018**, *125*, 96–107, doi:10.1016/J.MICPATH.2018.09.003.

117. Dardevet, L.; Rani, D.; el Aziz, T.A.; Bazin, I.; Sabatier, J.M.; Fadl, M.; Brambilla, E.; de Waard, M. Chlorotoxin: A Helpful Natural Scorpion Peptide to Diagnose Glioma and Fight Tumor Invasion. *Toxins* 2015, *7*, 1079–1101.

118. Nascimento, F.D.; Sancey, L.; Pereira, A.; Rome, C.; Oliveira, V.; Oliveira, E.B.; Nader, H.B.; Yamane, T.; Kerkis, I.; Tersariol, I.L.S.; et al. The Natural Cell-Penetrating Peptide Crotamine Targets Tumor Tissue in Vivo and Triggers a Lethal

Calcium-Dependent Pathway in Cultured Cells. *Molecular Pharmaceutics* **2012**, *9*, 211–221, doi:10.1021/mp2000605.

119. Wu, M.; Ming, W.; Tang, Y.; Zhou, S.; Kong, T.; Dong, W. The Anticancer Effect of Cytotoxin 1 from Naja Atra Cantor Venom Is Mediated by a Lysosomal Cell Death Pathway Involving Lysosomal Membrane Permeabilization and Cathepsin B Release. *American Journal of Chinese Medicine* **2013**, *41*, 643–663, doi:10.1142/S0192415X13500456.

120. Yu, R.; Wang, M.; Wang, M.; Han, L. Melittin Suppresses Growth and Induces Apoptosis of Non-Small-Cell Lung Cancer Cells via down-Regulation of Tgf-β-Mediated Erk Signal Pathway. *Brazilian Journal of Medical and Biological Research* **2021**, *54*, 1–9, doi:10.1590/1414-431x20209017.

121. Soliman, C.; Eastwood, S.; Truong, V.K.; Ramsland, P.A.; Elbourne, A. The Membrane Effects of Melittin on Gastric and Colorectal Cancer. *PLoS ONE* **2019**, *14*, 1–16, doi:10.1371/journal.pone.0224028.

122. Chaisakul, J.; Hodgson, W.C.; Kuruppu, S.; Prasongsook, N. Effects of Animal Venoms and Toxins on Hallmarks of Cancer. *Journal of Cancer* **2016**, *7*, 1571–1578, doi:10.7150/jca.15309.

123. Heylen, D.J.A.; Matthysen, E. Contrasting Detachment Strategies in Two Congeneric Ticks (Ixodidae) Parasitizing the Same Songbird. *Parasitology* **2010**, *137*, 661–667, doi:10.1017/S0031182009991582.

124. Kada, S.; McCoy, K.D.; Boulinier, T. Impact of Life Stage-Dependent Dispersal on the Colonization Dynamics of Host Patches by Ticks and Tick-Borne Infectious Agents. *Parasites and Vectors* **2017**, *10*, 375, doi:10.1186/s13071-017-2261-y.

125. Kazimírová, M.; Štibrániová, I. Tick Salivary Compounds: Their Role in Modulation of Host Defences and Pathogen Transmission. *Frontiers in Cellular and Infection Microbiology* 2013, *4*, 43.

126. Wikel, S. Ticks and Tick-Borne Pathogens at the Cutaneous Interface: Host Defenses, Tick Countermeasures, and a Suitable Environment for Pathogen Establishment. *Frontiers in Microbiology* **2013**, *4*, 337, doi:10.3389/fmicb.2013.00337.

127. Chmelař, J.; Kotál, J.; Karim, S.; Kopacek, P.; Francischetti, I.M.B.; Pedra, J.H.F.; Kotsyfakis, M. Sialomes and Mialomes: A Systems-Biology View of Tick Tissues and Tick–Host Interactions. *Trends in Parasitology* **2016**, *32*, 242–254, doi:10.1016/j.pt.2015.10.002.

128. Francischetti, I.M.B.; Sa-Nunes, A.; Mans, B.J.; Santos, I.M.; Ribeiro, J.M.C. The Role of Saliva in Tick Feeding. *Frontiers in Bioscience* **2009**, *14*, 2051–2088, doi:10.2741/3363.

129. Nuttall, P.A. Wonders of Tick Saliva. *Ticks and Tick-borne Diseases* 2019, *10*, 470–481.

130. Bitencourth, K.; Amorim, M.; de Oliveira, S. v.; Caetano, R.L.; Voloch, C.M.; GazÊta, G.S. Amblyomma Sculptum: Genetic Diversity and Rickettsias in the Brazilian Cerrado Biome. *Medical and Veterinary Entomology* **2017**, *31*, 427–437, doi:10.1111/mve.12249.

131. Martins, K.; Menezes, F. CARRAPATO Amblyomma Sculptum (ACARI : IXODIDAE). **2017**.

132. Nunes, E.D.C.; Vizzoni, V.F.; Navarro, D.L.; de Melo Iani, F.C.; Durães, L.S.; Daemon, E.; Soares, C.A.G.; Gazeta, G.S. Rickettsia Amblyommii Infecting

Amblyomma Sculptum in Endemic Spotted Fever Area from Southeastern Brazil. *Memorias do Instituto Oswaldo Cruz* **2015**, *110*, 1058–1061, doi:10.1590/0074-02760150266.

133. Beati, L.; Nava, S.; Burkman, E.J.; Barros-Battesti, D.M.; Labruna, M.B.; Guglielmone, A.A.; Cáceres, A.G.; Guzmán-Cornejo, C.M.; León, R.; Durden, L.A.; et al. Amblyomma Cajennense (Fabricius, 1787) (Acari: Ixodidae), the Cayenne Tick: Phylogeography and Evidence for Allopatric Speciation. *BMC Evolutionary Biology* **2013**, *13*, 267, doi:10.1186/1471-2148-13-267.

134. Batista, I.F.C.; Chudzinski-Tavassi, A.M.; Faria, F.; Simons, S.M.; Barros-Batestti, D.M.; Labruna, M.B.; Leão, L.I.; Ho, P.L.; Junqueira-de-Azevedo, I.L.M. Expressed Sequence Tags (ESTs) from the Salivary Glands of the Tick Amblyomma Cajennense (Acari: Ixodidae). *Toxicon* **2008**, *51*, 823–834, doi:10.1016/j.toxicon.2007.12.011.

135. Monteiro, R.Q.; Rezaie, A.R.; Ribeiro, J.M.C.; Francischetti, I.M.B. Ixolaris: A Factor Xa Heparin-Binding Exosite Inhibitor. *Biochemical Journal* **2005**, *387*, 871–877, doi:10.1042/BJ20041738.

136. Batista, I.F.C.; Ramos, O.H.P.; Ventura, J.S.; Junqueira-de-Azevedo, I.L.M.; Ho, P.L.; Chudzinski-Tavassi, A.M. A New Factor Xa Inhibitor from Amblyomma Cajennense with a Unique Domain Composition. *Archives of Biochemistry and Biophysics* **2010**, *493*, 151–156, doi:10.1016/j.abb.2009.10.009.

137. Prosdocimi, C.C.; Bechara, G.H.; Luduvério, D.J.; Otávio, F.M.S.; del Vecchio, R.E. Innate Immunity in Wooless Lamb to Larvae of Amblyomma Cajennense Tick (Fabricius, 1787) (Acari: Ixodidae). *Transboundary and Emerging Diseases* **2010**, *57*, 75–76, doi:10.1111/j.1865-1682.2010.01114.x.

138. Franco, P.F.; Silva, N.C.S.; Fazito do Vale, V.; Abreu, J.F.; Santos, V.C.; Gontijo, N.F.; Valenzuela, J.G.; Pereira, M.H.; Sant'Anna, M.R.V.; Gomes, A.P.S.; et al. Inhibition of the Classical Pathway of the Complement System by Saliva of Amblyomma Cajennense (Acari: Ixodidae). *Experimental Parasitology* **2016**, *164*, 91–96, doi:10.1016/j.exppara.2016.03.002.

139. Carvalho-Costa, T.M.; Mendes, M.T.; da Silva, M.V.; da Costa, T.A.; Tiburcio, M.G.S.; Anhê, A.C.B.M.; Rodrigues, V.; Oliveira, C.J.F. Immunosuppressive Effects of Amblyomma Cajennense Tick Saliva on Murine Bone Marrow-Derived Dendritic Cells. *Parasites and Vectors* **2015**, *8*, 22, doi:10.1186/s13071-015-0634-7.

140. Nascimento, T.G.; Vieira, P.S.; Cogo, S.C.; Dias-Netipanyj, M.F.; França Junior, N.; Câmara, D.A.D.; Porcacchia, A.S.; Mendonça, R.Z.; Moreno-Amaral, A.N.; Sá Junior, P.L.; et al. Antitumoral Effects of Amblyomma Sculptum Berlese Saliva in Neuroblastoma Cell Lines Involve Cytoskeletal Deconstruction and Cell Cycle Arrest. *Revista Brasileira de Parasitologia Veterinaria* **2019**, *28*, doi:10.1590/s1984-296120180098.

141. Salomon, J.; Hamer, S.A.; Swei, A. A Beginner's Guide to Collecting Questing Hard Ticks (Acari: Ixodidae): A Standardized Tick Dragging Protocol. *Journal of Insect Science* **2020**, *20*, doi:10.1093/JISESA/IEAA073.

142. Oliveira, D.G.L.L.; Simons, S.M.; Chudzinski-Tavassi, A.M.; Zamboni, C.B. Analysis of Saliva from Amblyomma Cajennense (Acari: Ixodidae) Species from Brazil by NAA. *Journal of Radioanalytical and Nuclear Chemistry* **2012**, *291*, 385–388, doi:10.1007/s10967-011-1265-x.

143. MM, B. A Rapid and Sensitive Method for the Quantitation of Microgram Quantities of Protein Utilizing the Principle of Protein-Dye Binding. *Analytical biochemistry* **1976**, *72*, 248–254, doi:10.1006/ABIO.1976.9999.

144. Stoscheck, C.M. Quantitation of Protein. *Methods in enzymology* **1990**, *182*, 50–68, doi:10.1016/0076-6879(90)82008-P.

145. Morgenstern, J.P.; Land, H. Advanced Mammalian Gene Transfer: High Titre Retroviral Vectors with Multiple Drug Selection Markers and a Complementary Helper-Free Packaging Cell Line. *Nucleic acids research* **1990**, *18*, 3587–3596, doi:10.1093/NAR/18.12.3587.

146. Morizot, A.; Mérino, D.; Lalaoui, N.; Jacquemin, G.; Granci, V.; Iessi, E.; Lanneau, D.; Bouyer, F.; Solary, E.; Chauffert, B.; et al. Chemotherapy Overcomes TRAIL-R4-Mediated TRAIL Resistance at the DISC Level. *Cell death and differentiation* **2011**, *18*, 700–711, doi:10.1038/CDD.2010.144.

147. Morlé, A.; Garrido, C.; Micheau, O. Hyperthermia Restores Apoptosis Induced by Death Receptors through Aggregation-Induced c-FLIP Cytosolic Depletion. *Cell death & disease* **2015**, *6*, doi:10.1038/CDDIS.2015.12.

148. Morel, C.; Carlson, S.M.; White, F.M.; Davis, R.J. Mcl-1 Integrates the Opposing Actions of Signaling Pathways That Mediate Survival and Apoptosis. *Molecular and cellular biology* **2009**, *29*, 3845–3852, doi:10.1128/MCB.00279-09.

149. Ehrhardt, C.; Schmolke, M.; Matzke, A.; Knoblauch, A.; Will, C.; Wixler, V.; Ludwig, S. Polyethylenimine, a Cost-Effective Transfection Reagent. *Signal Transduction* **2006**, *6*, 179–184, doi:10.1002/SITA.200500073.

150. Dufour, F.; Rattier, T.; Shirley, S.; Picarda, G.; Constantinescu, A.A.; Morlé, A.; Zakaria, A.B.; Marcion, G.; Causse, S.; Szegezdi, E.; et al. N-Glycosylation of Mouse TRAIL-R and Human TRAIL-R1 Enhances TRAIL-Induced Death. *Cell Death and Differentiation* **2017**, *24*, 500–510, doi:10.1038/cdd.2016.150.

151. Elmallah, M.I.Y.; Cogo, S.; Constantinescu, A.A.; Elifio-Esposito, S.; Abdelfattah, M.S.; Micheau, O. Marine Actinomycetes-Derived Secondary Metabolites Overcome TRAIL-Resistance via the Intrinsic Pathway through Downregulation of Survivin and XIAP. *Cells* **2020**, *9*, doi:10.3390/cells9081760.

152. McComb, S.; Aguadé-Gorgorió, J.; Harder, L.; Marovca, B.; Cario, G.; Eckert, C.; Schrappe, M.; Stanulla, M.; von Stackelberg, A.; Bourquin, J.P.; et al. Activation of Concurrent Apoptosis and Necroptosis by SMAC Mimetics for the Treatment of Refractory and Relapsed ALL. *Science translational medicine* **2016**, *8*, doi:10.1126/SCITRANSLMED.AAD2986.

153. Zhang, J.F.; Zhang, J.G.; Kuai, X.L.; Zhang, H.; Jiang, W.; Ding, W.F.; Li, Z.L.; Zhu, H.J.; Mao, Z.B. Reactivation of the Homeotic Tumor Suppressor Gene CDX2 by 5-Aza-2'-Deoxycytidine-Induced Demethylation Inhibits Cell Proliferation and Induces Caspase-Independent Apoptosis in Gastric Cancer Cells. *Experimental and Therapeutic Medicine* **2013**, *5*, 735–741, doi:10.3892/etm.2013.901.

154. Felice, D.L.; Sun, J.; Liu, R.H. A Modified Methylene Blue Assay for Accurate Cell Counting. *Journal of Functional Foods* **2009**, *1*, 109–118, doi:10.1016/J.JFF.2008.09.014.

155. Dubuisson, A.; Favreau, C.; Fourmaux, E.; Lareure, S.; Rodrigues-Saraiva, R.; Pellat-Deceunynck, C.; el Alaoui, S.; Micheau, O. Generation and Characterization of Novel Anti-DR4 and Anti-DR5 Antibodies Developed by Genetic Immunization. *Cell death & disease* **2019**, *10*, doi:10.1038/S41419-019-1343-5.

156. Sassaki, G.L.; Souza, L.M.; Serrato, R. v.; Cipriani, T.R.; Gorin, P.A.J.; Iacomini, M. Application of Acetate Derivatives for Gas Chromatography-Mass Spectrometry: Novel Approaches on Carbohydrates, Lipids and Amino Acids Analysis. *Journal of chromatography. A* **2008**, *1208*, 215–222, doi:10.1016/J.CHROMA.2008.08.083.

157. Sassaki, G.L.; Riter, D.S.; Santana Filho, A.P.; Guerrini, M.; Lima, M.A.; Cosentino, C.; Souza, L.M.; Cipriani, T.R.; Rudd, T.R.; Nader, H.B.; et al. A Robust Method to Quantify Low Molecular Weight Contaminants in Heparin: Detection of Tris(2-n-Butoxyethyl) Phosphate. *Analyst* **2011**, *136*, 2330–2338, doi:10.1039/C0AN01010C.

158. Seelan, R.S.; Mukhopadhyay, P.; Pisano, M.M.; Greene, R.M. Effects of 5-Aza-2′-Deoxycytidine (Decitabine) on Gene Expression. *Drug Metabolism Reviews* 2018, *50*, 193–207.

159. Wang, L.; Dong, C.; Li, X.; Han, W.; Su, X. Anticancer Potential of Bioactive Peptides from Animal Sources (Review). *Oncology Reports* 2017, *38*, 637–651.

160. Simons, S.M.; Júnior, P.L. de S.; Faria, F.; Batista, I. de F.C.; Barros-Battesti, D.M.; Labruna, M.B.; Chudzinski-Tavassi, A.M. The Action of Amblyomma Cajennense Tick Saliva in Compounds of the Hemostatic System and Cytotoxicity in Tumor Cell Lines. *Biomedicine and Pharmacotherapy* **2011**, *65*, 443–450, doi:10.1016/j.biopha.2011.04.030.

161. Simons, S.M.; Júnior, P.L. de S.; Faria, F.; Batista, I. de F.C.; Barros-Battesti, D.M.; Labruna, M.B.; Chudzinski-Tavassi, A.M. The Action of Amblyomma Cajennense Tick Saliva in Compounds of the Hemostatic System and Cytotoxicity in Tumor Cell Lines. *Biomedicine and Pharmacotherapy* **2011**, *65*, 443–450, doi:10.1016/j.biopha.2011.04.030.

162. Drewes, C.C.; Dias, R.Y.S.; Hebeda, C.B.; Simons, S.M.; Barreto, S.A.; Ferreira, J.M.; Chudzinski-Tavassi, A.M.; Farsky, S.H.P. Actions of the Kunitz-Type Serine Protease Inhibitor Amblyomin-X on VEGF-A-Induced Angiogenesis. *Toxicon* **2012**, *60*, 333–340, doi:10.1016/j.toxicon.2012.04.349.

163. Takita, J.; Yang, H.W.; Chen, Y.Y.; Hanada, R.; Yamamoto, K.; Teitz, T.; Kidd, V.; Hayashi, Y. Allelic Imbalance on Chromosome 2q and Alterations of the Caspase 8 Gene in Neuroblastoma. *Oncogene* **2001**, *20*, 4424–4432, doi:10.1038/sj.onc.1204521.

164. Teitz, T.; Lahti, J.M.; Kidd, V.J. Aggressive Childhood Neuroblastomas Do Not Express Caspase-8: An Important Component of Programmed Cell Death. *Journal of Molecular Medicine* **2001**, *79*, 428–436, doi:10.1007/s001090100233.

165. Harada, K.; Toyooka, S.; Shivapurkar, N.; Maitra, A.; Reddy, J.L.; Matta, H.; Miyajima, K.; Timmons, C.F.; Tomlinson, G.E.; Mastrangelo, D.; et al. Deregulation of Caspase 8 and 10 Expression in Pediatric Tumors and Cell Lines. *Cancer Research* **2002**, *62*, 5897–5901.

166. Stupack, D.G.; Teitz, T.; Potter, M.D.; Mikolon, D.; Houghton, P.J.; Kidd, V.J.; Lahti, J.M.; Cheresh, D.A. Potentiation of Neuroblastoma Metastasis by Loss of Caspase-8. *Nature* **2006**, *439*, 95–99, doi:10.1038/nature04323.

167. Hopkins-Donaldson, S.; Bodmer, J.L.; Bourloud, K.B.; Brognara, C.B.; Tschopp, J.; Gross, N. Loss of Caspase-8 Expression in Highly Malignant Human Neuroblastoma Cells Correlates with Resistance to Tumor Necrosis Factor-Related Apoptosis-Inducing Ligand-Induced Apoptosis. *Cancer Research* **2000**, *60*, 4315–4319.

168. Teitz, T.; Wei, T.; Valentine, M.B.; Vanin, E.F.; Grenet, J.; Valentine, V.A.; Behm, F.G.; Look, A.T.; Lahti, J.M.; Kidd, V.J. Caspase 8 Is Deleted or Silenced

Preferentially in Childhood Neuroblastomas with Amplification of MYCN. *Nature Medicine* **2000**, *6*, 529–535, doi:10.1038/75007.

169. Sheard, M.A.; Asgharzadeh, S.; Liu, Y.; Lin, T.Y.; Wu, H.W.; Ji, L.; Groshen, S.; Lee, D.A.; Seeger, R.C. Membrane-Bound TRAIL Supplements Natural Killer Cell Cytotoxicity against Neuroblastoma Cells. *Journal of Immunotherapy* **2013**, *36*, 319–329, doi:10.1097/CJI.0b013e31829b4493.

170. Eggert, A.; Grotzer, M.A.; Zuzak, T.J.; Wiewrodt, B.R.; Ho, R.; Ikegaki, N.; Brodeur, G.M. Resistance to Tumor Necrosis Factor-Related Apoptosis-Inducing Ligand (TRAIL)-Induced Apoptosis in Neuroblastoma Cells Correlates with a Loss of Caspase-8 Expression. *Cancer Research* **2001**, *61*, 1314–1319.

171. Christman, J.K. 5-Azacytidine and 5-Aza-2′-Deoxycytidine as Inhibitors of DNA Methylation: Mechanistic Studies and Their Implications for Cancer Therapy. *Oncogene* 2002, *21*, 5483–5495.

172. Bate-Eya, L.T.; den Hartog, I.J.M.; van der Ploeg, I.; Schild, L.; Koster, J.; Santo, E.E.; Westerhout, E.M.; Versteeg, R.; Caron, H.N.; Molenaar, J.J.; et al. High Efficacy of the BCL-2 Inhibitor ABT199 (Venetoclax) in BCL-2 High-Expressing Neuroblastoma Cell Lines and Xenografts and Rational for Combination with MCL-1 Inhibition. *Oncotarget* **2016**, *7*, 27946–27958, doi:10.18632/ONCOTARGET.8547.

173. Jeng, P.S.; Inoue-Yamauchi, A.; Hsieh, J.J.; Cheng, E.H. BH3-Dependent and Independent Activation of BAX and BAK in Mitochondrial Apoptosis. *Current Opinion in Physiology* **2018**, *3*, 71–81, doi:10.1016/J.COPHYS.2018.03.005.

174. Puthalakath, H.; Strasser, A. Keeping Killers on a Tight Leash: Transcriptional and Post-Translational Control of the pro-Apoptotic Activity of BH3-Only Proteins. *Cell Death & Differentiation 2002 9:5* **2002**, *9*, 505–512, doi:10.1038/sj.cdd.4400998.

175. Yu, J.; Zhang, L. PUMA, a Potent Killer with or without P53. *Oncogene* **2008**, *27*, S71, doi:10.1038/ONC.2009.45.

176. Mihailidou, C.; Chatzistamou, I.; Papavassiliou, A.G.; Kiaris, H. Improvement of Chemotherapeutic Drug Efficacy by Endoplasmic Reticulum Stress., doi:10.1530/ERC-15-0019.

177. Yoneda, T.; Imaizumi, K.; Oono, K.; Yui, D.; Gomi, F.; Katayama, T.; Tohyama, M. Activation of Caspase-12, an Endoplastic Reticulum (ER) Resident Caspase, through Tumor Necrosis Factor Receptor-Associated Factor 2-Dependent Mechanism in Response to the ER Stress. *The Journal of biological chemistry* **2001**, *276*, 13935–13940, doi:10.1074/JBC.M010677200.

178. Nishitoh, H.; Matsuzawa, A.; Tobiume, K.; Saegusa, K.; Takeda, K.; Inoue, K.; Hori, S.; Kakizuka, A.; Ichijo, H. ASK1 Is Essential for Endoplasmic Reticulum Stress-Induced Neuronal Cell Death Triggered by Expanded Polyglutamine Repeats. *Genes & development* **2002**, *16*, 1345–1355, doi:10.1101/GAD.992302.

179. Walczak, H. Death Receptor–Ligand Systems in Cancer, Cell Death, and Inflammation. *Cold Spring Harbor Perspectives in Biology* **2013**, *5*, doi:10.1101/CSHPERSPECT.A008698.

180. Dhanasekaran, D.N.; Reddy, E.P. *JNK-Signaling: A Multiplexing Hub in Programmed Cell Death*; 2017; Vol. 8;.

181. Abe, J.I.; Morrell, C. Pyroptosis as a Regulated Form of Necrosis: PI+/Annexin V-/High Caspase 1/Low Caspase 9 Activity in Cells = Pyroptosis? *Circulation research* **2016**, *118*, 1457–1460, doi:10.1161/CIRCRESAHA.116.308699.

182. Redza-Dutordoir, M.; Averill-Bates, D.A. Activation of Apoptosis Signalling Pathways by Reactive Oxygen Species. *Biochimica et Biophysica Acta (BBA) - Molecular Cell Research* **2016**, *1863*, 2977–2992, doi:10.1016/J.BBAMCR.2016.09.012.

183. Datta, K.; Babbar, P.; Srivastava, T.; Sinha, S.; Chattopadhyay, P. P53 Dependent Apoptosis in Glioma Cell Lines in Response to Hydrogen Peroxide Induced Oxidative Stress. *The International Journal of Biochemistry & Cell Biology* **2002**, *34*, 148–157, doi:10.1016/S1357-2725(01)00106-6.

184. Circu, M.L.; Aw, T.Y. Reactive Oxygen Species, Cellular Redox Systems, and Apoptosis. *Free Radical Biology and Medicine* **2010**, *48*, 749–762, doi:10.1016/J.FREERADBIOMED.2009.12.022.

185. Maher, H.; Zeeshan, A.; Lee, G.H.; Kim, H.-R.; Chae, H.-J. Molecular Sciences Endoplasmic Reticulum Stress and Associated ROS. **2016**, doi:10.3390/ijms17030327.

186. Zuo, Y.; Xiang, B.; Yang, J.; Sun, X.; Wang, Y.; Cang, H.; Yi, J. Oxidative Modification of Caspase-9 Facilitates Its Activation via Disulfide-Mediated Interaction with Apaf-1. *Cell Research 2009 19:4* **2009**, *19*, 449–457, doi:10.1038/cr.2009.19.

187. Prasad, V.; Chandele, A.; Jagtap, J.C.; Kumar P., S.; Shastry, P. ROS-Triggered Caspase 2 Activation and Feedback Amplification Loop in β-Carotene-Induced Apoptosis. *Free Radical Biology and Medicine* **2006**, *41*, 431–442, doi:10.1016/J.FREERADBIOMED.2006.03.009.

188. Pallepati, P.; Averill-Bates, D.A. Mild Thermotolerance Induced at 40 °C Protects HeLa Cells against Activation of Death Receptor-Mediated Apoptosis by Hydrogen Peroxide. *Free Radical Biology and Medicine* **2011**, *50*, 667–679, doi:10.1016/J.FREERADBIOMED.2010.11.022.

189. Mellier, G.; Pervaiz, S. The Three Rs along the TRAIL: Resistance, Re-Sensitization and Reactive Oxygen Species (ROS). *http://dx.doi.org/10.3109/10715762.2012.690514* **2012**, *46*, 996–1003, doi:10.3109/10715762.2012.690514.

190. Chinopoulos, C.; Tretter, L.; Adam-Vizi, V. Depolarization of in Situ Mitochondria Due to Hydrogen Peroxide-Induced Oxidative Stress in Nerve Terminals: Inhibition of Alpha-Ketoglutarate Dehydrogenase. *Journal of neurochemistry* **1999**, *73*, 220–228, doi:10.1046/J.1471-4159.1999.0730220.X.

191. Quast, S.A.; Berger, A.; Eberle, J. ROS-Dependent Phosphorylation of Bax by Wortmannin Sensitizes Melanoma Cells for TRAIL-Induced Apoptosis. *Cell Death & Disease 2013 4:10* **2013**, *4*, e839–e839, doi:10.1038/cddis.2013.344.

192. Orrenius, S.; Gogvadze, V.; Zhivotovsky, B. Calcium and Mitochondria in the Regulation of Cell Death. *Biochemical and Biophysical Research Communications* **2015**, *460*, 72–81, doi:10.1016/J.BBRC.2015.01.137.

193. Giorgi, C.; Baldassari, F.; Bononi, A.; Bonora, M.; de Marchi, E.; Marchi, S.; Missiroli, S.; Patergnani, S.; Rimessi, A.; Suski, J.M.; et al. Mitochondrial Ca2+ and Apoptosis. *Cell Calcium* **2012**, *52*, 36–43, doi:10.1016/J.CECA.2012.02.008.

194. Halestrap, A.P. What Is the Mitochondrial Permeability Transition Pore? *Journal of molecular and cellular cardiology* **2009**, *46*, 821–831, doi:10.1016/J.YJMCC.2009.02.021.

195. Li, C.; Wang, X.; Vais, H.; Thompson, C.B.; Foskett, J.K.; White, C. Apoptosis Regulation by Bcl-XL Modulation of Mammalian Inositol 1,4,5-Trisphosphate Receptor Channel Isoform Gating. *Proceedings of the National Academy of Sciences of the United States of America* **2007**, *104*, 12565–12570, doi:10.1073/PNAS.0702489104.

196. Distelhorst, C.W.; Shore, G.C. Bcl-2 and Calcium: Controversy beneath the Surface. *Oncogene 2004 23:16* **2004**, *23*, 2875–2880, doi:10.1038/sj.onc.1207519.

197. Gomes, A.; Bhattacharjee, P.; Mishra, R.; Biswas, A.K.; Dasgupta, S.C.; Giri, B.; Debnath, A.; Gupta, S. das; Das, T.; Gomes, A. Anticancer Potential of Animal Venoms and Toxins. *Indian Journal of Experimental Biology* **2010**, *48*, 93–103.

198. Chaisakul, J.; Hodgson, W.C.; Kuruppu, S.; Prasongsook, N. Effects of Animal Venoms and Toxins on Hallmarks of Cancer. *Journal of Cancer* 2016, *7*, 1571–1578.

199. Cordeiro, F.A.; Amorim, F.G.; Anjolette, F.A.P.; Arantes, E.C. Arachnids of Medical Importance in Brazil: Main Active Compounds Present in Scorpion and Spider Venoms and Tick Saliva. *Journal of Venomous Animals and Toxins Including Tropical Diseases* 2015, *21*.

200. Bordon, K. de C.F.; Cologna, C.T.; Fornari-Baldo, E.C.; Pinheiro-Júnior, E.L.; Cerni, F.A.; Amorim, F.G.; Anjolette, F.A.P.; Cordeiro, F.A.; Wiezel, G.A.; Cardoso, I.A.; et al. From Animal Poisons and Venoms to Medicines: Achievements, Challenges and Perspectives in Drug Discovery. *Frontiers in Pharmacology* **2020**, *11*, 1132, doi:10.3389/FPHAR.2020.01132/BIBTEX.

201. Sweeney, P.J.; Walker, J.M. Proteinase K (EC 3.4.21.14). *Methods in molecular biology (Clifton, N.J.)* **1993**, *16*, 305–311, doi:10.1385/0-89603-234-5:305.

202. Esteves, E.; Bizzarro, B.; Costa, F.B.; Ramírez-Hernández, A.; Peti, A.P.F.; Cataneo, A.H.D.; Wowk, P.F.; Timóteo, R.P.; Labruna, M.B.; Silva, P.I.; et al. Amblyomma Sculptum Salivary PGE 2 Modulates the Dendritic Cell Rickettsia Rickettsii Interactions in Vitro and in Vivo. *Frontiers in Immunology* **2019**, *10*, 1–15, doi:10.3389/fimmu.2019.00118.

203. Herzig, V.; King, G.F. The Cystine Knot Is Responsible for the Exceptional Stability of the Insecticidal Spider Toxin ω-Hexatoxin-Hv1a. *Toxins* **2015**, *7*, 4366–4380, doi:10.3390/toxins7104366.

204. Kikuchi, K.; Sugiura, M.; Kimura, T. High Proteolytic Resistance of Spider-Derived Inhibitor Cystine Knots. *International Journal of Peptides* **2015**, *2015*, doi:10.1155/2015/537508.

205. Craik, D.J.; Daly, N.L.; Waine, C. The Cystine Knot Motif in Toxins and Implications for Drug Design. *Toxicon* 2001, *39*, 43–60.

206. Kintzing, J.R.; Cochran, J.R. Engineered Knottin Peptides as Diagnostics, Therapeutics, and Drug Delivery Vehicles. *Current Opinion in Chemical Biology* 2016, *34*, 143–150.

207. Deng, M.; Luo, X.; Xiao, Y.; Sun, Z.; Jiang, L.; Liu, Z.; Zeng, X.; Chen, H.; Tang, J.; Zeng, W.; et al. Huwentoxin-XVI, an Analgesic, Highly Reversible Mammalian N-Type Calcium Channel Antagonist from Chinese Tarantula Ornithoctonus Huwena. *Neuropharmacology* **2014**, *79*, 657–667, doi:10.1016/j.neuropharm.2014.01.017.

208. Regier, J.C.; Shultz, J.W.; Zwick, A.; Hussey, A.; Ball, B.; Wetzer, R.; Martin, J.W.; Cunningham, C.W. Arthropod Relationships Revealed by Phylogenomic Analysis of

Nuclear Protein-Coding Sequences. *Nature* **2010**, *463*, 1079–1083, doi:10.1038/nature08742.

209. A, C.-C.; JJ, V. Are Ticks Venomous Animals? *Frontiers in Zoology* **2014**, *11*, 47–47, doi:10.1186/1742-9994-11-47.

210. Konno, K.; Kazuma, K.; Rangel, M.; Stolarz-De-oliveira, J.; Fontana, R.; Kawano, M.; Fuchino, H.; Hide, I.; Yasuhara, T.; Nakata, Y. New Mastoparan Peptides in the Venom of the Solitary Eumenine Wasp Eumenes Micado. *Toxins* **2019**, *11*, 155, doi:10.3390/toxins11030155.

211. Gupta, S. das; Gomes, A.; Debnath, A.; Saha, A.; Gomes, A. Apoptosis Induction in Human Leukemic Cells by a Novel Protein Bengalin, Isolated from Indian Black Scorpion Venom: Through Mitochondrial Pathway and Inhibition of Heat Shock Proteins. *Chemico-Biological Interactions* **2010**, *183*, 293–303, doi:10.1016/j.cbi.2009.11.006.

212. Liu, Z.; Deng, M.; Xiang, J.; Ma, H.; Hu, W.; Zhao, Y.; Li, D.W.-C.; Liang, S. A Novel Spider Peptide Toxin Suppresses Tumor Growth Through Dual Signaling Pathways. *Current Molecular Medicine* **2012**, *12*, 1350–1360, doi:10.2174/156652412803833643.

213. McLachlan, A.; Kekre, N.; McNulty, J.; Pandey, S. Pancratistatin: A Natural Anti-Cancer Compound That Targets Mitochondria Specifically in Cancer Cells to Induce Apoptosis. *Apoptosis* **2005**, *10*, 619–630, doi:10.1007/s10495-005-1896-x.

214. Senji Laxme, R.R.; Suranse, V.; Sunagar, K. Arthropod Venoms: Biochemistry, Ecology and Evolution. *Toxicon* 2019, *158*, 84–103.

ANNEX I – PUBLISHED ARTICLES

Original Article

Antitumoral effects of *Amblyomma sculptum* Berlese saliva in neuroblastoma cell lines involve cytoskeletal deconstruction and cell cycle arrest

Efeito antitumoral da saliva do carrapato *Amblyomma sculptum* Berlese em células de neuroblastoma envolve desconstrução do citoesqueleto e parada do ciclo celular

Thatyanne Gradowski do Nascimento[1]; Priscilla Santos Vieira[2]; Sheron Campos Cogo[1];
Marcela Ferreira Dias-Netipanyj[1]; Nilton de França Junior[1]; Diana Aparecida Dias Câmara[3]; Allan Saj Porcacchia[3];
Ronaldo Zucatelli Mendonça[4]; Andréa Novais Moreno-Amaral[1]; Paulo Luiz de Sá Junior[3]; Simone Michaela Simons[4];
Luciana Zischler[2]; Selene Elifio-Esposito[1]*

[1] Programa de Ciências da Saúde, Pontifícia Universidade Católica do Paraná – PUCPR, Curitiba, PR, Brasil

[2] Escola de Ciências da Vida, Pontifícia Universidade Católica do Paraná – PUCPR, Curitiba, PR, Brasil

[3] Laboratório de Genética, Instituto Butantan, São Paulo, SP, Brasil

[4] Laboratório de Parasitologia, Instituto Butantan, São Paulo, SP, Brasil

Abstract

The antitumor properties of ticks salivary gland extracts or recombinant proteins have been reported recently, but little is known about the antitumor properties of the secreted components of saliva. The goal of this study was to investigate the *in vitro* effect of the saliva of the hard tick *Amblyomma sculptum* on neuroblastoma cell lines. SK-N-SK, SH-SY5Y, Be(2)-M17, IMR-32, and CHLA-20 cells were susceptible to saliva, with 80% reduction in their viability compared to untreated controls, as demonstrated by the methylene blue assay. Further investigation using CHLA-20 revealed apoptosis, with approximately 30% of annexin-V positive cells, and G0/G1-phase accumulation (>60%) after treatment with saliva. Mitochondrial membrane potential ($\Delta\psi$m) was slightly, but significantly ($p < 0.05$), reduced and the actin cytoskeleton was disarranged, as indicated by fluorescent microscopy. The viability of human fibroblast (HFF-1 cells) used as a non-tumoral control decreased by approximately 40%. However, no alterations in cell cycle progression, morphology, and $\Delta\psi$m were observed in these cells. The present work provides new perspectives for the characterization of the molecules present in saliva and their antitumor properties.

Keywords: Tick saliva, animal toxin, tumor cell death, pediatric cancer.

Minireview

An overview of neuroblastoma cell lineage phenotypes and *in vitro* models

Sheron Campos Cogo[1], Thatyanne Gradowski Farias da Costa do Nascimento[1], Fernanda de Almeida Brehm Pinhatti[1] ⓘ, Nilton de França Junior[1], Bruna Santos Rodrigues[1], Luciane Regina Cavalli[2,3] and Selene Elifio-Esposito[1] ⓘ

[1]Graduate Program in Health Sciences, Pontifícia Universidade Católica do Paraná, Curitiba 80215-901, Brazil; [2]Instituto de Pesquisa Pelé Pequeno Príncipe, Faculdades Pequeno Príncipe, Curitiba 80250-060, Brazil; [3]Lombardi Comprehensive Cancer Center, Georgetown University, Washington, DC 20007, USA
Corresponding author: Elifio-Esposito Selene. Email: seleneesposito@gmail.com

Impact statement

This review provides an update on the mostly used cell line *in vitro* models for neuroblastoma (NB), a heterogeneous disease with high metastatic potential and resistance to treatment. The genetic and phenotypic profiles of the most used NB cell lines in the last 10 years are presented, considering the molecular markers that are involved in the distinct NB tumor phenotypes, including distinct core regulatory circuitries and non-coding RNAs. This gathered information can assist in the selection of the most appropriate NB *in vitro* model, based on the specific goals and objectives of each study.

Abstract

This review was conducted to present the main neuroblastoma (NB) clinical characteristics and the most common genetic alterations present in these pediatric tumors, highlighting their impact in tumor cell aggressiveness behavior, including metastatic development and treatment resistance, and patients' prognosis. The distinct three NB cell lineage phenotypes, S-type, N-type, and I-type, which are characterized by unique cell surface markers and gene expression patterns, are also reviewed. Finally, an overview of the most used NB cell lines currently available for *in vitro* studies and their unique cellular and molecular characteristics, which should be taken into account for the selection of the most appropriate model for NB pre-clinical studies, is presented. These valuable models can be complemented by the generation of NB reprogrammed tumor cells or organoids, derived directly from patients' tumor specimens, in the direction toward personalized medicine.

Introduction

Neuroblastoma (NB) is an extracranial solid tumor in children and comprehends 8% to 10% of all pediatric cancers.[1] It is a heterogeneous disease that presents a broad spectrum of clinical behaviors; in children aged 18 months or older, it is often unresectable or metastatic, requires intensive multimodal therapy, and is associated with a survival rate lower than 50%.[2] On the other side of the spectrum, NB with spontaneous regression without chemotherapy is seen in low-risk subgroups.[3]

NB is derived from cells within the neural crest, likely sympathoadrenal progenitor cells that differentiate to sympathetic ganglion and adrenal catecholamine-secreting chromaffin cells.[4] The presentation and symptoms at diagnosis reflect the tumor location, commonly in the adrenal medulla or anywhere along the sympathetic ganglia.

Metastases are present in about 50% of patients at diagnosis, with bone marrow metastases corresponding to 80% of the cases. Metastases are also found in bones and regional lymph nodes, while the involvement of the central nervous system and lungs is rare.[5]

The International Committee of Pathology of Neuroblastoma classifies NB tumors into distinct subtypes, according to histological findings, which include the amount of Schwannian stroma present in the tumor and the mitosis-karyorrhexis index (MKI).[6] Generally, the poorly differentiated or undifferentiated histology confers a worse prognosis to patients. Age is also an important prognostic indicator; in <18-month-old patients, poorly differentiated NB is still considered a favorable prognosis if the MKI is not high; however, in patients aged >18 months, poorly differentiated NB is invariably unfavorable.[7]

Marine Actinomycetes-Derived Secondary Metabolites Overcome TRAIL-Resistance via the Intrinsic Pathway through Downregulation of Survivin and XIAP

Mohammed I. Y. Elmallah [1,2,3,*], Sheron Cogo [1,2,4], Andrei A. Constantinescu [1,2], Selene Elifio-Esposito [4], Mohammed S. Abdelfattah [3,5] and Olivier Micheau [1,2,*]

[1] LNC, INSERM, UMR1231, F-21079 Dijon, France; sheron_cogo@hotmail.com (S.C.); andrei.ac@windowslive.com (A.A.C.)

[2] UFR Science de Santé, Université de Bourgogne Franche-Comté, F-21079 Dijon, France

[3] Chemistry Department, Faculty of Science, Helwan University, 11795 Ain Helwan, Cairo 11795, Egypt; mabdelfattah@science.helwan.edu.eg

[4] Graduate Programme in Health Sciences, Pontifícia Universidade Catolica do Parana, Curitiba 80215–901, Parana, Brazil; seleneesposito@gmail.com

[5] Marine Natural Products Unit (MNPRU), Faculty of Science, Helwan University, 11795 Ain Helwan, Cairo 11795, Egypt

[*] Correspondence: mohamed_almallah@science.helwan.edu.eg (M.I.Y.E.); omicheau@u-bourgogne.fr (O.M.)

Abstract: Resistance of cancer cells to tumor necrosis factor-related apoptosis-inducing ligand (TRAIL)-induced apoptosis represents the major hurdle to the clinical use of TRAIL or its derivatives. The discovery and development of lead compounds able to sensitize tumor cells to TRAIL-induced cell death is thus likely to overcome this limitation. We recently reported that marine actinomycetes' crude extracts could restore TRAIL sensitivity of the MDA-MB-231 resistant triple negative breast cancer cell line. We demonstrate in this study, that purified secondary metabolites originating from distinct marine actinomycetes (sharkquinone (1), resistomycin (2), undecylprodigiosin (3), butylcyclopentylprodigiosin (4), elloxizanone A (5) and B (6), carboxyexfoliazone (7), and exfoliazone (8)), alone, and in a concentration-dependent manner, induce killing in both MDA-MB-231 and HCT116 cell lines. Combined with TRAIL, these compounds displayed additive to synergistic apoptotic activity in the Jurkat, HCT116 and MDA-MB-231 cell lines. Mechanistically, these secondary metabolites induced and enhanced procaspase-10, -8, -9 and -3 activation leading to an increase in PARP and lamin A/C cleavage. Apoptosis induced by these compounds was blocked by the pan-caspase inhibitor QvD, but not by a deficiency in caspase-8, FADD or TRAIL agonist receptors. Activation of the intrinsic pathway, on the other hand, is likely to explain both their ability to trigger cell death and to restore sensitivity to TRAIL, as it was evidenced that these compounds could induce the downregulation of XIAP and survivin. Our data further highlight that compounds derived from marine sources may lead to novel anti-cancer drug discovery.

Keywords: TRAIL; marine actinomycetes; apoptosis; therapy

ELSEVIER

Evidence that BJcuL, a C-type lectin from *Bothrops jararacussu* venom, influences deubiquitinase activity, resulting in the accumulation of anti-apoptotic proteins in two colorectal cancer cell lines

L. Zischler [a], S.C. Cogo [a], O. Micheau [b,c], S. Elifio-Esposito [a,*]

[a] Graduate Program in Health Sciences, Pontifícia Universidade Católica do Paraná, 80215-901, Curitiba, Paraná, Brasil
[b] University of Bourgogne Franche-Comté, LNC UMR1231, F-21000 Dijon, France
[c] INSERM, LNC UMR1231, F-21000 Dijon, France

ARTICLE INFO

ABSTRACT

BJcuL is a snake venom C-type lectin (SVCTL) purified from the snake's venom *Bothrops jararacussu*. It has been previously demonstrated that BJcuL induces the accumulation of pro-apoptotic proteins of the extrinsic pathway, such as FADD and caspase-8, in the colorectal cancer cell line HT29, suggesting that the lectin may be able to enhance TRAIL-induced apoptosis. To test this hypothesis, we exposed two colorectal cancer cell lines, HT29 and HCT116, to increasing concentrations of BJcuL (1–20 μg/mL) in the presence or absence of TRAIL. Contrary to our expectations, however, BJcuL was unable to induce apoptosis in these cells, as shown by annexin-V/7AAD, clonogenic assays, and immunoblotting. Nevertheless, BJcuL was able to induce the accumulation of FADD and caspase-8, as well as anti-apoptotic proteins such as c-FLIP and survivin and poly-ubiquitinated proteins. Incubation with the deubiquitinase inhibitor WP1130 (10 μM) resulted in decreased BJcuL-induced survivin levels. Altogether, our results evince the effects of SVCTL on the ubiquitin-proteasome system *in vitro* for the first time. Compounds that can influence such system are important tools in the search for new therapeutic or diagnostic targets in cancer since they can elucidate the molecular mechanisms involved in determining cell fate as well as contributing to drug-development strategies in partnership with the pharmaceutical industry.

1. Introduction

Snake venom toxins are promising sources of novel biologically active molecules and pharmacological agents [1]. Snake venom C-type lectins (SVCTL) are among the best-known and most active components, exhibiting a peculiar ability to interact with specific glycoligands and affect extensive biological processes [2]. The antitumor activity of SVCTL, for example, has been attributed to its involvement in apoptosis induction [3] through mechanisms that remain only partially understood. BJcuL is an SVCTL purified from *Bothrops jararacussu* venom. It has a pro-inflammatory capacity, as demonstrated by the activation of neutrophils and macrophages *in vitro* [4–7]. BJcuL can also decrease the growth of breast, pancreatic, renal, ovarian, and glioma tumor cells [8,9] and induce apoptosis in MKN45 and AGS gastric tumor cell lines [10]. When assessing the effects of BJcuL on colorectal cancer (CRC) cell line HT29, increased immunocytochemistry staining of the death receptor TRAIL, FADD, caspase 8, and Bax have been observed, as well as a decreased cellular respiration rate followed by an increase in the release of cytochrome c [11]. These previous findings appear to suggest that BJcuL may exert an extrinsic pro-apoptotic effect on HT29 cells and that it could be involved in TRAIL-induced apoptosis.

Apoptosis is a mechanism of programmed cell death that is constantly regulated to maintain cellular homeostasis. In cancer, the apoptotic pathway is typically inhibited by a wide variety of conditions that may occur at three levels: (1) the membrane level, by the recruitment of c-FLIP [cellular FLICE (FADD-like IL-1β-converting enzyme)-inhibitory protein], a key inhibitor of extrinsic apoptosis that competes with caspases 8 or 10 for interaction with the adaptor protein FADD (Fas-associated Death Domain) in the assembly of the membrane-bound DISC (death-inducing signaling complex) [12]; (2) the mitochondrial level, where anti-apoptotic proteins from the Bcl-2 family inhibit Bax/Bak oligomerization, preventing the mitochondrial outer